Palaeolimnology of Adelaide Tarn, a ~14,000-year-old low-alpine glacial lake, northwestern South Island, New Zealand

A thesis submitted in partial fulfilment

of the requirements for the degree

of

Master of Science

in Earth Sciences

at

The University of Waikato

by

Courtney Renee Foster

The University of Waikato
2013

THE UNIVERSITY OF
WAIKATO
Te Whare Wānanga o Waikato

Abstract

A palaeolimnology study has been carried out on a ~14,000 calendar [cal]-year-old low-alpine glacial lake, Adelaide Tarn. The lake is located in a cirque basin at ~1260 m elevation in the Tasman Mountains, just below present-day treeline, within Kahurangi National Park, northern South Island, New Zealand. A 5.6-m long sediment core was retrieved from the lake by staff of GNS Science. The chronology of the core was constructed from 15 ^{14}C dates obtained via AMS on 14 samples of in-situ plant macrofossils and one sample of bulk organic sediment. The core was divided into lithozones 1, 2, and 3 from the base through to the top of the core. Lithozone 1 (5.6–4.8 m) comprises inorganic (carbon content 0.3 to 4%) grey silts with gravel (Munsell colour 5Y 6/1) and these sediments, primarily composed of angular particles identifed by scanning electron microscopy (SEM), date to a little earlier than ~13,932 cal yr BP. Lithozone 2 consists of organic (carbon content up to 15%) brownish black (10YR 2/3) silt and clay and extends from ~13,932 to ~7709 cal yr BP. In lithozone 2, diatoms appear, as identified by SEM. Lithozone 3 is made up of dark brown (10YR 3/4) organic silt (carbon content 5 to 10%) and extends from ~7709 cal yr BP through to the top of the core which has an age estimated to be a little older than ~700 cal yr BP on the basis of a ^{14}C date (~926 cal yr BP) at 13 cm depth and a pollen record that shows neither a Polynesian deforestation signal (i.e. the sediments likely pre-date ~700 cal yr BP) nor European adventives (i.e. the sediments pre-date ~1840 AD). Lithozone 3 is diatom-rich with subordinate angular particles. Intermittent yellow/brown (10YR 6/8) laminae occur throughout lithozones 2 and 3; one lamination occurs near the top of lithozone 1. These yellow/brown laminae comprise mainly angular clastic particles (evident in SEM micrographs) and show a slight increase in sand compared with non-laminated sediments, and the laminae are inferred to reflect terrigenous input to the lake as a consequence of storms or during intense rainfall events. These possible storm events may correspond with ENSO events as described/identified in Lake Tutira in Hawke's Bay.

Multiple components of the sediment archive were analysed to reconstruct the history of the lake and its catchment. Properties included were X-radiography,

grey-scale, magnetic susceptibility, grain size, plant macrofossil assemblages, organic carbon content, and isotopes $\delta^{15}N$ and $\delta^{13}C$.

The results show four phases of climate variability (Adelaide Tarn climate events, AT-CEs) from the onset of lake formation ~14,000 cal yr BP. **AT-CE1**: early sediments ~14,000 cal yr BP show enhanced terrigenous input (fine-grained grey silts, with gravel layers, of lithozone 1), consistent with fluvio-glacial in-wash during retreat from the Adelaide Tarn basin of a local cirque glacier. **AT-CE2**: from ~13,932 to ~10,000 cal yr BP, erosion of the catchment is much diminished, indicated by decreases in modal grain size and magnetic susceptibility, and lake productivity concomitantly commences as shown by the $\delta^{13}C$ and $\delta^{15}N$ isotope records. *Poaceae* species dominate the macrofossil plant assemblages with no tree-species found. AT-CE2 (~13,932 to ~10,000 cal yr BP) is inferred to be one of warming but the catchment was not yet stable and little or no soil formation occurred that would allow habitation by tree species. **AT-CE3**: the third palaeoenvironmental phase, from ~10,000 to ~2400 cal yr BP, is marked by an expansion of *Nothofagus* (*Nothofagus menziesii* and *Nothofagus fusca*) forest with minor constituents of *Libocedrus biwillii* and *Phyllocladus alpinus*. This phase is inferred to be one of sustained warm conditions and a stable catchment. Adelaide Tarn is situated 250 m higher than the present-day altitudinal limit of *N. fusca* and the presence of macrofossils of this species in the sediment record suggests that between ~6400 and ~2400 cal yr BP the mean annual temperature was possibly ~1.2˚C warmer than present based on an observed environmental lapse rate of 0.47˚C/100 m. There was slight increase in denitrification from ~8000 through to ~3000 cal yr BP, suggesting that primary productivity increased in the lake. **AT-CE4**: from ~2400 cal yr BP, the fourth phase, the plant assemblage shifted to *Poaceae*-dominated; cold-sensitive taxa were forced to descend, marked by disappearance of forest species from the plant macrofossil assemblage. The climate is inferred to have deteriorated and the tree-line descended to near the present-day position.

The Adelaide Tarn record is one of only a few spanning the last ~14,000 years in central New Zealand, and is especially useful in adding to the plant macrofossil records, which are rare. The Adelaide Tarn record was compared with the newly-

published New Zealand climate event stratigraphy (NZ-CES), with the proposed tripartite subdivision of the Holocene, and with a number of records across New Zealand that are based on various proxies including speleothems and pollen assemblages. None of the NZ-CES events were clearly evident in the Adelaide Tarn record (apart from NZce-1), and the proposed boundaries of the subdivided Holocene (at ~8.2 ka and 4.2 ka) were not evident. A palynological record spanning the last ~12,000 years from Cropp Valley, western South Island, showed close consistency with the Adelaide Tarn record.

Acknowledgements

I would like to express my gratitude to my chief supervisor Professor David Lowe for his full support, constant enthusiasm, his willingness to help at any time (day or night), for always having faith in me to help me progress, and for helping with revising and editing my chapters. I feel very privileged to have had David as a supervisor; he has encouraged me and inspired me throughout the whole process. I would also like to thank his wife Maria for her understanding regarding the time David puts into his students.

I would like to acknowledge my co-supervisors Professor Rewi Newnham of Victoria University of Wellington (VUW) and Dr Marcus Vandergoes of the Geological and Nuclear Sciences Institute (GNS). Meetings I have had with them in designing the project and in discussing sampling and analytical procedures were very beneficial and I always gained a lot from them. I also feel very privileged to have had them on board this project, their great passion and enthusiasm for this field have encouraged and inspired me. I would like to thank Marcus and his colleagues for the retrieval of the sediment core, for providing the radiocarbon ages, for his supervision throughout the sampling process, and especially for making me feel very welcome and comfortable throughout my work at GNS Science. Rewi also helped with revising and editing of chapters and is thanked for giving me the last push to make them better

I would like to thank Ignacio Jara of VUW for providing the detailed pollen record and the work on the age model, for his help with the sampling, his willingness to help and provide data and his full support throughout. Ignacio has been very easy going but very professional, and great to work with.

I am very grateful for the funding I have acquired to help see me through university and this thesis project. I would like to thank the Bay of Plenty Trust for providing me with funding since 2007, the University of Waikato Masterate Research Scholarship, and the Broad Memorial Fund.

I thank all of the university staff who have helped me in some way. Janine Ryburn, Annette Rodgers, Renat Radiosinsky and Toni Cornes are thanked for their help in the labs. I also thank the following people for their assistance with various techniques

I have used: Professor Bruce Clarkson (taxonomy of plant macrofossils), Dr Mike Clearwater (botany knowledge), Anjana Rajendram (isotope analysis), Dr Chris Hendy and Dr Adam Hartland (interpretation of isotopes), Dr Barry O'Brien (for his guidance and for the use of his microscope and camera), Dr David Campbell (general knowledge of the Adelaide Tarn area and photographs of the lake and catchment), Helen Turner (SEM micrographs), Associate Professor Murray Jorgensen and Dr Willem de Lange (for help with "R"), and a special thanks to Sydney Wright (administrative help).

I would like to acknowledge Dr Allan Orpin from NIWA for the use of the X-radiography machine and help with the acquisition, Heidi Roop for providing software and detailed notes for grey-scale analysis, Dr Lynda Petherick (University of Queensland) for the initial help with "R" and the mixdist package, and Dr Gillian Turner (VUW) for her help with magnetic susceptibility measurements.

I would like to thank my friends. My fellow masterate students provided enduring support throughout the project, especially Erin and Diana with whom I shared an office. Both have been absolutely amazing and have helped me right to the end. I would like to give special thanks to Alex McClaren and her family for hosting me for the two weeks while I was working in Wellington at GNS Science. Thanks are also due to Lauren Wolting, Kaylee Mahoney and Ali Horsley (the last even while undertaking a masters of her own at the time); my three oldest friends who have always understood, supported and had faith in me to finish.

Finally, I would like to thank my most important support team, my family. I would like to thank my parents (Steve and Bev) for providing me with love and support throughout, always showing that special interest in what I was doing, having faith in me and giving me that last bit of confidence I needed to finish. I would like to thank my sister Amanda, my brother Nick and their partners (Joseph and Lisa) for their unconditional love and support and for just being my best and forever friends. Finally Josh, who has loved and supported me throughout especially during the most stressful points – he has always understood the way I work and has continuously had faith in me, and I cannot thank him enough.

Table of Contents

List of figures

List of tables

Chapter 1. Introduction

1.0 Introduction

This thesis focuses on reconstructing the history of Adelaide Tarn and its catchment from the time of the lake's formation ~14,000 calendar (cal) yr before present (BP) through to ~700 cal yr BP. Adelaide Tarn is a low-alpine lake (zone based on Ryan et al., 2012) close to tree-line in the North-west Nelson region of the northern South Island (section 1.2). A core taken from the lake provides an archive to study palaeoenvironmental change in the lake and catchment, inferred from plant macrofossil assemblages and various chemical and physical properties of the sediments. This is the first research undertaken on Adelaide Tarn.

Establishing precisely dated patterns in palaeoenvironmental records is the key to understanding the changes and intensities of the climatic modes spanning the Quaternary. Three broad climate cycles occur at different time scales (Barrell et al., 2013): (1) long-term glacial through to interglacial cycles (~10,000 to ~100,000 years), (2) intermediate-term or millennial-scale cycles such as the Antarctic Cold Reversal (ACR), in the Southern Hemisphere (~100 to 1,000 years), and (3) short-term decadal to centennial scales such as the El Nino Southern Oscillation (ENSO) (~1 to 10 years).

Quaternary records from New Zealand can help to track changes in climate at these scales, for a part of the world where evidence is comparatively sparse.

The New Zealand landmass today extends approximately north-south for about 1500 km across the middle latitudes (34°–47°*S*) of the Southern Hemisphere and is one of only a few sizeable landmasses in these latitudes (Alloway et al., 2007). This situation makes the New Zealand evidence particularly important at wider scales in developing palaeoenvironmental change records and understanding the past to predict future patterns (Newnham et al., 1999).

The New Zealand's landscape has high-altitude axial ranges and these have made for an ideal environment for the development of ice caps in the South Island during glacials that have great sensitivity and relatively fast response times to changing climate. Evidence of the changing extent of glaciers through the Quaternary are preserved in the present-day landscape as moraines, glacial dammed water bodies such as lakes or wetlands, and ice-carved basins (Barrell et al., 2011). The elongated archipelago of New Zealand is located at the convergence of subtropical waters from the north and the Antarctic Circumpolar Current from the south (Alloway et al., 2007; Barrell et al., 2013). Amidst this setting, New Zealand terrestrial and marine records of palaeoenvironmental change have been examined to develop a model of climatic change for the past 30,000 years that comprises a high-resolution New Zealand climate event stratigraphy (NZ-CES) as part of the Australasian INTIMATE project (INTegration of Ice-core, MArine, and TErrestrial records) (Alloway et al., 2007; Newnham et al., 2012; Barrell et al., 2013).

Palaeolimnology, the study of lake sediments to interpret lake history based on characteristics preserved within the lake (Green & Lowe, 1992), plays an important role in this process (e.g., Newnham & Lowe, 1991; McGlone, 2002; Sandiford et al., 2003; Newnham et al., 2012; Augustinus et al., 2012, Heyng et al., 2012). Processes occurring within the lake, and changes in the surrounding catchment, result in deposition of sediment at the lake bottom and these sediments provide an archive from which proxies can be examined to reconstruct past events. A 'causal chain' in palaeoenvironmental reconstructions is summarised as follows (D.J. Lowe pers comm., 2013) (Fig. 1.0):

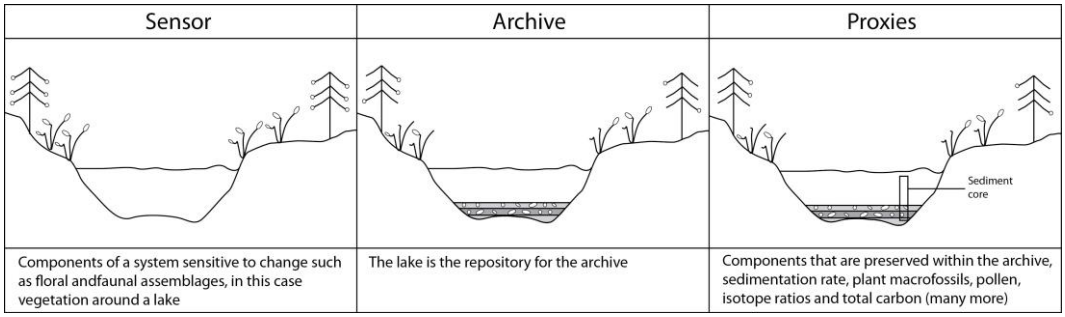

Figure 1.0 Palaeoenvironmental reconstruction from lake sediments based on the "causal chain".

The development of a timescale for the accumulation of lake sediment is an essential requirement for palaeolimnological studies. For the late Quaternary, the radiocarbon method (^{14}C) has been the most widely used, together with tephrochronology in North Island especially (Lowe et al., 2008).

1.1 Aim and objectives

The primary aim of this thesis is to reconstruct the history of Adelaide Tarn and its catchment since 14,000 cal years ago, and to develop a dated record of climatic and environmental changes using a range of biological, chemical, and physical proxies.

The following objectives were constructed to aid in the completion of the principal aim.

- Develop a stratigraphy and chronology of the core by assessing the lithology and obtaining radiocarbon dates from in-situ plant macrofossil remains.

- Undertake a range of analyses from some of the proxies preserved in the lake archive:
    - Physical properties:
        - X-radiography
        - Grey-scale analysis
        - Magnetic susceptibility
        - Grain size

    - Biological properties
        - Identification of plant macrofossils

    - Chemical properties
        - Carbon content
        - Stable isotopes: $\delta^{13}C$ and $\delta^{15}N$

- Construct a lake history and interpret palaeoenvironmental changes spanning the last ~14,000 cal years
- Synthesise palaeoenvironmental changes from the Adelaide Tarn record and compare with other New Zealand records including the NZ-CES.

1.1.1 Collaborative investigations of Adelaide Tarn

Firstly, I would like to acknowledge Dr Marcus Vandergoes of the Geological and Nuclear Sciences (GNS Science), Wellington, for acquiring and providing the Adelaide Tarn core and radiocarbon dates, and for supervising core sampling and X-radiographic analyses.

Pollen record: Ignacio Jara from Victoria University of Wellington has undertaken pollen analysis.

Stomatal density: Alex Hincke is investigating stomatal density on *Nothofagus* leaves throughout the core in order to reconstruct CO_2 changes through time.

1.2 Introduction to Adelaide tarn

1.2.1 Location

Adelaide Tarn is located in the Tasman Mountains at ~1260 m above sea level (asl) within the Kahurangi National Park in the North-west Nelson region. Three main ridges, extending from 1483 to 1563 m asl, enclose the catchment basin:

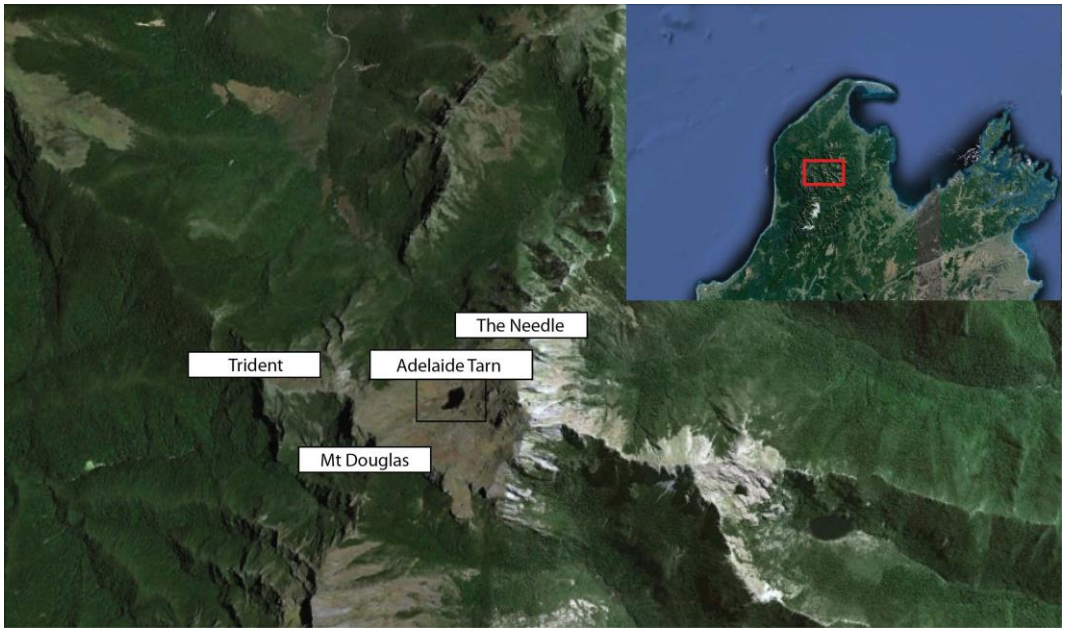

Figure 1.1 Map showing location of Adelaide Tarn (Google Earth).

Trident and Mount Douglas to the west and The Needle to the east of the lake (Fig. 1.1). Lakes are common in this landscape with several close to Adelaide Tarn, such as Boulder Lake, Lake Clara, and Darby's pond to the north and Lake Sparrow and Lake Lindsay to the southeast (Fig. 1.1). Adelaide Tarn was chosen for this study primarily because it is situated at an altitude that currently forms the transition between forest and alpine vegetation in the region today (Fig. 1.1) and its sediments were expected to provide a long-term record of changes to these regionally extensive ecotones.

1.2.2 Geology

Adelaide Tarn is situated within rocks of the Buller terrane, west of the Anotoki Fault, which is the most sizeable fault in the North-west Nelson region (Roser et al., 1996; Rattenbury et al., 1998). The Anatoki Fault has a diagnostic breccia, mylonite and cataclastite appearance along its fringe and this marks the eastern boundary of the Buller terrane and the western perimeter of the Takaka terrane (Rattenbury et al., 1998).

1.2.2.1 Buller terrane

The Buller terrane and associated formations were deposited during the late Cambrian through to late Ordovician (~500–430 Ma). The Buller terrane comprises quartz-rich continental-derived metaturbidites with sandstone and mudstone sequences, along with black shale and quartz sandstone, which can be subdivided into the Greenland and the Golden Bay Groups, respectively (Roser et al., 1996; Rattenbury et al., 1998). The Buller terrane has undergone many deformational phases with the oldest of these preserved between Adelaide Tarn and Kakapo Peak. These units are tightly folded and most abundant within the Douglas Formation of the Golden Bay Group (Jongens, 2006).

1.2.2.2 Douglas Formation

The early Late Ordovician Douglas Formation forms the youngest part of the Golden Bay Group and conformably overlies the Leslie Formation (Jongens, 2006). The bedrock beneath and surrounding Adelaide Tarn is primarily Douglas Formation that grades into the Leslie Formation at the Douglas Range, west of the lake (Fig. 1.2). The Douglas Formation consists of a grey, well-laminated siltstone with infrequent quartz sandstone beds (Jongen, 2006).

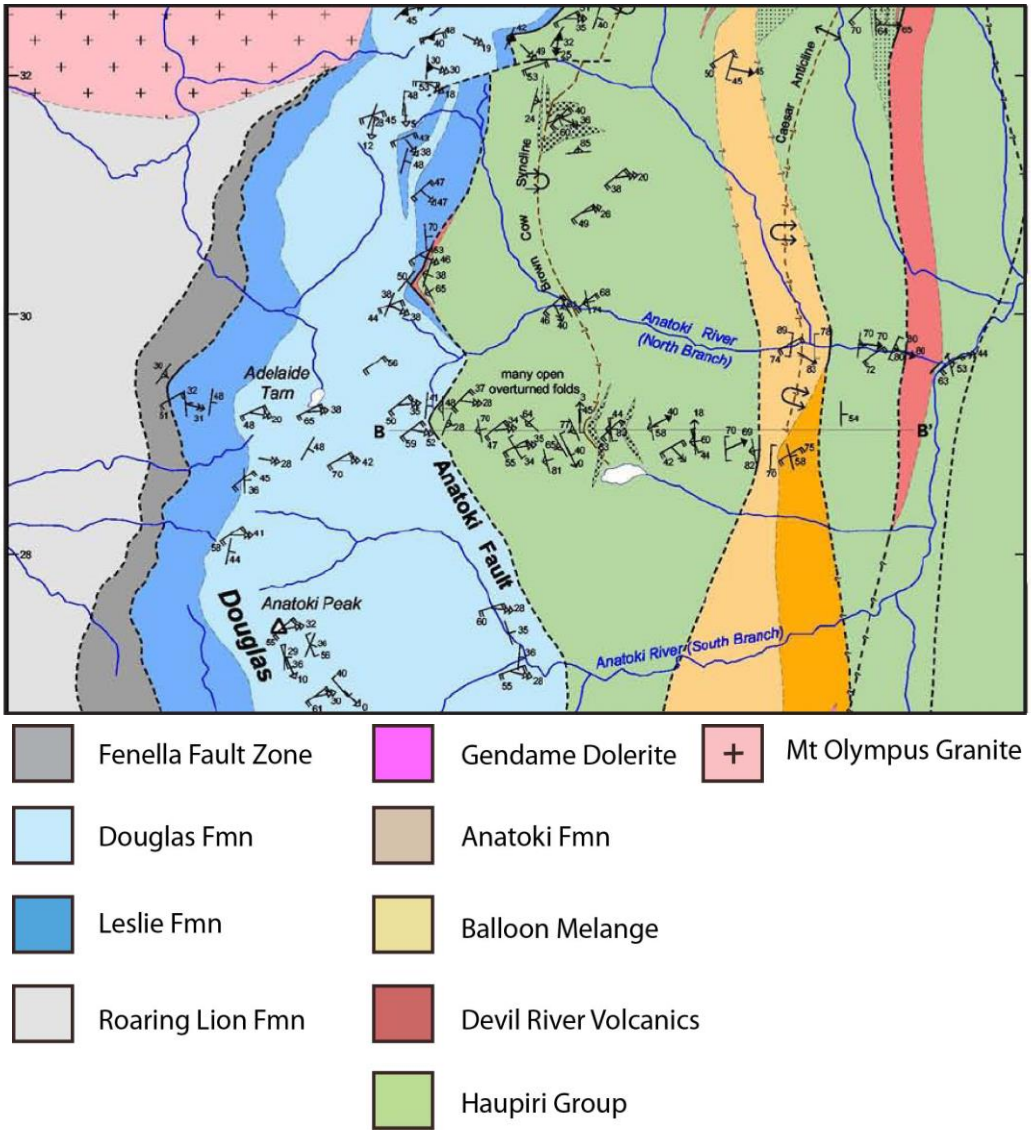

Figure 1.2 Geological map of the Adelaide Tarn region (the lake is shown white) showing the Buller and Takaka terranes intersected by the Anatoki Fault. Map adapted from Jongens (2006).

1.2.3 Geomorphology

The lake formed approximately (~) 14,000 cal yr BP (based on results of this study) within a closed cirque basin. My interpretation is that ice movements prior to ~14,000 cal yr BP carved out a circular basin in the landscape and poured over the northern rim pushing bedrock over the southern rim of the basin into the surrounding valley (Fig. 1.3B). There is no evidence of moraines in the vicinity of the lake but the cirque basin in which the lake has formed has relatively low relief and has been smoothed out by glacierisation (D.I. Campbell pers. comm., 2013). Bedrock surrounds the lake with shallow soils in some places. The bedrock is relatively close to the surface because of the shallow soil depth and this allows for overland flow directly into the lake. The low relief of the surrounding basin allows for the formation of shallow soils in rock and in slight depressions water has accumulated to form wetlands. Wetlands occur on the lower slopes of Trident and Mount Douglas on the western side of the closed basin (Fig. 1.1). The Needle to the east of the lake has the highest relief with steep rocky sides where there is little to no soil formation. Recent landslide processes are evident at the saddle just north of The Needle (Fig. 1.1) but not on the slopes surrounding the lake (D.I. Campbell pers. comm., 2013).

The current maximum depth of the lake is 7.6 m and there is one small inlet entering the lake to the southwest. There is one outlet discharging from the northern edge flowing into the Clark River and eventually joining up to the much larger Aorere River.

1.2.4 Present-day vegetation patterns

There are three main vegetation patterns around the lake and these are primarily based on soil thickness, wetness, and angle of slopes. On the low relief slopes, water accumulates and creates a niche for water tolerant plants such as the rush-like species *Empodisma minus* and large snow tussocks (*Chionochloa spp.*). In the saturated areas there is peat formation raising the surface higher than the surrounding lower relief slopes. Shorter tussock species dominate on the marginally steeper ridges of Trident and Mount Douglas, where there is mainly

bedrock exposed and little or no soil. On the remaining low-angle slopes around the lake, thicker soils allow for a larger variety of plant species. The third main vegetation pattern consists of alpine herbs such as Hebe and *Coprosma*, mountain daisies/herbs (*Celmisia spp.*), mountain flax (*Phormium cookianum* and *Astelia spp.*), Spaniard grass (*Aciphylla spp.*), leatherwood (*Oleria colensoi*) and other typical alpine scrub. One aquatic plant was observed in Adelaide Tarn belonging to the *Potamogeton* genus.

The regional tree-line is currently 30 to 100 m above the lake, although there is no forest growing in the closed basin (Fig. 1.1) presumably due to recent clearances for grazing. The closest patch of forest is on the southern rim of the basin and this is north-facing (Fig. 1.3). The forest is dominated by beech species (*Nothofagus menziesii* and *N. solandri var. cliffortioides*) with other minor constituents such as mountain/southern rata (*Metrosideros umbellata*), mountain toatoa (*Phyllocladus alpinus*), mountain neinei (*Dracophyllum traversii*) and inaka (*Dracophyllum longifolium*) (Fig. 1.3A).

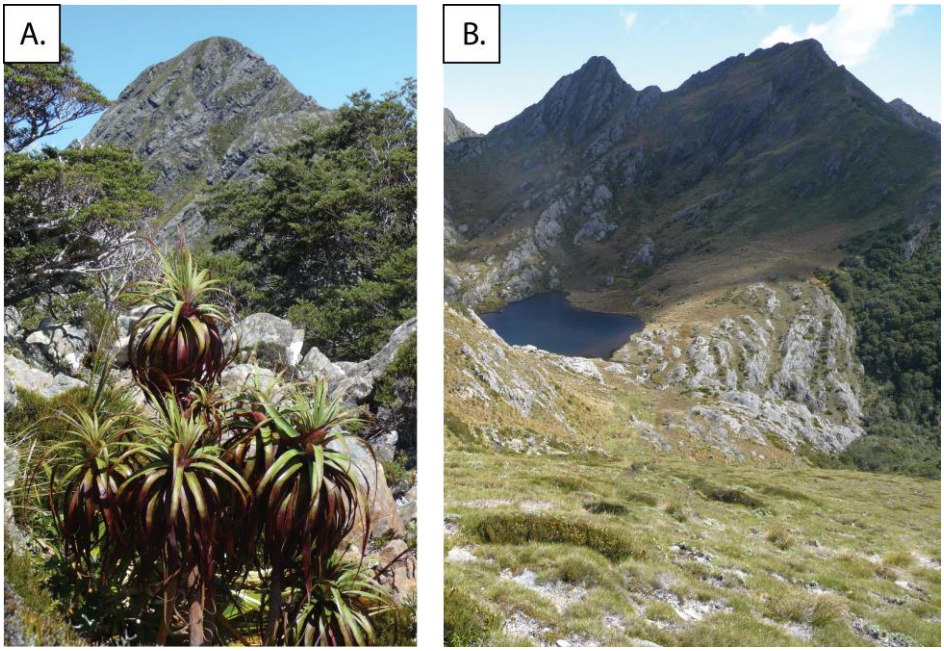

Figure 1.3 (A) Some of the present-day vegetation with *Nothofagus* in the background and *Dracophyllum traversii* in the foreground, (B) Adelaide Tarn, occupying a cirque basin in the transitional vegetation zone between *Nothofagus* forest (centre right, at southern rim of basin) and alpine herb communities (photographs courtesy of Dr David Campbell).

The species mentioned here are only some of the many that surround the lake and there has been no extensive vegetation study undertaken at this site. However, Druce (1985) compiled a thorough vegetation list at Snowden Range that is likely to be similar to that surrounding Adelaide Tarn, and hence can be used to infer changes in species assemblages through time. Snowden Range is approximately 15 km southwest of Adelaide Tarn and ranges between 1300 and 1700 m asl (Fig. 1.4).

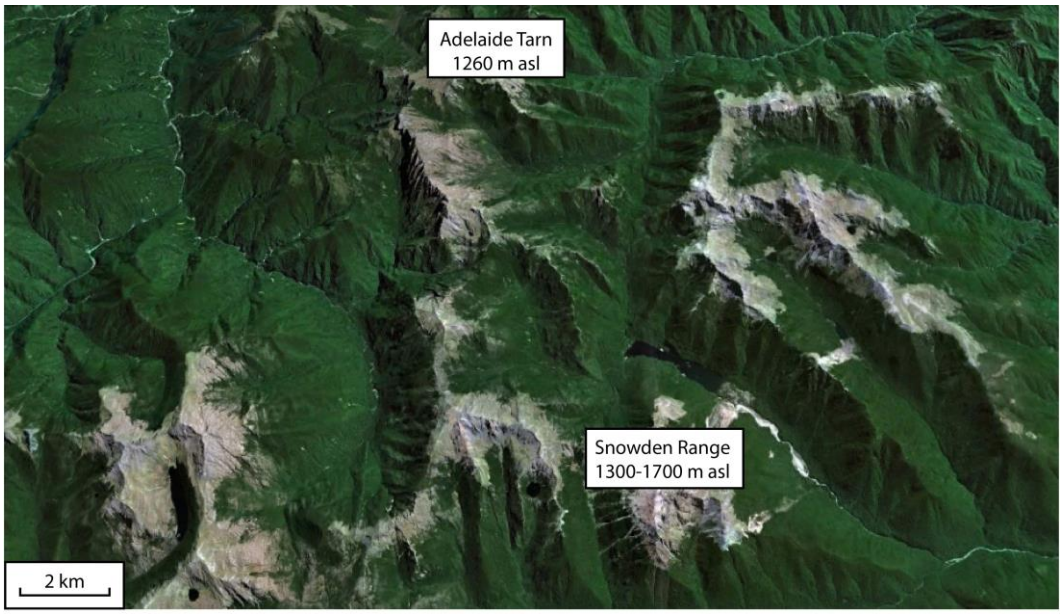

Figure 1.4 Map showing location of Snowden Range in proximity to Adelaide Tarn (Google Earth).

1.2.5 Present-day climate

There are currently no climate stations around Adelaide Tarn and the nearest stations are at a much lower elevation. McCarthy et al. (2008) acquired some useful data from Boulder Lake and wind direction and mean annual temperature from a Cobb Valley weather station. Boulder Lake is located 5.6 km north of the study site and at 985 m asl, similar to that of Adelaide Tarn. I have also used two other databases based on 30 years of climate records for comparative value: (1) GIS raster data, and (2) Landcare Research database.

Table 1.0 Climate data from three sources.

Source	McCarthy et al. (2008)	GIS raster data Wratt et al. (2006)	Landcare database Leathwick et al. (2002)
Climate parameter			
Mean annual temperature (℃)	8.2 (Cobb Valley)	6.1	5.8
Mean annual rainfall (mm)	3100 (Boulder Lake)	6181	3636
Dominant wind direction	Westerly (Cobb Valley)		

The mean annual temperature from the GIS raster data and the Landcare Research database are similar but the data from McCarthy et al. (2008) are obtained from the Cobb Valley weather station and the mean temperature is 2 ℃ higher. The rainfall for Boulder Lake is similar to that acquired from the Landcare database but the GIS raster-derived rainfall data is almost double the rainfall recorded for the other two sources. For the purpose of my research I will use the mean annual rainfall from Boulder Lake (3100 mm) (McCarthy et al., 2008), the dominant westerly wind direction from Cobb Valley (McCarthy et al., 2008) and the mean annual temperature from the GIS raster data (6.1 °C) (Wratt et al., 2006).

1.3 Structure of thesis

- In **Chapter 1** I have given a general introduction to this research and why it is important. The primary aim has been stated followed by objectives chosen to help achieve the primary aim. Lastly, the location of the study site has been described along with background information on surrounding geology, present-day geomorphology, vegetation, and climate.

- In **Chapter 2** I have defined palaeolimnology and its importance in reconstructing palaeoenvironmental change. Previous studies from New Zealand are mentioned in relation to palaeolimnology. Climate events from the last-glacial to interglacial-transition (LGIT) through to present day in New Zealand have been discussed covering a wide range of environments. The New Zealand INTIMATE project is considered in this chapter and why additional research is needed. Lastly, climatic cycles that influence New Zealand's climate are discussed.

- In **Chapter 3** I present the coring methods involved in obtaining the sediment core and methods related to its sampling. I describe the stratigraphy of the 5.6-m long core along with its lithology. Chronological methods are stated and the age model is presented.

- In **Chapter 4** I explain the physical components of the core, X-radiography, grey-scale, magnetic susceptibility, and grain size. This chapter is broken into three sections with a short introduction along with methods, results and discussions about each component that has been measured.

- In **Chapter 5** I examine the biological and chemical components, in particular plant macrofossils, and stable isotopes $\delta^{13}C$ and $\delta^{15}N$. This chapter is subdivided into these two components with introduction/background, methods, results and discussions on each.

- In **Chapter 6** I have synthesised the findings of measurements made of all of the components analysed and their palaeoenvironmental interpretations to develop a lake and catchment history and a climate event stratigraphy for Adelaide Tarn. The Adelaide Tarn climate record is compared to various New Zealand records including the NZ-CES constructed by Barrell et al. (2013).

- In **Chapter 7**, the final chapter, the main findings of my study are summarised and recommendations for further research are stated.

Chapter2. Literature review

2.0 Introduction

This chapter provides critical context to this research providing information on what palaeolimnology is and how lakes can be utilized as an archive for reconstructing past environments. This review highlights the relevance of undertaking analysis on lake sediment archives using plant macrofossils in particular and how the Adelaide Tarn record will fit into the late-glacial and Holocene palaeoclimate record of New Zealand.

2.1 Palaeolimnology

Palaeolimnology is the reconstruction of the past history of lakes and their catchments from studies of lake sediment cores (Green & Lowe, 1992; Newnham et al., 1999). Such analyses of lake sediments provide a multidisciplinary basis for palaeoenvironmental and palaeoclimate reconstructions, and for determining human impacts through time (e.g. Birks and Birks, 2006). Techniques to analyse and interpret lake sediments were initially developed in the 1920s but palaeolimnology did not develop further until the 1940s (Battarbee & Bennion, 2011). The first study undertaken in New Zealand was by E. Deevey in 1955 in the Canterbury area (Green & Lowe, 1992).

Sediments accumulate on the lakebed through processes that occur within the lake, from material entering the lake from the surrounding catchment, and from distant regions. Changes in these key processes will be reflected in the stratigraphy of the cores and preserved under the right conditions. The core stratigraphy can hold key information to past environmental states. The local climate is the primary variable influencing lake environments including catchment ecosystems, such as the surrounding vegetation pattern (Green & Lowe, 1992).

There are several ways to acquire sediment cores from lakes and these are all dependent on depth, research aim, and accessibility of the lake. Piston coring is the most common and easiest way to obtain sediment with minimal compression and deformation of the stratigraphy and this was the method employed for this study (Glew et al., 2001). Piston cores can be collected in 1-m sections and can be continuously taken in the same place off a boat or raft system and with relatively little contamination. Continuous cores up to ~6-m-long can be obtained using a modified Livingston corer (e.g. Green and Lowe, 1985; Newnham et al., 2004), however. Once the core has been obtained, the stratigraphy, lithology, and other features are recorded in detail before undertaking analyses.

2.1.1 Dating methods

Having a sound numerical age model is essential to date changes through time. The technique used for dating lake sediments is dependent on the research aim and the limiting age range. If the idealised age range for the study is relatively recent (~100 years) then lead-210 (^{210}Pb) may be useful and this method normally performs well for dating sediments in low energy environments such as lakes (e.g. Newnham et al., 1998a; Jeter, 2000). A method of dating lake sediments deposited since the 1950s is the use of caesium-137 (^{137}Cs). ^{137}Cs is a human-made radionuclide that is generated by nuclear bomb explosions and absorbed by the soil. The peak in ^{137}Cs can help to determine sediments that are of this age or younger (Yan et al., 2002). The most common dating technique used globally and in New Zealand is radiocarbon dating (^{14}C) (Alloway et al., 2007). Radiocarbon dates can be obtained from bulk sediment samples or from plant macro/microfossils such as leaves or pollen, respectively (Bjorck & Wohlfarth, 2001; Newnham et al., 2007). Radiocarbon dating (via liquid scintillation spectrometry or accelerator mass spectrometry, AMS) is used for dating carbon-bearing material dating back to ~60,000 calendar (cal) years before present (BP) (Hogg et al., 2006; Alloway et al., 2007). AMS-based ^{14}C dating is employed in this study, mainly on in-situ plant macrofossil remains.

2.1.2 Lake origins

A lake is an isolated body of standing water within a basin that is disconnected from the sea (Lowe & Green, 1992). The isolated water body is able to occur because of a pre-existing depression with a perimeter higher than that of the deepest point, allowing water to accumulate. Lakes can be formed over a wide range of timescales under one or a combination of different processes. Origins of lakes can be classed into ten broad categories: (1) glacial, (2) tectonic, (3), volcanic, (4), fluvial or riverine, (5) barrier-coast (coastal), (6) dune, (7) solution (sinkholes), (8) landslides, (9), peat, and (10) artificial (Lowe & Green, 1992; Cohen, 2003). In New Zealand, lakes are able to be grouped into distinct lake districts because of the dominance of particular geological processes in different areas, and 'glacial lakes', which are found only in the South Island, are the most common lake type in the country (38%) (Lowe & Green, 1992). Most glacial lakes are at high altitude, small in size, and were formed because of extensive glacial action and reworking of subsequent deposits during the Quaternary glaciations (e.g. see Barrell et al., 2011). They may be grouped into four main types, including lakes in ice-excavated rock depressions described as 'cirque lakes', and 'piedmont lakes' (Lowe and Green, 1992). Cirque lakes, of which Adelaide Tarn is an example, are discussed further below.

2.1.2.1 Cirque lakes

Cirque lakes occupy basins that have been carved by fluctuations of ice in glacierised valleys (Lowe & Green, 1992). The basin or amphitheatre formation is typically circular in plan view with a gently sloping floor, connected to, or dammed by, steep headwalls (Evan & Cox, 1974; Brook et al., 2006) (Fig. 2.0). Cirque glaciers can either form in direct contact with a glacier or indirectly through glacier advancement or melt-water (Cohen, 2003; Brook et al., 2006). Gordon (2001) discussed two main models of cirque development: (1) ice dammed in the basin and rotational movements (flow caused by the constant addition of snow and the melt-water at the outlet) of the ice within the basin causes the walls to erode and deepen; and (2) larger glaciers confining a basin or lake beneath and scouring the valley head/walls as the descending movement

occurs. Adelaide Tarn occupies a cirque basin and was formed through either of the two mechanisms mentioned above, but (1) is favoured because of the isolated steep walls that surround the tarn today (Fig. 2.1).

As well as ice/frost riving, freeze-thawing is likely to have occurred at Adelaide Tarn, causing large fragments of bedrock to detach, and thereby eroding the future depocentre. In New Zealand, the Scandinavian word 'tarn' represents a small mountain glacial lake and tarns may be cirque or kettle lakes formed through glacial corrosion or melting (Lowe & Green, 1992).

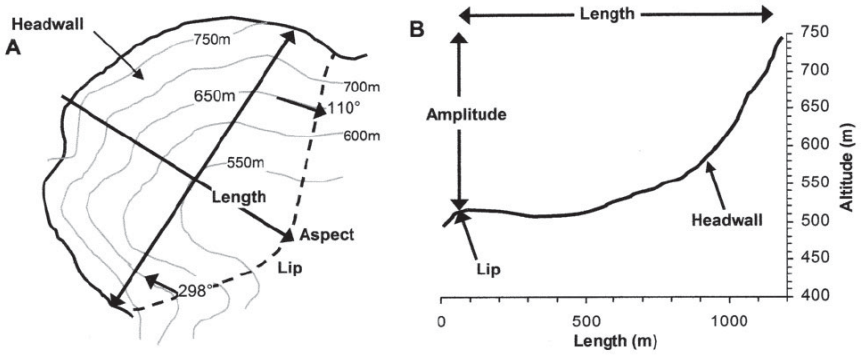

Figure 2.0 (A) A typical plan view of a cirque basin and (B) associated deepening shown in the cross-section profile (from Brook et al., 2006).

Figure 2.1 A wide view of Adelaide Tarn highlighting its isolation in a closed cirque basin (cf. the narrower view of Adelaide Tarn shown in Fig. 1.4) (photograph courtesy of Dr David Campbell).

2.1.3 Lake systems and sensors

Lake sediments are natural archives that record lake processes, productivity and local environmental change (Anderson, 1995; Birks and Birks, 2006). This is because lake systems are highly dynamic and respond physically, chemically and biologically to changes in the local climate (abiotic components) (Battarbee, 2000). The sensors or biotic components of the system include flora and faunal species assemblages within the lake and the catchment, and abiotic components (from the forcing of biotic changes) include soil, topography, climate, water chemistry and water temperature (Birks et al., 2010) (Fig. 2.2). Changes in the catchment will likely lead to changes in the sedimentation rate. Fluctuations in sedimentation rate can be attributed to various events, some of which relate to disturbance or change in the catchment or beyond, which are described as allochthonous events (e.g. storms, earthquakes, climate change).

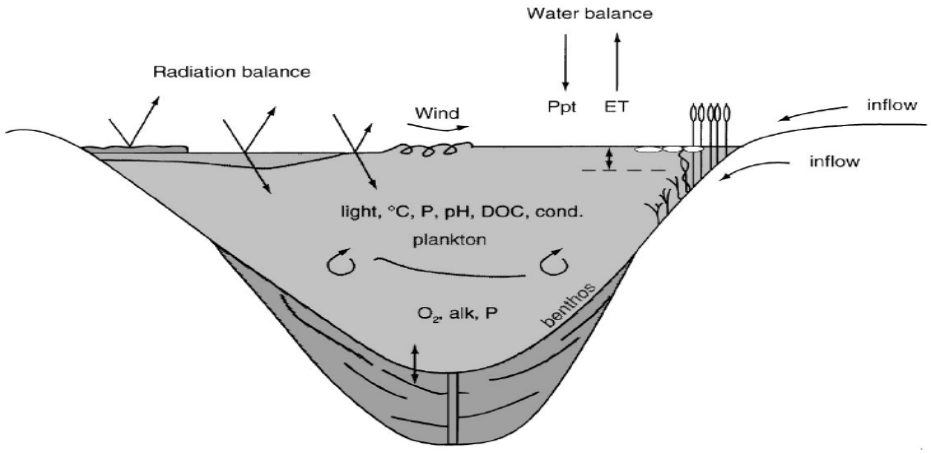

Figure 2.2 A simplified schematic showing lake processes and the main driving forces of these (from Cohen, 2003).

Fluctuations may also be the result of in-lake processes, which are described as authochthonous (e.g. sediment focussing, changes in trophic status) (Battarbee, 2000; Gasiorowski, 2008). Small alpine lakes in the mid-latitudes are regarded as particularly sensitive to climate changes because they are considered to be highly sensitive to small changes in climate, and studies of their sediments thus provide

an opportunity to describe variations in, for example, biological assemblages through time, and hence enable researchers to identify and evaluate climatic events (Sporka et al., 2002; Vanhoutte et al., 2006).

It is important therefore to understand how present-day lake systems function in terms of responses to climatic parameters. Radiation is the key driver along with wind, precipitation and temperature (Fig. 2.2). Observing the effects of these parameters in a modern system can help a researcher to infer changes in biological, chemical and physical proxies in the archive (Battarbee, 2000).

The amount of radiation that can be absorbed by a lake in an alpine environment is influenced by ice and snow cover in relation to albedo and reflected light. Reduced radiation means that lake temperatures in winter are lower and hence species within the lake will generally have wide optimal temperature ranges and so will be sensitive to fluctuations. Biological assemblages are largely driven by temperature, nutrients, predators and water level (Korhola et al., 2000). Lake levels (in closed basins with minor or no inlets or outlets) are broadly driven by precipitation and evaporation (e.g. Lowe et al., 1997).

An important physical process in lakes is the formation of a thermocline because of temperature stratification during warmer months. Not all lakes produce a thermocline and may remain mixed all year round.

2.1.4 Lacustrine archives

A lake archive is derived from three main processes: (1) in-wash of sediment from the catchment that may contain minerals from bedrock, soil, humus, pollen, vegetation remains, and wind-blown material, (2) biological productivity within the lake where the dead organic matter accumulates on the lake bed, and (3) geochemical components such as nitrogen and phosphorus in the water column (Gornez, 2009). Relationships between proxies can provide information on past climate parameters, such as wind, temperature, precipitation, and the structure of the biological system at the time. Listed below are common proxies that can be preserved in lake sediments and the interpretation(s) that can be made from each

(Table 2.0). A multi-proxy approach is essential and can help in determining biotic responses to climate change through time. Each proxy has limitations but correlations between two or more can give a more definitive interpretation (Birks and Birks, 2006; Birks et al., 2010).

Table 2.0 Available proxies from lake sediments and information potentially gained from these.

Interpretations	Proxies from lake sediment archive
Temperature (through transfer functions or modern analogue technique)	Diatoms Chironomids Beetles Pollen
Floral assemblages (temperature and wet/dry conditions)	Pollen Plant macrofossils Ancient DNA Phytoliths
Lake productivity	Lipids Pigments Isotope analysis (^{13}C, ^{15}N, ^{18}O)* TOC*, C/N* Biogenic silica Mineral assemblage from XRD* Diatoms (pH)
Wind circulation	Floral and faunal assemblages Grain size Fingerprint sediment chemistry through XRF*
Catchment disturbance by storms, earthquakes, and heightened erosion; distant volcanic eruptions	Grain size Magnetic susceptibility X- radiography Tephra layers or cryptotephras

*TOC = total organic carbon, C = carbon, N = nitrogen, O = oxygen, XRF = X-ray fluorescence, XRD= X-ray diffraction

I have chosen to take a multi-proxy approach in sampling variables from each of the three components, biological, chemical and physical. This approach provides supporting (independent) evidence for changes through time and enables such changes to be interpreted more reliably. The table below outlines the proxies chosen for this research (Table 2.1). These are discussed in subsequent chapters.

Table 2.1 Proxies chosen for this research and associated advantages and limitations.

Proxy	Information	Advantages	Limitations	References
Biological				
Plant macrofossils	Local presence of certain plant species and related environmental factors	Located close to source and can be identified to a species level	Species have different rates of preservation. May be located far from preservation site. Serendipitous record	Birks & Birks (2003), Finsinger& Wagner-Cremer (2009), Mauquoy et al. (2010)
Physical				
Grain size	Lithological characteristics. Catchment disturbance, e.g., storm frequency, earthquakes, and erosion	Local sediment transport, insight into climate conditions, eg. increased precipitation	Can cause disturbances in other proxies; environmental interpretations may be confounded by local site factors	Last (2001), Parris et al. (2009)
Magnetic susceptibility	Changes in landscape and catchment in relation to erosion	Based on changes in significant minerals. Fast easy and non-destructive	Mixing of sediment; reliant upon magnetic properties not always consistently present	Lee et al. (1998), Balascio& Bradley (2012)
X-radiography	Changes in core stratigraphy are enhanced	Fast, easy and non-destructive	May show no significant changes	Tiljander et al. (2002)
Grey-scale	Changes in core density, can give idea of in-lake or terrestrial processes	Fluctuations can link up with other proxies	May show no significant changes; multiple possible causes	Saarinen &Petterson (2001)
Chemical				
^{13}C	Abundance of plant matter. Can determine the source of organic matter	Stable isotopes do not degrade	Dependent on concentration of CO_2 in the atmosphere; subject to plant-specific fractionation and other biotic factors	Talbot &Laerdal (2000), Augustinus et al. (2008)
^{15}N	Lake productivity	Stable isotopes do not degrade	Can be ambiguous and complex on its own	Talbot, (2001)

2.1.5 Palaeolimnology in New Zealand

This section outlines some of the research undertaken in the field of palaeolimnology in New Zealand and studies that have used the same proxies that have been chosen for this research (Table 2.2). The locations of the lakes mentioned can be seen in Fig. 2.3.

Table 2.2 An outline of palaeolimnology studies in New Zealand that have used the same or similar properties that have been chosen for this research on Adelaide Tarn, and information that has been gained that may assist in the reconstruction of this record.

	Lake	Information	Interpretations	References
Physical properties	X-radiography			
	Lake Onepoto	X-radiography, grey-scale and laminae count to reconstruct ENSO cycles	Results indicate that El Nino and possibly IPO operated prior to LGM* and were supressed or absent in NI during the Holocene	Pepper et al. (2004)
	Lake Tekapo	X-radiography, grey-scale to interpret varve couplets	Interpreted as seasonal to annual depositions	Mildenhall et al. (2006)
	Lake Waihola	X-radiography to define stratigraphy	Identified two distinct changes in stratigraphy in relation to estuarine influence	Schallenberg et al. (2012)
	Magnetic susceptibility			
	Lake Pounui	Magnetisation of sediments to reconstruct palaeomagnetism	West-ward shift of palaeomagnetic drift over the last 2500 years (can now be used as a dating tool)	Turner & Lillis (1994)
	Lake Tutira and Lake Waikopiro	Palaeomagnetism in relation to the impact of human settlement	Increased magnetic susceptibility during storm events post-human settlement	Turner (1997)
	Lake Omapere	Palaeomagnetism in relation to onset of burning of vegetation	Heightened magnetism consistent with pollen analysis of extensive burning	Newnham et al. (2004)
	Grain size			
	Lake Pupuke	%>32 μm grains interpreted as terrigenous input	Increased %>32 μm after 8.2 ka	Augustinus et al. (2008)
	Lake Tutira	To characterise lithotypes	Storm events generated larger grain sizes and inorganic lithologies	Page et al. (2010)

	Lake Omapere	Lake and catchment history	A sandy pre-lake composition to finer muddier lake sediments	Newnham et al. (2004)
Biological component	Plant macrofossils			
	Lake Omapere	Charcoal is used to interpret onset of burning period	Deforestation ~600 to 700 cal yr BP	Newnham et al. (2004)
Chemical properties	Carbon content			
	Lake Pupuke	Biological productivity	Highest auto and allochthonous biomass from the LGIT through to the Holocene	Stephens et al. (2012)
	Lake Waihola	Characterisation of sediment	Decrease in carbon content after AD 1860 and this is also the boundary of a major stratigraphic change	Schallenberg et al. (2012)
	$\delta^{15}N$ and $\delta^{13}C$ isotopes			
	Lake Pupuke	$\delta^{13}C$ used to determine in-washing of terrigenous carbon	Influx after 8.2 ka coincidentwith increased grain size.	Augustinus et al. (2008)
	Lake Tutira	$\delta^{13}C$ was used to characterise lithotypes	Storm events had slightly more positive $\delta^{13}C$, catchment derived	Page et al. (2010)
	Lake Pupuke	Both isotopes were used to determine lake productivity and source or organic matter	Found little allochthonous input throughout most of the core and isotopes were inferred to be dominated by in-lake processes during the last 7000 years.	Heyng et al. (2012)

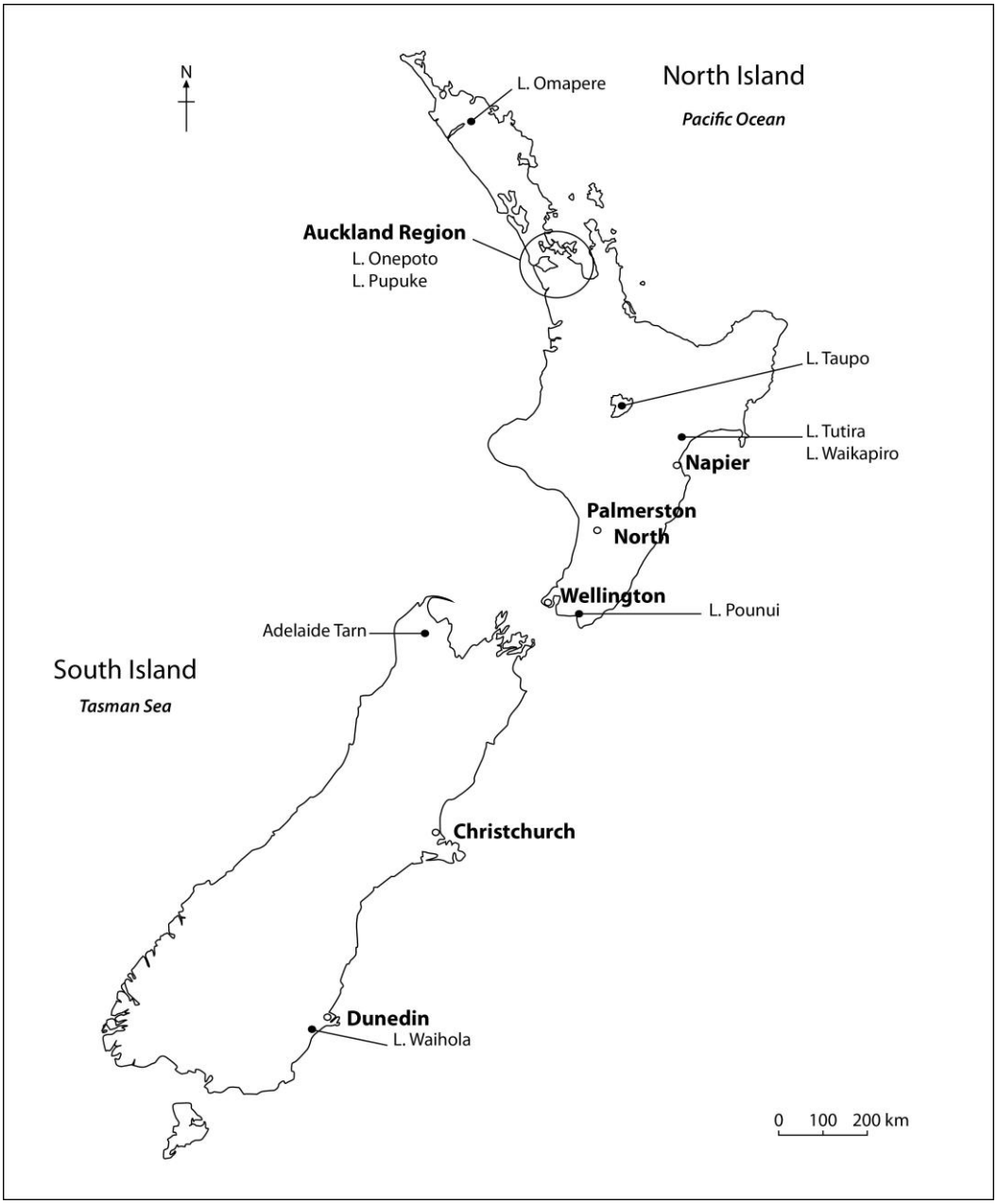

Figure 2.3 Locations of lakes that have been mentioned in Table 2.3.

The studies mentioned in Table 2.2 have used multiple proxies to reconstruct past lake and catchment changes. Some of these proxies have been chosen for my research on Adelaide Tarn. The papers representative of X-radiography highlight the point that multiple interpretations that can be made from X-radiography and why it can be a useful and non-destructive tool (Pepper et al., 2004; Mildenhall et al., 2006; Schallenberg et al., 2012). X-radiography can assist in defining boundaries between major stratigraphic units and enhance further laminations that may not have been picked up otherwise. Studies chosen to represent palaeomagnetism in lake sediments relate to the increase of magnetics in relation to storm events and the onset of burning following initial human settlement (Turner, 1997; Newnham et al., 2004). The relationship between grain size and magnetic susceptibility has been used to infer increased storm events or terrigenous input and lake catchment history (Newnham et al., 2004; Augustinus et al., 2008; Page et al., 2010). Isotope analyses have been used by Augustinus et al. (2008) and Page et al. (2010) to infer changes in autochthonous- and allochthonous-derived organic matter, and both studies found more positive values of $\delta^{13}C$ during storm or terrigenous in-wash events. Heyng et al. (2012) attempted to fingerprint the source of organic matter using both $\delta^{15}N$ and $\delta^{13}C$ isotopes along with interpreting a history of lake productivity of Lake Pupuke. They saw a marked change in the in-lake processes dating from 7000 cal yr BP.

An important point made by this table is the paucity of plant macrofossil-based reconstructions obtained from studies of lake sediments. The majority of palaeolimnological research is based on pollen assemblages and has not had the support of plant macrofossils (Newnham et al., 1998a, 1998b; Turney et al., 2003; Wilmshurt et al., 2007; Li et al., 2008). Lakes close to tree-line are going to preserve sensitive changes in the position of the tree-line from in-situ plant macrofossils rather than pollen that can be blown in from outside of the catchment, i.e. pollen represents a more regional context (e.g. Newnham et al., 1995; Drake and Burrows, 1980; Pocknall, 1980). This paucity illustrates the importance of the study on Adelaide Tarn sediments that contain abundant plant macrofossils in places, and the use of plant macrofossils as a biological sensor in support of the detailed pollen record being constructed by Ignacio Jara at Victoria University of Wellington (VUW).

2.1.6 Plant macrofossil research in New Zealand

The use of plant macrofossils to reconstruct late-glacial or Holocene vegetation is uncommon in New Zealand. Studies include those of Pocknall (1980), Drake & Burrows (1980), Clarkson et al. (1995), Newnham et al. (1995), McGlone et al. (2004), and McGlone et al. (2011). Clarkson et al. (1995) reconstructed vegetation patterns using pollen and plant macrofossils pre-Taupo eruption (i.e. before ~AD 232). They found that plant macrofossils represented local vegetation and pollen was a representation of both local and regional vegetation. Both pollen and the plant macrofossils identified the same forest type of conifer/broadleaf forest, and therefore supported each another. Newnham et al. (1995) reconstructed late-glacial to Holocene vegetation history and climate from Kopouatai Bog. The pollen and macrofossil assemblages together provided an excellent and detailed record of past vegetation and climate history, although the limitations of each were reported (Newnham et al., 1995). McGlone et al. (2004) constructed a palaeoclimate record at Kettle Bog (Cass Basin) from pollen, plant macrofossils and various other proxies. McGlone et al. (2011) noted tall tree and shrub macrofossils found at Kettle Bog along with pollen assemblages and inferred past temperatures between 8200 and 300 cal yr BP.

2.2 Palaeoenvironmental reconstruction in New Zealand spanning the last 14,000 years

2.2.1 New Zealand climate event stratigraphy (NZ-CES)

The INTIMATE project (North Atlanic region) was founded in 1995 with a primary aim of developing ways to improve dating, correlation and resolution of climate records spanning the last 30,000 cal years, and was focussed on an integration of marine, ice and terrestrial records (Bjork et al., 1998; J.J. Lowe et al., 2008; Blockley et al., 2012).). The Australasian-INTIMATE project began in 2003 with two subgroups, the NZ-INTIMATE and the OZ-INTIMATE groups (Alloway et al., 2007). Initial objectives of the NZ-INTIMATE were to obtain and identify records that had high-resolution, good chronology, were continuous and had clear definitions of major climate events spanning the marine and

terrestrial realms and across a range of latitudes and altitudes. Alloway et al. (2007) presented a series of reference records derived from key sites on both main islands and also from the marine realm, together with fragmentary-type records for New Zealand spanning the last 30,000 cal years (also presented in poster form by Barrell et al., 2005). D.J. Lowe et al. (2008) presented new geochemical data and age models for a group of widespread tephras useful for NZ-INTIMATE. An important conclusion reached by the NZ-INTIMATE community subsequently is that no single record provides a definitive reference standard for the New Zealand region (Lowe et al., 2013). The most recent initiative has therefore been to formalise a New Zealand climate event stratigraphy (NZ-CES), tied to a composite inter-regional stratotype of three high-quality proxy terrestrial records that will facilitate enquiry into event rationality, and leads or lags in timing of events (Barrell et al., 2013). The NZ-CES presents a time period from present day to 30,000 cal. years BP and focuses on one type of proxy, pollen (Fig. 2.4).

The NZ-CES provides a regional template against which the Adelaide Tarn record may be compared. The Adelaide Tarn record dates back to ~14,000 cal years (see Chapter 3) and so includes four of the newly-defined climate events of the NZ-CES (NZce-4 to NZce-1) that span the late part of the LGIT through to the Holocene Interglacial. Events NZce-4 to -2 have been defined and have type records that have marked changes in pollen assemblages (Barrell et al., 2013; Lowe et al., 2013) (Fig. 2.4). The Holocene interglacial is undefined in this scheme but Lake Maratoto, near Hamilton in the Waikato region, has been suggested as a provisional stratotype for the Holocene (Barrell et al., 2013) partly because it has been studied in detail and because of its status as a global parastratotype (Green & Lowe, 1985; Walker et al., 2009).

NZce-4, from ca. 15.6 to 13.74 cal ka (ka = thousands of years ago), is defined at Kaipo bog where the peat shows a pollen assemblage dominated by lowland tall trees. This assemblage suggests mild climate conditions at this time (Newnham and Lowe, 2000; Hajdas et al., 2006). NZce-3, also defined at Kaipo bog, commenced at ca. 13.74 and ended ca. 12.55 cal ka and is characterised by cool climate conditions. The pollen record shows a higher ratio of grass species to tall trees than that for NZce-4. Prior to the Holocene there is a marked amelioration

and this is shown in the Kaipo bog pollen where tall trees progressively take over the assemblage again. The climate becomes progressively warmer allowing trees to occupy the environment again from ca. 12.55 through to ca. 11.88 cal ka (Newnham and Lowe, 2000; Hajdas et al., 2006; Lowe et al., 2013). The boundary timings do not convey the measurement or calibration errors of the ages on which they are based, although the underlying errors are reported in detail in Barrell et al. (2013), and Lowe et al. (2013) and are also likely to vary between sites.

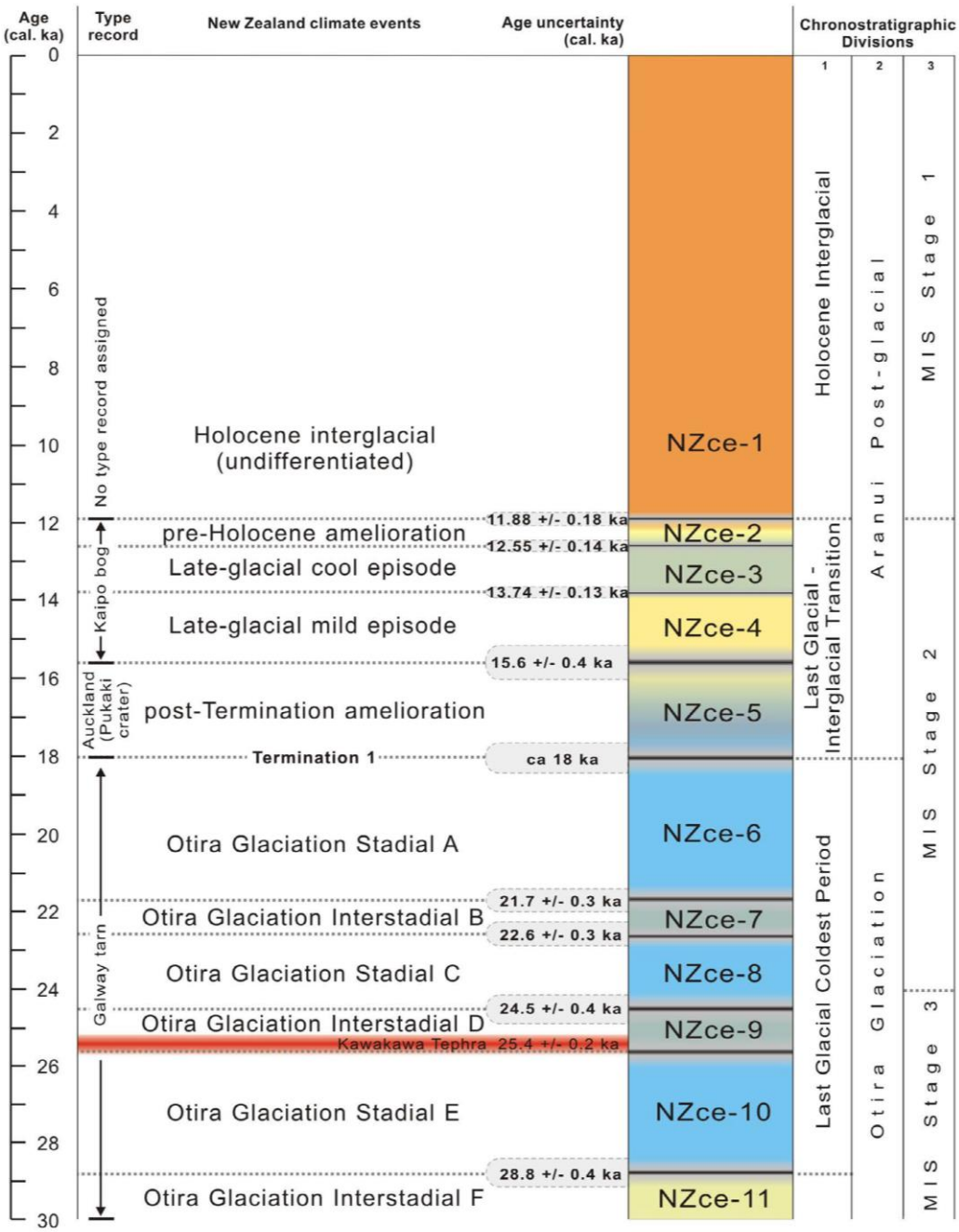

Figure 2.4 The New Zealand climate event stratigraphy from 30,000 to 8000 cal years BP (from Barrell et al., 2013).

2.2.2 Late Quaternary palaeoenvironmental reconstruction

Climatic archives in New Zealand cover an array of media, including peat, lacustrine sediments, marine sediments, speleothems, loess, volcanic deposits, tree rings, and glacial moraines (Newnham et al., 1999, 2012; Carter & Lian, 2000; Carter et al., 2008; Williams et al., 2010; Barrell et al., 2011; Neukom & Gergis, 2011; Bostock et al., 2013). Sites chosen for palaeoenvironmental reconstruction range over a variety of latitudes and altitudes across the landmass and offshore, ensuring the capture of local and regional climate change (Alloway et al., 2007). Of these records, only a few tree-ring records have annual resolution, whilst the remainder have chronologies with age uncertainties ranging from 10-100 years (Barrell et al., 2013).

2.2.2.1 Late-glacial cool episode and the Holocene Epoch

This section is a summary of the of key climate changes inferred from palaeoclimate records spanning the last ~14,000 years (Table 2.3). It is recognised that not all records will show the same timing of events because of the range of localities, altitudes and latitudes (Newnham et al., 2012; Barrell et al., 2013). Each record will show potential lead and lags of the key climate changes spanning this period and the records will also have different local climate imprints. In the table below (Table 2.4), the Holocene has been spilt into Early, Middle and Late based on the proposed tripartite subdivision by Walker et al. (2012). The 8.2 ka event (a cool episode identified in various records but thus far there is only one potential record in New Zealand) is the boundary for Early to Middle Holocene. The 4.2 ka event (a similar cool episode identified around the world, and in the EPICA core, but currently not yet found in any records in New Zealand) that is proposed for the boundary between Middle and Early Holocene. The records that will be used in the synthesis chapter (Chapter 6) to compare to the Adelaide Tarn record are shaded grey in Table 2.4.

Table 2.3 Selected records spanning the last 14,000 years and key climate changes inferred over this time (*ka, thousands of years ago).

Name of record	Location	Type of proxy	Interpretations	Age range (cal ka*))	Reference(s)
Late-glacial cool period					
Lake Pupuke	Auckland	A range of physical and chemical proxies	Low lake level, low biomass and heightened erosional influx	14.5–13.8	Stephens et al. (2012)
Holocene speleothem records	Various locations	Speleothem	A positive excursion of $\delta^{18}O$	13.4–11.2	Williams et al. (2010)
Kaipo Bog	Urewera mountains	Pollen	Marked change in vegetation, higher grass: podocarp ratio	13.8–12.6	Hajdas et al. (2006)
Mean annual temperatures (MAT)	Southern sites	Pollen	Cold tolerant taxa, low MAT	14–12	Wilmshurst et al. (2007)
Kettle Bog	Cass Basin, South Island	Pollen and plant macrofossils	Forest retreat	14.6–13.6	McGlone et al. (2004)
Early Holocene optimum					
Lake Pupuke	Auckland	A range of physical and chemical proxies	Higher biomass and a decrease in allochthonous sedimentation (decrease in grain size)	10.2–8.0	Stephens et al. (2012)
Holocene speleothem records	Various locations	Speleothem	Negative excursion of $\delta^{18}O$ values; this marks a phase of warming consistent with retreat of South Is. glaciers	10.8	Williams et al. (2004, 2010)
Lake Poukawa	Near Napier	Pollen	A shift from shrub and grassland to forest dominated	10.6–6.5	McGlone (2002)

Cameron Glacier	Southern Alps	Moraine deposits	Net loss of New Zealand Southern Alps glaciers showing warming temperatures	From 11 ka	Putnam et al. (2012)
Cropp Valley	Southern Alps	Pollen	Grass, shrub and other cold tolerant species. No trees seen in assemblage	12–10	McGlone & Basher (2012)
MAT	Southern sites	Pollen	Warming temperatures	12–9	Wilmshurst et al. (2007)
Kettle Bog	Cass Basin, South Island	Pollen and plant macrofossils	Podocarp expansion as climate ameliorated followed by mild moist then warm conditions	13.6–11 11–9.2 9.2–7.6	McGlone et al. (2004)
Mid Holocene					
Pupuke	Auckland	Number of proxies	Synchronous changes most all proxies	8.2–7.8	Augustinus et al. (2008)
Sponge swamp	Near Haast	Pollen	Pollen evidence indicates moist warm conditions and becoming slightly warmer. Warm taxa decline again	7.7–6.8 6.8–6.5 6.5–3	Li et al. (2008)
Cropp Valley	Southern Alps	Pollen			McGlone & Basher (2012)
MAT	Southern sites	Pollen	Warm conditions followed by cooler temperatures consistent with glacial readvance.	5.5 (glacial advance)	Wilmshurst et al. (2007)
Kettle Bog	Cass Basin, South Island	Pollen and plant macrofossils	Cooler more variable conditions	7.8–present	McGlone et al. (2004)
Late Holocene					
Lake Maratoto, MAT, Kettle Bog, and Cropp Valley	All records show slight climate deterioration in the late Holocene, the tree-line has descended and increased frostiness since ~1.8 ka				Green & Lowe (1985), McGlone et al. (2004), Wilmshurst et al. (2007), McGlone & Basher (2012)

2.2.2.2 Central New Zealand: southern North Island, northern South Island, and northern Westland

This section introduces Late Quaternary records from sites in the 'central New Zealand' area (Fig. 2.5). The northernmost site chosen is Lake Poukawa where McGlone (2002) constructed a pollen record. Avian fossils found spanning the late glacial through to the Early Holocene period suggest a shrub and grassland vegetation assemblage was predominant until ~10,000 cal yr BP and open forest became apparent until 6,500 years ago. A cooler phase took over from 6,500 years and this was seen in a vegetation change to closed podocarp-broadleaved type until removal by humans ~800 years ago. McGlone (2002) suggested a change from north-westerly to an easterly and southerly airflow from the mid-late Holocene caused the changes.

Five sites in the Ruhaine Ranges have been studied by Lees (1986) and pollen records were constructed for each (Fig. 2.5). Podocarp-broadleaved forest dominated the foothills at ~12,900 cal yr BP and a cooler drier climate than present was inferred from this assemblage pattern. At 10,350 cal yr BP, *Dacrydium cupressinum,* which prefers mild and moist climate, takes over the floral assemblage until ~5000 cal yr BP. A drought and frost-tender species, *Ascarina lucida*, occupied the vegetation pattern from 3400 to 1800 cal yr BP where it almost disappeared and is nearly absent in the present day vegetation in the area.

Carter & Lian (2000) constructed a phytolith sequence at Bidwill Hill from a loess deposit resting conformably on lacustrine sediments. The sequence spans the late glacial period through to the Holocene. Tree and shrub species steadily increase through the later LGIT with complete re-forestation in the Early Holocene (~11,000 cal yr BP). There is a slight decline in tree species at 10,000 cal yr BP and another decrease possibly attributed to heightened erosion around time of European settlement in the 19th Century.

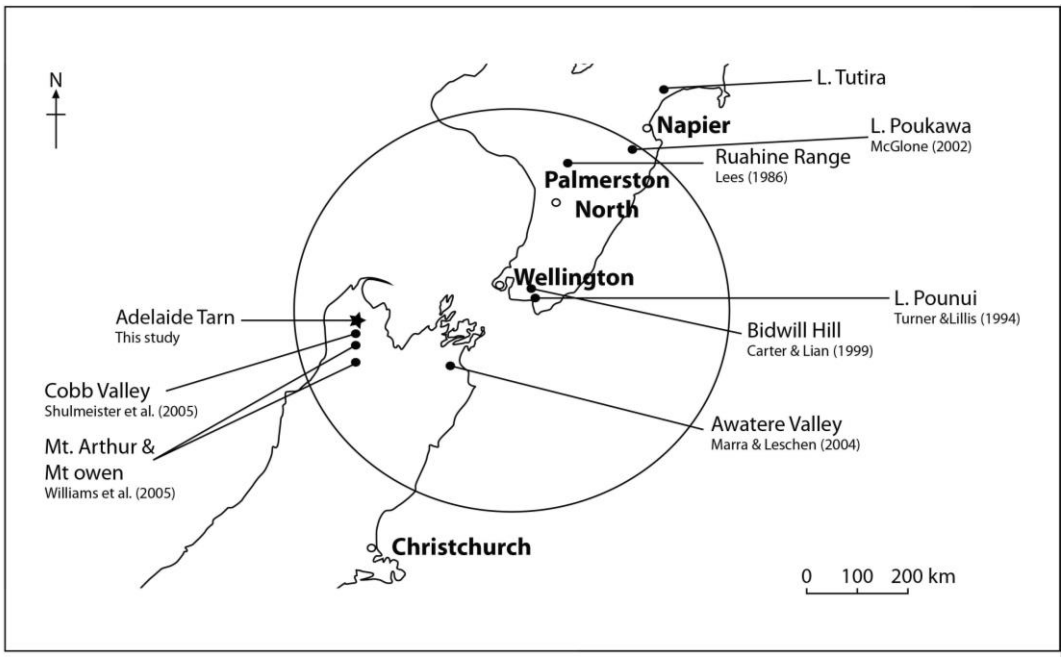

Figure 2.5 Map showing locations of records in central New Zealand and in proximity to Adelaide Tarn, spanning ~18,000 years to present.

Turner and Lillis (1994) focused on constructing past palaeomagnetism at Lake Pounui near Wellington. The record spanned 2500 years and showed two marked changes. Approximately 1500 years ago there was a change in declination to the west and gradual change to an eastward trend to present day. These marked changes can be used for dating methods in records throughout New Zealand and, because of the small size of the landmass, the signal will be essentially uniform.

Beetles and pollen were two proxies used at Awatere Valley in a study undertaken by Marra & Leschen (2004). In the Early Holocene the climate was warm and *Nothofagus* (possibly a relict patch) persisted at the site through to 8,500 cal yr BP where a diverse podocarp assemblage became more prominent indicating a change to colder conditions. During the podocarp expansion, beetles also increased and higher beetle species diversity is associated with these trees. Podocarps prevailed from the mid-Holocene through to anthropogenic deforestation ~500 years ago.

Barrell et al. (2011) compiled a review of Quaternary glaciation in New Zealand. They stated that the Tasman Mountains were glaciated during glacial periods but

only with minor ice volumes in comparison to the ice extent on the Southern Alps. Higher ranges show the distinct U-shaped valleys and south-east-facing cirque basins. There is little to no evidence of moraines and only inferred ice limits. The Cobb Valley glacial chronology indicates complete ice removal by ~14,000 cal years BP (Shulmeister et al., 2005).

Speleothem records from Mt Arthur and Mt Owen (Fig. 2.5) show distinct phases of positive and negative $\delta^{18}O$. From 14,700 to 13,530 (cal) yr ago the speleothem records show warm conditions with a positive phase of $\delta^{18}O$ and this becomes negative from 13,530 to 11,140 yr ago, suggesting a cooler climate. The cooling appears to overlap the ACR and the entire YD chronozone (Williams et al., 2005). Two more positive phases occurred between 11,140 and 6910–6470 yr ago and temperature drops from 6000 to 2000 yr ago.

The central New Zealand area is lacking in records from the Holocene and majority of reconstructions that have been done were 10 to 20 years ago and dating and age modelling have improved markedly since then. The Adelaide Tarn record can add to or support previous work undertaken in this area.

2.2.3 Major climate circulations influencing New Zealand's environments

Southern Annular Mode (SAM)

The SAM is an atmospheric circulation based on changes in pressure gradients in the Southern Hemisphere acting on the high latitudes of Antarctica and the Southern Ocean (50–70°) and the middle latitudes, including New Zealand (Renwick & Thompson, 2006; Gomez et al., 2011). SAM acts in two phases over the Southern Ocean: in the positive phase high pressures are located at mid-latitudes over the South Island of New Zealand (Fig. 2.6) and opposite in the negative phase (Renwick & Thompson, 2006). The phases of SAM influence the position and strength of the south-westerly winds: in the negative phase winds become stronger over New Zealand increasing storms and generating cooler temperatures and more-than-average precipitation.

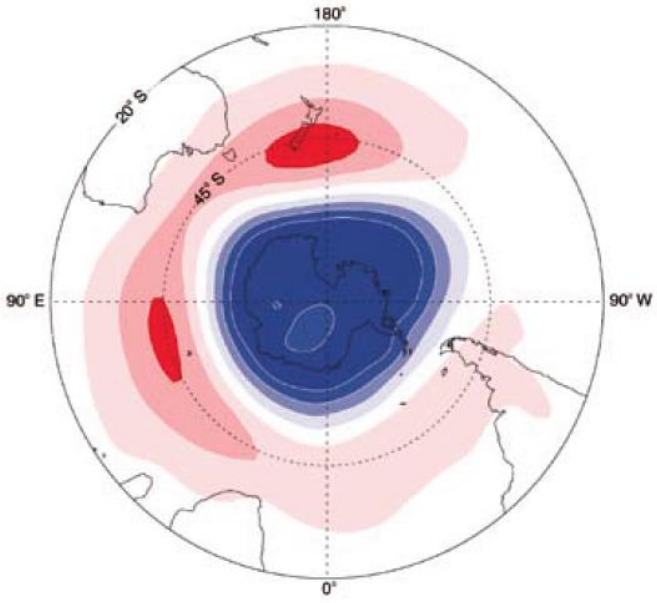

Figure 2.6 Positive phase of SAM, high pressure to low-pressure gradient towards Antarctica. The pattern is reversed in the negative phase of SAM. Red is showing high pressure and blue is low pressure over Antarctica (from Renwick & Thompson, 2006).

In the positive phase of SAM, the westerly winds move towards Antarctica enhancing north-easterlies over the North Island and thus introducing more rain

over the eastern North Island (Gomez et al., 2011). Research has been undertaken to reconstruct the movement of the westerly winds in the Southern Ocean and the correlation between changes in CO_2 in the atmosphere (Moreno et al., 2010). The strength of the south-westerly winds influences the upwelling of nutrient-rich cool deep waters to the surface near Antarctica, releasing CO_2 into the atmosphere (Moreno et al., 2010). Research into the westerly winds over Patagonia (at similar latitudes to those in New Zealand) during the Holocene by Moreno et al. (2010) found a strong influence of westerly winds from ~14 to 10.5 cal ka and another increase from 7.8 cal ka to the present. The decrease in westerly influence from 10.5 to 7.8 cal ka may be due to reduced radiation temperature gradients during this time. The release of CO_2 has a direct impact on temperature and may explain glacial advances during 8.5 and 6.5 cal ka in Patagonia and New Zealand, respectively (Moreno et al., 2010). The SAM and ENSO cycles also interrelate over New Zealand causing higher or lower storm frequencies.

El Nino Southern Oscillation (ENSO)

ENSO cycles are major changes in atmospheric pressure gradients and ocean circulation in the Pacific Ocean. The El Nino phase forces winds from the south, generating colder and wetter climates over the archipelago during winter, and droughts in eastern North Island during summer. The La Nina phase forces the winds from the north-east, generating higher-than-normal precipitation on the north-east of the North Island, less rainfall in the south, and warmer temperatures from the north-eastern subtropical waters. This pattern is similar to the weather associated with the positive phase of SAM.

A study was undertaken by Moy et al. (2002) in Ecuador aimed to reconstruct ENSO cyclicity over the Holocene. They found that in cycles of 2,000 years the ENSO cycle strengthened and weaken over this time, and from ~7000 to 1200 cal yr BP, ENSO events increased in magnitude (Fig. 2.7).The interpretations of the ENSO cycles were based on light-coloured bands in the lake sediment core, which were interpreted as alluvial inputs arising from increased catchment erosion during storms (Moy et al., 2002). ENSO cycles have also been reconstructed in a New Zealand setting at Lake Tutira by Gomez et al. (2011). Lake Tutira is located

in Hawke's Bay, which is on the eastern side of the North Island; storms are driven by the La Nina phase of the ENSO cycles. From the Mid to Late Holocene, the average number of storms per 100 years has increased from 4 to 16 between ~5000 and 2000 cal. yr BP. The frequency of storms in this region roughly coincides with the increased ENSO cycles per 100 years by Moy et al. (2002).

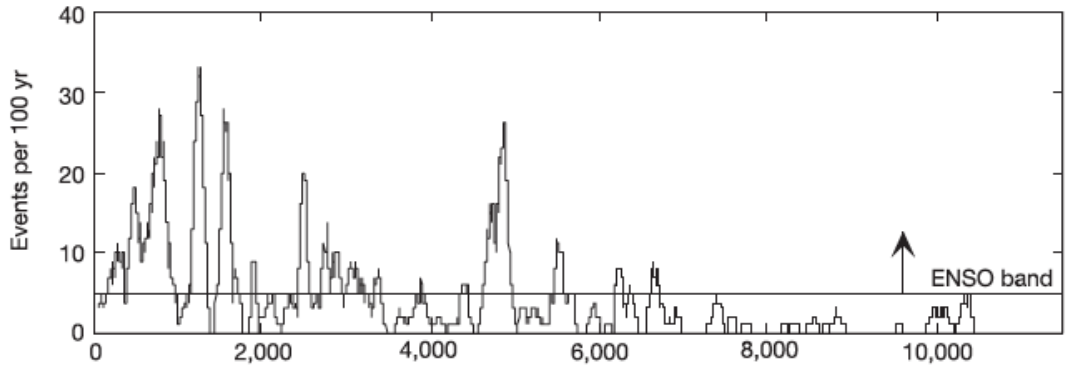

Figure 2.7 ENSO cyclicity and events per year, spanning ~12,000 cal. years (from Moy et al., 2002).

Chapter 3. Stratigraphy and chronology

3.0 Introduction

This chapter describes the coring technique used in the acquisition of the core. The sediment stratigraphy is described and characterised. The age model is presented along with sedimentation rates between known ages. Lastly, past lake history is inferred from stratigraphy and sedimentation in relation to chronology.

3.1 Coring

3.1.1 Coring method

A team led by Dr Marcus Vandergoes, from GNS Science, took sediment cores from Adelaide Tarn in the summer of 2011 using a Livingstone piston corer, as described below. Minor compression and loss of material can occur during insertion of the core barrel into the sediment, or when extruding the core. Hence it is beneficial to take more than one continuous core in a similar location. Two consecutive cores were thus taken from Adelaide Tarn at 172 ° 32.636 E, 40° 56.513 S, and are named as 1115 and 1116 throughout this section. An additional 1 m-long core, AD3, was taken which overlaps the top two thrusts of 1115 and 1116. The coring method captures 1 m of sediment at a time (as a 1-m-long thrust); six 1 m-thrusts (T1-T6) were obtained for each of the cores 1115 and 1116.

Livingstone piston corer

Piston cores were developed for the use of limnological research in the 1950s (Glew et al., 2001). There are three main parts to the coring system: (1) a piston attached to a cable, (2) the core tube and, (3) the driver head and associated rods. The piston is located within the core tube with minimal space in between but

enough for the piston to move freely when necessary (Fig. 3.0A). When the system is lowered to the required coring depth the piston is situated at the bottom of the core barrel and is held in place by the driving rods. Driving rods are added until the desired depth is reached, and tension is kept on the piston cable whilst lowering. When the depth is reached for acquisition of the core then the piston is set into place, in this case using vise grips (important to maintain tension on the cable) (Fig. 3.0B).

The drive rod is lifted and turned anti-clockwise to lock the core into place and a rubber catcher (already in place at the bottom of the coring system) captures the sediment inside the core tube. The piston is now located at the top of the core barrel next to the drive head (Fig. 3.0C). The driving rods are removed as the corer is brought to the surface and the core barrel is placed onto a flat surface in preparation for extruding the core (Glew et al., 2001; Mybro & Wright, 2008). Once the coring system is at the surface a pre-prepared PVC (half) tube is ready for collecting the extruded core. The drive head is unlocked and a winch set up is used to drive the core out of the barrel which is then carefully caught in the PVC pipe. The core is wrapped in tight plastic immediately, labelled top and bottom with the correct core and thrust number (e.g. 1115 T1). The symmetrical PVC half pipe is placed on top, taped together and labelled again.

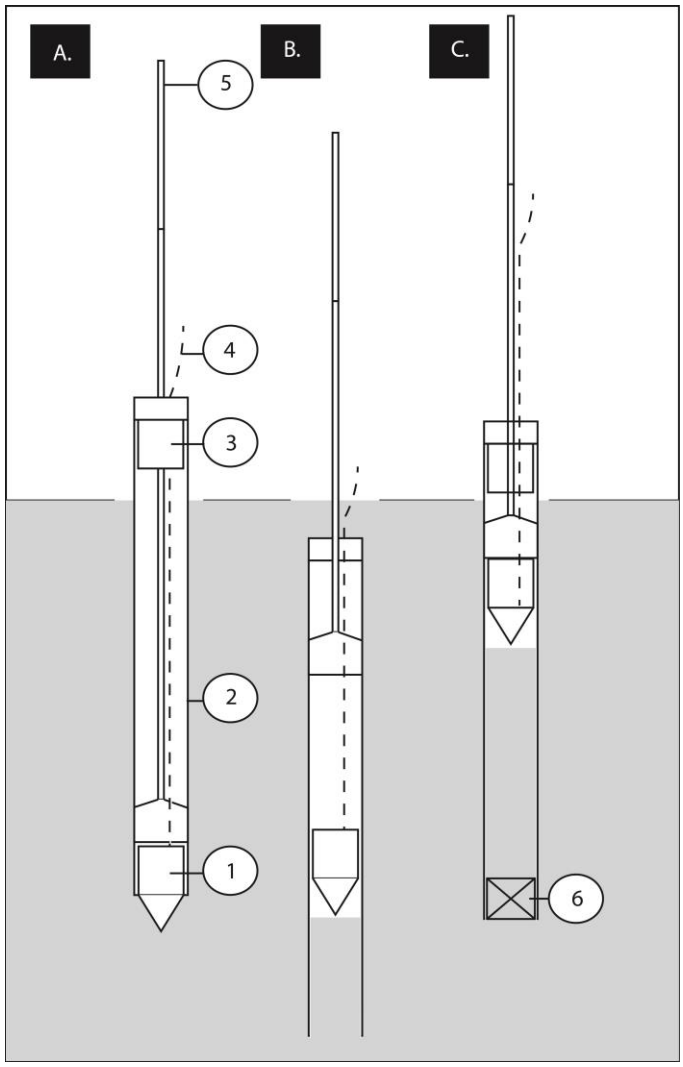

Figure 3.0 Illustration showing basic operation of Livingstone piston corer. (A) Coring system lowering into sediment, (B) capturing sample as piston moves up the core barrel and (C) full capture of 1 m core thrust. (1) Piston, (2) core barrel, (3) driver head, (4) piston cable, (5) driving rods and, (6) core catcher. Adapted from Glew et al. (2001).

3.1.2 Core processing and description

In order for the different thrusts of the cores to be correlated, preparation and cleaning were undertaken. Firstly, cores from each of the six thrusts relating to cores 1115 and 1116 were split using a piece of wire passed through one half of the PVC pipe. The wire was pulled along the length of the tube with great care

taken to ensure that there was minimal distortion of the sediment. One half of each thrust was re-wrapped in tight plastic and labelled as an archive half. Once splitting was completed, colour and lithological changes became more visible and these were noted down. When deciding on which thrusts were more useful for sampling, any contamination, loss and distortion were taken into consideration (Fig. 3.1).

The cores were cleaned with a sterile scalpel to remove possible contamination from splitting and this cleaning also helped to reveal the thickness and nature of the lithology and colour changes. The scraping allowed more adequate visual ties between the cores to construct an undisturbed total core length. A tape measure was placed down the length of each thrust and details such as length of the thrust, colour changes, positions and colour of laminae, and texture (grain size), were recorded. Thrusts that were used for sampling were prepared for photographing and pictures were taken in 30 cm intervals in order to capture an ideal resolution. Once the core processing and description were complete, thrusts from both cores 1115 and 1116 were placed on a flat surface to observe correlations between the adjacent cores. Distinct laminae patterns between cores made correlating the 1 m thrusts reasonably straightforward (Fig. 3.1).

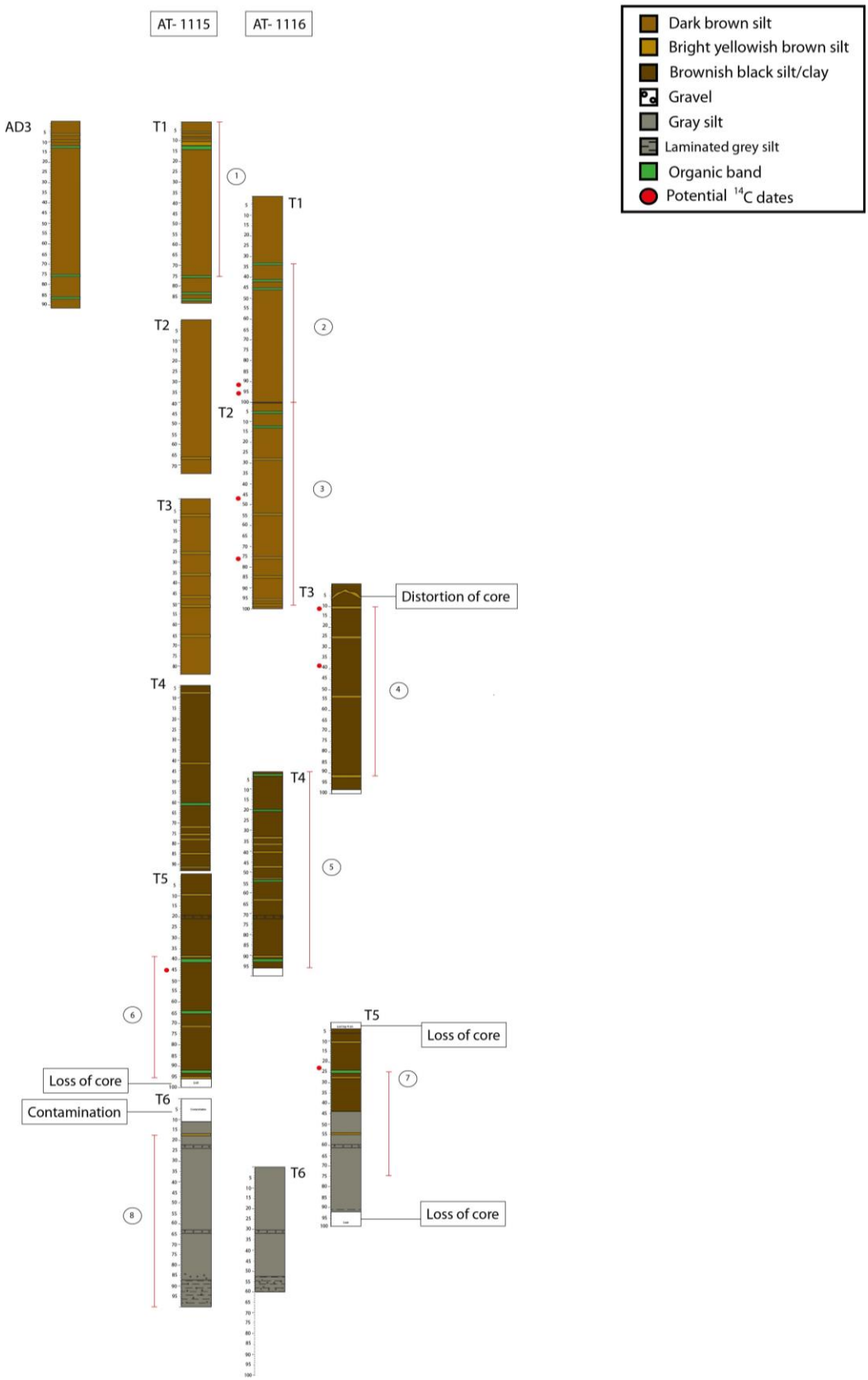

Figure 3.1 Illustration showing cores 1115 and 1116 with additional AD3 core overlapping thrust-1 of both cores. Cores were correlated with distinctive lithological patterns. The red lines show cores or segments chosen for sampling.

3.1.3 Sampling procedure

The PVC pipe was used to mark 1-cm intervals along the length of the core with the top end being at 0 cm. A 0.5 cm spatula was used to take a smear of sediment every centimetre down the core (working from top to bottom of the core) and this smear sample was later used for particle size analysis. In between taking each smear sample, the spatula was cleaned with distilled water to remove any contamination.

Each thrust was then cut into 1-cm-thick samples. Each sample was later used for plant macrofossil identification, pollen, and carbon and isotope analyses. A sanitized knife was used to cut the core and each 1-cm slice was placed onto a piece of tinfoil and trimmed on the outside to remove possible contamination. In between slicing, the knife was washed with distilled water. Each slice was placed into a pre-labelled bag and chilled ready for analysis.

The true depth of the core was calculated to a maximum length of 5.6 m and these depths weres placed alongside the sample numbers to help with interpretations. Every 5 cm point down the core was subsampled for plant macrofossil analysis, carbon content, and isotopes, and 1 cm^3 extracted for pollen analysis. Archived samples are kept at GNS Science, Wellington.

3.1.4 Sediment stratigraphy and characterisation

The 5.6-m long sediment core is predominantly made up of clay (< 3.9 μm fraction) and fine silt (3.9−6.3 μm fraction). Silts are defined as 3.9 to 62.5 μm in diameter, sand 62.5 μm to 2 mm, and gravel 2 to 64 mm (comprising granules and pebbles) (following Folk, 1968). The core can be divided into three distinct sediment ‘packages’ and these are characterised by differences in colour and by slight changes in grain size. The bottom of the core is a pale grey colour (0.8 m thick) transitioning into dark brown sediment (2.5 m thick) and then into brown at the top of the core (2.3 m thick). The three packages are henceforth referred to as lithozones 1−3 (from bottom to top of core), and are characterised further below. The core does not have evenly spaced laminae but pale yellow/brown layers, each

1−2 cm-thick, were deposited mainly in lithozones 2 and 3 at variable spacing. The layers are distinct and distinguishable from the surrounding sediment as they are a paler shade of brown with a yellowish/orange tinge. The grain size of the light yellow/brown layers is primarily fine silt (3.9−6.3 μm).

Lithozone 1 (5.6 m−4.8 m): This zone is located at the basal part of the core and consists of inorganic grey silts (Munsell colour 5Y 6/1). The base of the core is thinly laminated (1−2 mm thick) at 1 cm intervals until approximately 5.5 m and the rest of this zone is not laminated (5.5−4.8 m). There is only one yellowish brown (10YR 6/8) lamination in this section, 1 cm in thickness, located at ~ 4.8 m depth (characterised further in Table 3.0). Three gravel-dominated layers appear here ranging between 1−2.5 cm in thickness. The three gravel layers are located at the base of the core, at ~ 4.9 m and at 5.4 m and are bounded by and clay/silt (Fig. 3.2). The sediments in this zone are dominated by angular inorganic particles and no organics were found in scanning electron microscopy (SEM) (Fig. 3.3).

Lithozone 2 (4.8 m–2.3 m): Lithozone 1 transitions into organic brownish black silt/clay (10YR 2/3) between 5.0 m–4.8 m. The bright yellowish/brown (10YR 6/8) laminae are quite marked in this section with a very condensed segment between 3.5 and 3.8 m. The majority of the laminae in this section are 1 cm in thickness. A gravel layer occurs at 3.9 m depth with a thickness of 2 cm. The gravel is set in a matrix of silt/clay and a single granule is approximately 2 mm in diameter. Plant macrofossils such as leaves, stems, root and seeds start to appear at approximately 3 m depth, dispersed throughout and becoming more conspicuous up the core (Fig. 3.2). The plant macrofossils range from 2−15 mm in size and consist of fragments of plants and whole leaves. SEM images of the sediments in lithozone 2 show mainly angular inorganic particles with many diatoms (Fig. 3.3).

Lithozone 3 (2.38 to 0 m): The uppermost part of the core consists of dark brown organic silt (10YR 3/4) with interspersed laminae. There are three bright yellowish brown (10 YR 6/8) laminae in the top 20 cm and they range from 1−2 cm in thickness. Organic materials are evident in the deposits throughout this section in sporadic concentrations, and comprise tangled liverworts or mosses

(characterised in Table 3.0). Plant macrofossils disappear entirely from the sediments at a depth of around 1 m (Fig. 3.2). Lithozone 3 has abundant diatoms and some angular inorganic particles (Fig. 3.3). The species of diatoms that were identified from lithozone 3 are *Aulacosiera spp*., *Frustulia spp*., and *Stauroneis spp.* (Fig. 3.4).

Table 3.0 Summary of the main characteristics of lithozones and of distinct laminae

Lithozone	Depth (m)	Age (cal yr BP)	Sediment description	SEM characterisation	Munsell colour	$\delta^{13}C$ (‰) range	C %
1	5.6–4.8	>13,932*	Inorganic grey silts	Angular particles, inorganic	5Y 6/1	-21.86 to -25.85	0.3–8.8
2	4.8–2.3	13,932–7709	Organic brownish black silt/clay with plant macrofossils	Angular particles, organic and some diatoms	10YR 2/3	-26.21 to -27.56	3.6–15.0
3	2.3–0	7709–926 (or younger (pre~700 cal yr BP)	Dark brown organic silt	Diatom rich with angular inorganic particles	10YR 3/4	-26.67 to -28.21	5.0–10.1
Yellowish/ brown laminae	Various depths	Various ages	Yellowish brown silt/clay	Dominated by angular inorganic particles and few fragmented diatoms	10YR 6/8	-27.40	5.2
Organic layers	Various depths	Various ages	Tangled plant remains (mosses and liverworts) in silt/clay	-	10YR 3/4	-27.56	7.3–8.1

* NB: Any numerical ages below 4.8 m (i.e., older than 13,932 cal yr BP) are approximate only because these ages were estimated by extrapolating beyond our deepest radiocarbon age.

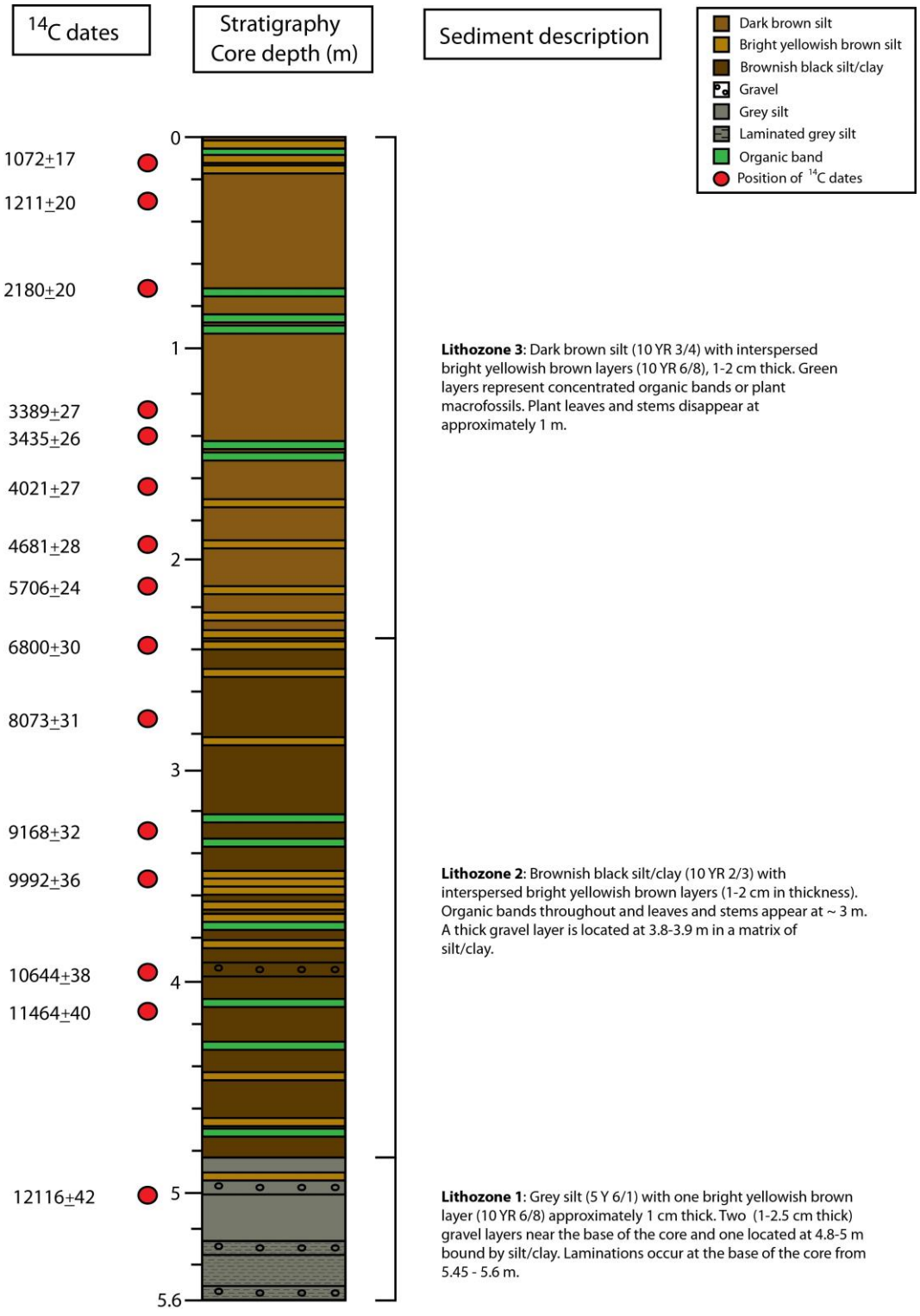

Figure 3.2 Stratigraphy of the core, descriptions of each of the three lithozones, and location of sampling positions for radiocarbon dates (ages recorded in ^{14}C yr BP ± 1 sd).

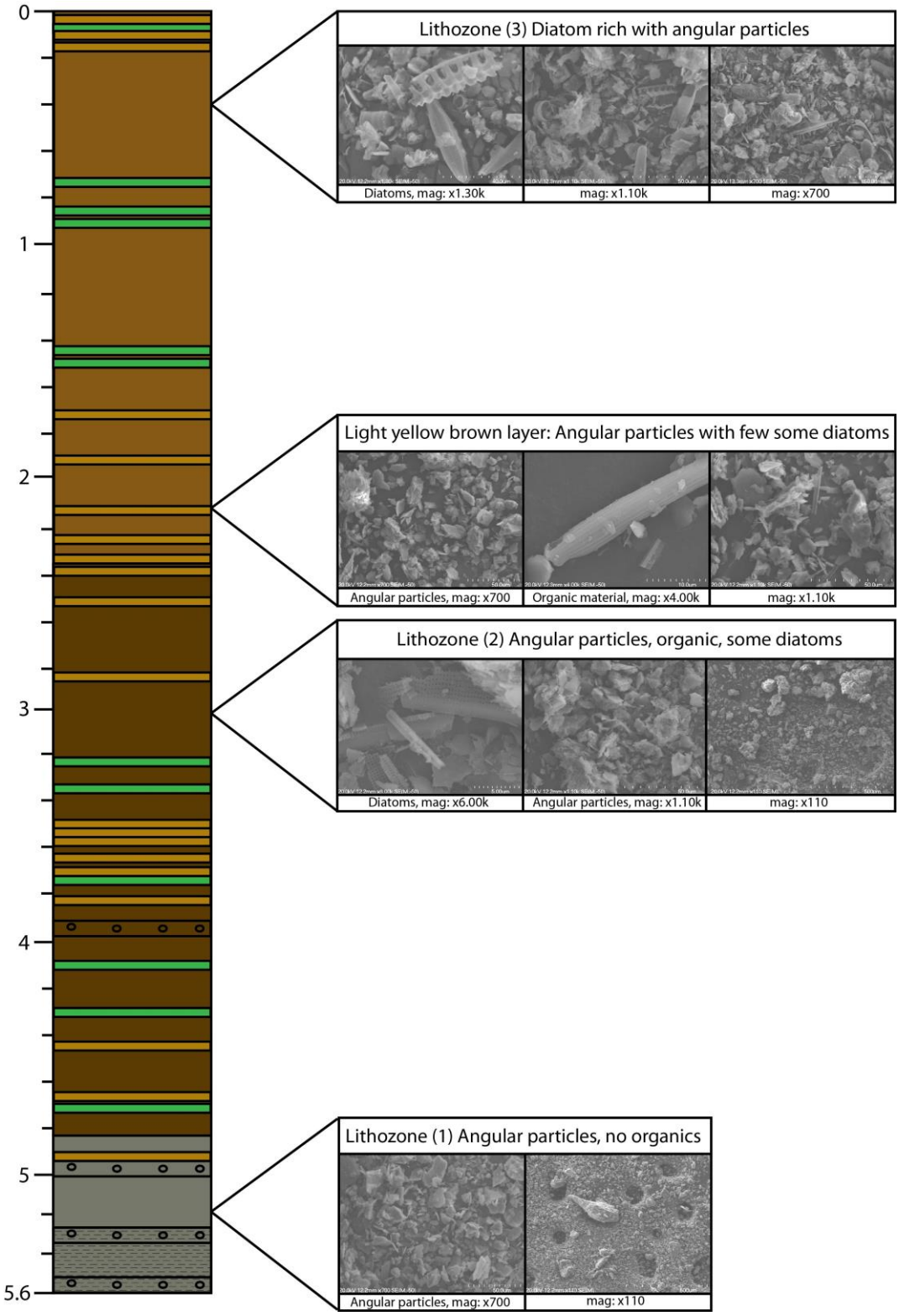

Figure 3.3 Scanning electron microscope (SEM) micrographs to further characterise the three lithozones and the laminae present in the core. Lithozone (1) SEMs are from the sample at 525 cm depth, (2) 300 cm depth, (3), 40 cm depth, and the light yellow/brown layer was sampled at 215 cm depth.

3.1.5 Diatom species identified

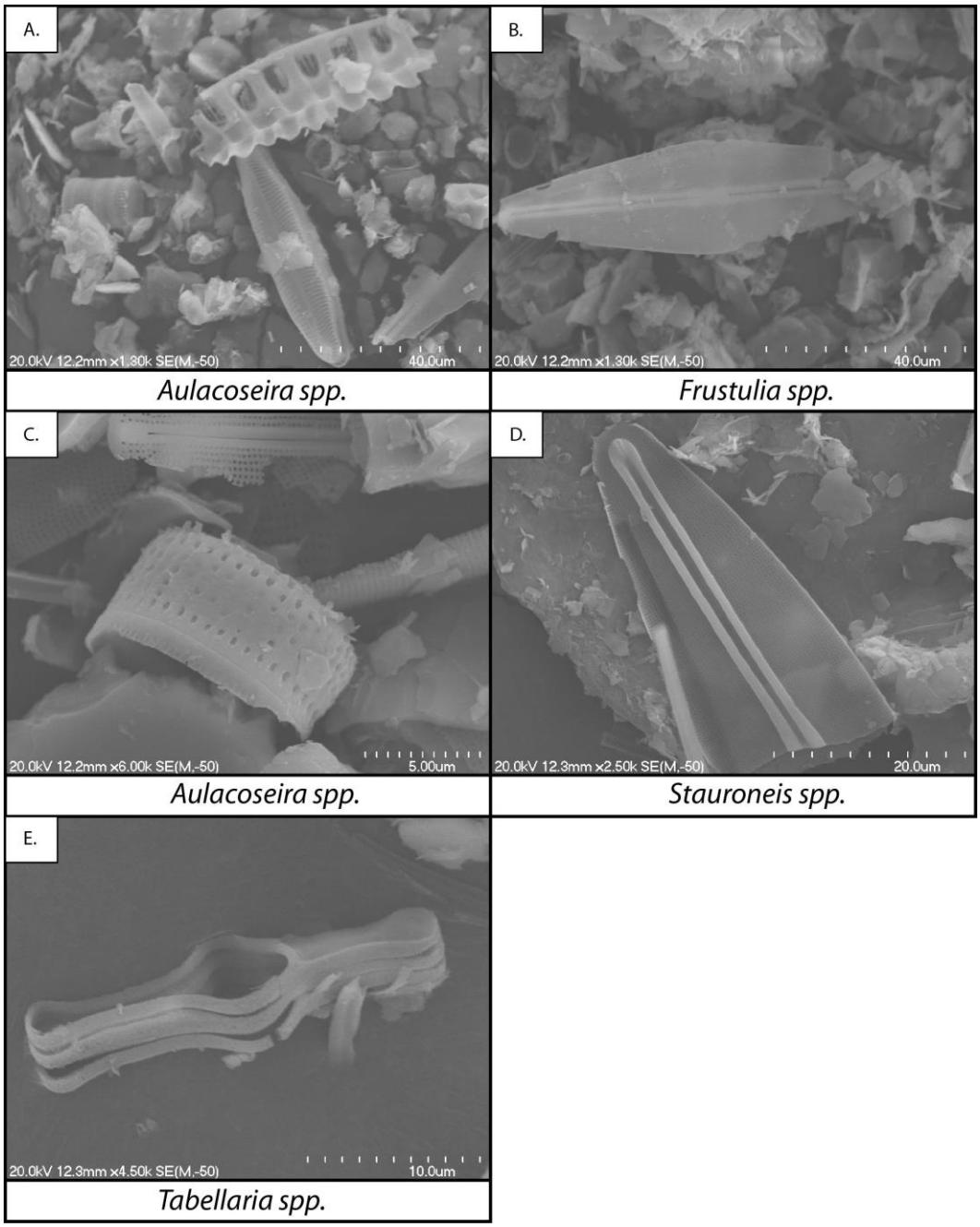

Figure 3.4 The diatom species identified from the representative samples. A—D are from lithozone 3 (40 cm depth) and E is from the light yellow brown layer (215 cm depth), the only non-fragmented diatom found.

3.2 Chronology

3.2.2 Sampling

In the sample preparation stage and whilst the core was being cleaned of potential contamination, plant macrofossils such as leaves, seeds and twigs were removed as potentially datable material. The datable material was placed into clean and sealed zip-lock bags to minimize contamination. Choosing potential items for dating was based on their stratigraphic position and their relation to the obvious changes in sediment lithology (Fig. 3.2). Potential material was selected from segments of cores not used in other sampling but are correlated to the same position in the cores selected for the other analyses. The selected ^{14}C material was sent to Rafter Radiocarbon Laboratory (Institute of Geological and Nuclear Sciences, lab code R40018) for AMS dating.

Sample treatment – Rafter Radiocarbon Laboratory

A range of initial sample weights of organic material (23–9000 mg) were given to the lab and these were subsampled under a microscope. Excess debris and clay were removed in the subsampling process with tweezers and then pre-treated with acid–alkali-acid. Samples were weighed again once the unwanted material was removed. Samples were then combusted to produce carbon in a sealed tube. Lastly, the samples were converted to graphite by reduction with hydrogen over an iron catalyst.

3.2.3 Radiocarbon dating

Fourteen plant macrofossil samples and one organic silt sample were dated (Table 3.1). The ^{14}C age ranges received from the Rafter Lab were between 1072 ± 17 and 12116 ± 42 years ^{14}C BP (± 1 sd). These conventional ^{14}C ages were then calibrated using INTCal04 with the calibrated ages ranging from 942 cal yr BP to 13,959 cal yr BP (Table. 3.1; errors are given in this table). All calibrated ages are in a consecutive order through the core (i.e., no age reversals). The youngest age (942 cal yr BP) is located at 13 cm depth, near the top of the core, and the oldest

at 500 cm depth. The 15 calibrated ages were then used to construct an age model to extrapolate between the fixed and known ages.

Table 3.1 Radiocarbon samples, associated depth, ^{14}C ages and calibrated ages. Ages courtesy of Dr Marcus Vandergoes.

* N. menz= *Nothofagus menziesii,* L. bid= *Libocedrus bidwillii.*

	Lab number	Core	Sample number	Plant material	True depth	^{14}C date ±1 σ	Calibration curve	oldest 2σ intercept	youngest 2σ intercept	Median probability
Unit			(cm)		(cm)	(years)		(cal yr BP)	(cal yr BP)	(cal yr BP)
1	NZA 51077	1115 T1	13	Seeds	13	1072±17	SHCal04	959	923	942
2		1115 T1	37-38	N. menz* leaf	37	1211±20	SHCal04	1170	982	1063
3		1115 T1	75-76	Horizontal stems	75	2180±20	SHCal04	2294	2002	2100
4	NZA 50821	1116 T1	91-92	N.menz leaf	133	3389 ± 27	SHCal04	3677	3469	3566
5	NZA 50822	1116 T1	95-96	N.menz leaf	137	3435 ± 26	SHCal04	3698	3484	3622
6	NZA 50823	1116 T2	21-22	N.menz leaf	161	4021 ± 27	SHCal04	4521	4295	4435
7	NZA 50824	1116 T2	48-49	L.bid* Leaf	188	4681 ± 28	SHCal04	5445	5307	5405
8	NZA 50905	1116 T2	75-76	N.menz leaf	215	5706 ± 24	SHCal04	6495	6318	6432
9	NZA 50825	1116 T3	11-12	Twig	239	6800 ± 30	SHCal04	7668	7520	7606
10	NZA 51059	1116 T3	39-40	Moss	267	8073 ± 31	SHCal04	9012	8725	8888
11	NZA 51060	1116 T4	6-7	Moss	324	9168 ± 32	SHCal04	10389	10200	10255
12	NZA 50826	1116 T4	33-34	Twig	351	9992 ± 36	SHCal04	11600	11237	11338
13	NZA 50829	1116 T4	71-72	Rootlet	389	10644 ± 38	IntCal09	12620	12541	12595
14	NZA 50827	1115 T5	46-47	Moss	417	11464 ± 40	IntCal09	13376	13220	13327
15	NZA 50828	1116 T5	24-25	Organic silt	500	12116 ± 42	IntCal09	14026	13814	13959

3.2.4 Age model

The 15 calibrated ages were used to construct an age model for the core. The median probability ages (cal yr BP) were plotted against depth of core (0–561 cm) in a statistical program called "R". A spline cubic function was applied to the plot in order to extrapolate between the known ages and create the age model (Fig. 3.5).

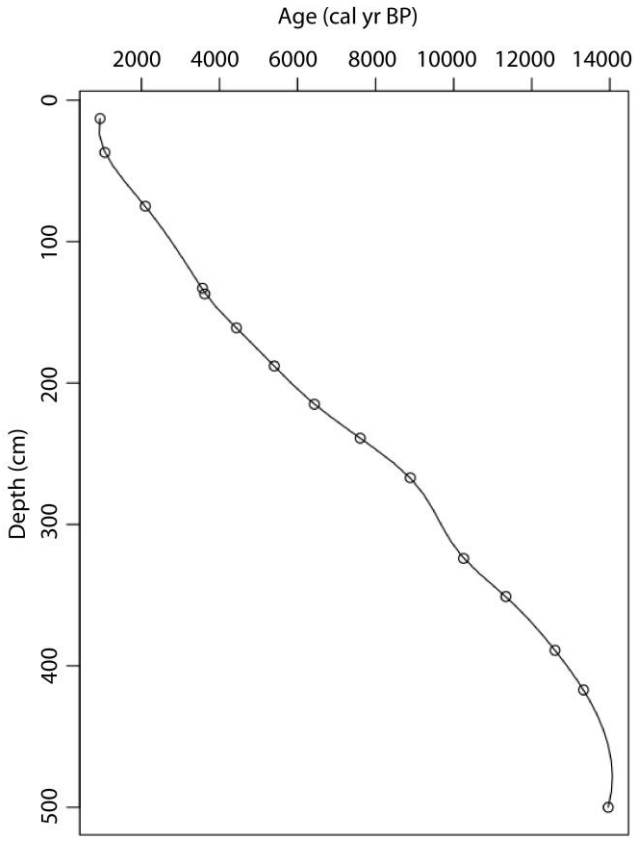

Figure 3.5 Spline cubic function age model used to extrapolate between dates.

The Adelaide tarn record thus spans about 14,000 cal years. The youngest age derived from the ^{14}C dates and the associated age modelling and calibration is ~930 calendar (cal) years BP at 13 cm depth in the core. Because of the amount of water in the sediment at the lake-bed and water interface there was most likely loss of sediment towards the top of the core. On the basis of extrapolation

between the ^{14}C dates, the top of the core is aged ~900 cal yr BP. That estimation is consistent with the results of pollen analysis undertaken by Mr Ignacio Jara (Victoria University of Wellington), which suggest the top of the core predates the earliest discernible anthropogenic impact in the region, assumed to be ~700 cal yr BP (R.M. Newnham pers. comm.., March 2013) (No European adventives are present in the sediments, meaning the core top definitely pre-dates ~1840 AD.)

3.3 Rates of sedimentation

The ^{14}C ages and their associated depths have been used to calculate sedimentation rates between known ages. A mean sedimentation rate can be calculated (in millimetres per year) between zones 1 to 15 as indicated in Table 3.2. An example of how the rates are calculated is that for zones 3 and 4 (grey shading):

Difference between known ages (cal yr BP): 3566 - 2100 = 1466 cal yr BP

Difference between depths of known ages (mm): 133 - 75 cm x 10 = 580 mm

Sedimentation rate between known ages: 580 mm/1466 cal yr BP =

0.40 mm/yr

Table 3.2 Calculated sedimentation rates between points of known age.

Zone	Age (cal yr BP)	Differences between ages	Depth (cm)	Differences between depths (mm)	Sedimentation rate (mm/yr)
			0		
1	942	942	13	130	
2	1063	121	37	240	1.98
3	2100	1037	75	380	0.37
4	3566	1466	133	580	0.40
5	3622	56	137	40	0.71
6	4435	813	161	240	0.30
7	5405	970	188	270	0.28
8	6432	1027	215	270	0.26
9	7606	1174	239	240	0.20
10	8888	1282	267	280	0.22
11	10255	1367	324	570	0.42
12	11338	1083	351	270	0.25
13	12595	1257	389	380	0.30
14	13327	732	417	280	0.38
15	13959	632	500	830	1.31

The sedimentation rates at Adelaide Tarn range between 0.20 mm/yr and 1.98 mm/yr with the maximum located near the top of the core (from 0 to 37 cm depth). The second highest sedimentation rate (1.31 mm/yr) is at the base of the core or between the oldest two known ages.

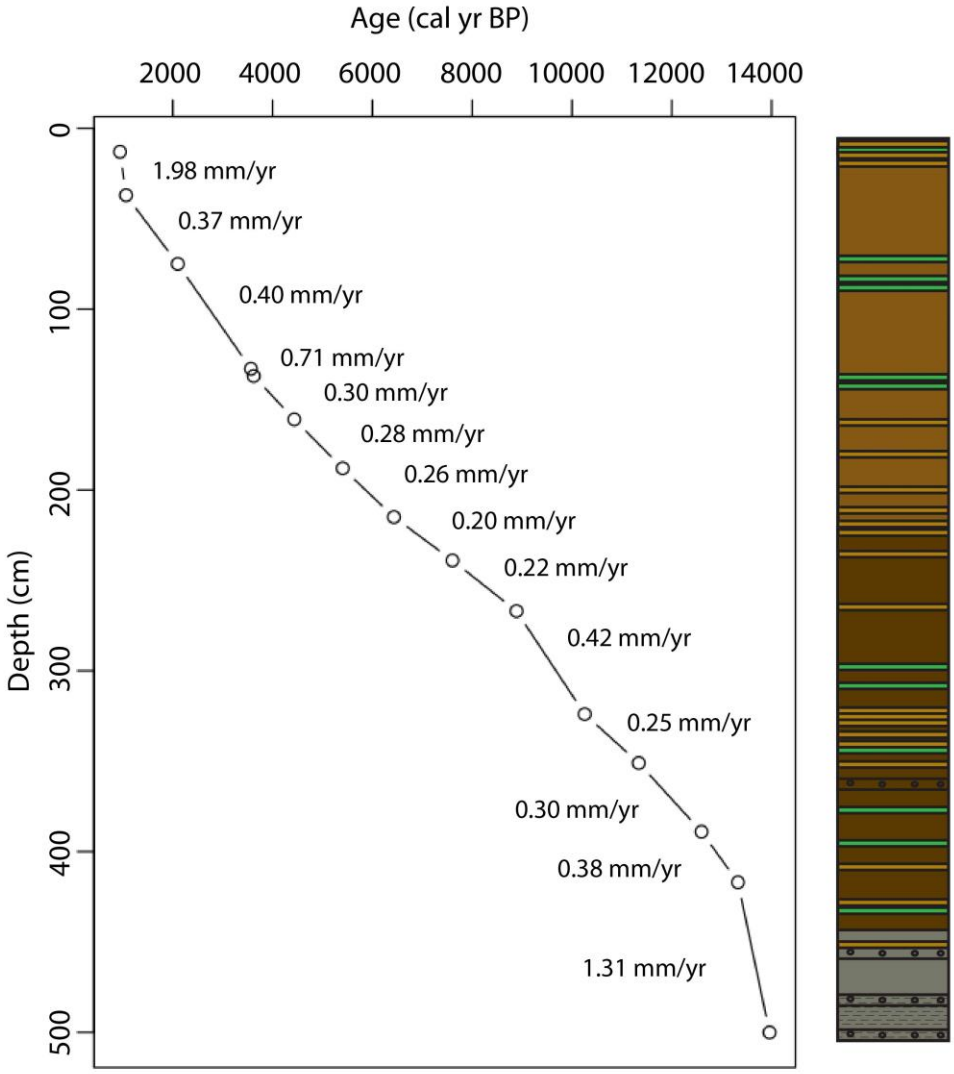

Figure 3.6 Calibrated ages, and mean sedimentation rates between dated points, in mm/yr. Stratigraphy is shown alongside.

From the base of the core, ~14,000 cal yr BP to 13,327 cal yr BP, the mean sedimentation rate (MSR) is initially quite high (1.31 mm/yr) and this is approximately coincident with the grey silts of lithozone 1. The MSR between 13,327 and 10,255 cal yr BP is relatively low, ranging from 0.25 to 0.38 mm/yr.

Between 10,255 and 8888 cal yr BP, the MSR slightly increases to 0.42 mm/yr, and from 8888 to 3622 cal yr BP, the MSR drops to 0.25 to 0.38 mm/yr. From 11,338 years to 3622 cal yr BP, the overall sedimentation is low over this time period in comparison to that for the basal sediments of the core. This low sedimentation rate roughly coincides with the majority of the laminae in the core. Condensed patches of laminae occur in other parts of the core (Fig. 3.6). From 3622 to 3566 cal yr BP, the MSR shows an increase to 0.71 mm/yr. Between 3566 and 1063 cal yr BP, the MSR decreases to 0.37−0.40 mm/yr. From 1063 years to 942 cal yr BP, the MSR increases to the fastest rate of 1.98 mm/yr. The age at the very top of the core is uncertain as noted above, and is likely to be before ~700 cal yr BP.

3.4 Origin and development of the lake on the basis of changes in lithozones and the age model

Lithozone 1: 5.6–4.8 m (~14,000 cal yr BP)

The sediments at the base of the core at 5.6 m depth consist of laminated inorganic grey silts (characterised by very low to low organic carbon contents of 0.3 to 4% at 5.6 m depth; see Chapter 5) and then transition into massive inorganic grey silts at ~5.45 m. Three thin gravel layers occur in this section, one at the base of the core and two more above that (as shown in Fig. 3.2). The MSR in lithozone 1 is 1.31 mm/yr, the second fastest rate in the entire core. There is only one ^{14}C date in this lithozone (at the base) and so the sedimentation rate is not securely constrained.

The high sedimentation rate and distinct lithology of this lithozone could relate to the conditions in the catchment soon after the formation of the lake around or just before ~14,000 cal yr BP. These greyish silts with gravel layers are typical for lakes formed under glacial conditions when there is limited vegetation in the catchment (Cohen, 2003). SEM photos from lithozone 1 sediments only contained angular particles and little or no organic matter. A cool period with a local active glacier (prior to ~14, 000 cal yr BP) probably led to the formation of a cirque glacier in the surrounding catchment. Temperatures then warmed causing the glacier to retreat and muds and gravels were deposited during this postulated retreat phase into the pre-carved antecedent cirque basin. Higher hydraulic transport is required to transport gravel-sized sediment and glacial melt water may have been the mechanism attributed to depositing this sediment into Adelaide tarn, with fluxes of material derived from erosion of the surrounding catchment. During a postulated cool period after ~14,000 cal yr BP (Chapter 6), the catchment was unstable with minimal vegetation around the basin, exposing slopes to more frequent erosion and subsequent deposition of this eroded sediment into the lake. The condensed layer of laminations at the base (5.6–5.45 m) alternating between white and grey sediment could be due to seasonal variations with ice melt in the summer and winter temperatures keeping the possible

remnants of the local glacier stable. These geomorphic and sedimentological features are similar to those at lakes nearby, which have also been ascribed a glacial origin, as follows. The record from Lake Doubtful, near Adelaide Tarn (Chapter 2), comprises a distinct stratigraphy with laminated clays and silts with interspersed gravel layers and drop stones. These Lake Doubtful sediments were derived from melt water from up-valley glaciers (Turner et al., 2003; see also McGlone & Basher, 2012). Similarly, the basal sediments, grey muds, at Boundary Tarn (Chapter 2) reflect fluctuations from cool to warming conditions relating to glacier retreat (Vandergoes et al., 2008). When temperatures warmed from 12,000–11,500 cal yr BP at Boundary Tarn Stream, inorganic sediments increased and, as the catchment stabilised, sediment became enriched in organic matter (Vandergoes et al., 2008). In Adelaide Tarn, the sediments also increase in organic carbon in the sediments of lithozone 2, where carbon content increases dramatically to 15.0 % as the Adelaide Tarn catchment becomes more stable.

Lithozone 2: 4.8–2.4 m (~13, 932 –7709 cal yr BP)

This section comprises a brownish black organic silt/clay with light yellow/brown laminae, some macrofossils, and organic-rich bands. These sediments have the highest content of organic matter of the three lithozones, attaining 15.0% organic carbon (Table. 3.0). The yellowish brown laminae become very abundant and six organic-rich layers are made up of tangled moss/liverworts. The organic layers are present at depths of 4.70, 4.35, 4.15, 3.75, 3.38, and 3.22 m. Plant macrofossils appear at approximately 3 m depth in the core (i.e. they are absent below that depth) and are scattered throughout the sediments above 3 m depth. The mean sedimentation rate decreases upwards, ranging between 0.20 and 0.38 mm/yr, and is comparatively low with respect to rates in the older sediments of lithozone 1. The laminae are more frequent between 3.8 and 3.2 m and this zone roughly coincides with the low MSRs. Although the sedimentation rates are only averages, their changes can be an indication of changes in lake productivity or changes in stability in the catchment, or both. The distinctly coloured laminae could also be a response to in-wash of sediment derived from erosion during storms or following earthquakes in this period (cf. Page et al., 2010). The SEM photos that have further characterised the laminae suggest that these are formed from storm events

washing in allochthonous sediment filled with angular particles and some organic matter and hence little to no diatoms (Fig. 3.3) (note that only one light yellow-brown layer was examined by SEM and that further characterisation is needed to support inferences made using lithological features). The rest of the sediment that is non-bedded has angular inorganic particles and more abundant diatoms that relate to high lake productivity.

The appearance of plant macrofossils at ~ 3 m depth and upwards in the sediments (details are given in Chapter 5) may signal the movement of the tree-line to higher altitudes and closer to the lake. Another hypothesis to explain the lack of plant macrofossils in the lowermost sediments is that the lake environment was too dynamic to allow conditions to develop to preserve any plant macrofossils.

Lithozone 3: 2.4–0 m (~7709 – 927 cal yr BP and younger (pre-700 cal yr BP))

Lithozone 3 consists of dark brown organic silt with increased plant macrofossils, condensed organic bands and yellowish brown laminae lessening up the core but with a zone of condensed laminae between 0.2 and 0 m. The colour of the sediment is related to amount of organic carbon content, which ranges from 5.0 to 10.2 % (Table. 3.3 and Chapter 5). Plant macrofossils disappear at around 1 m depth where there is a slight increase in organic bands above this point at 0.9, 0.89, 0.72 and 0.1 m. The sedimentation rate in this section fluctuates a lot more than in lithozones 1 and 2. There are two periods of high sedimentation of 0.71 mm/yr and 1.98 mm/yr between 3622–3566 cal yr BP and 1063–942 cal yr BP, respectively. The MSR in the uppermost sediments fluctuates between 0.26 mm/yr and 0.40 mm/yr. This part of the core has very abundant diatoms (in comparison to the other sections) within the non-bedded sections.

In this latter part of the lake's history, the lake catchment is considered to be relatively stable with fairly constant MSRs except where MSR increases to 0.71 and 1.98 mm/yr. The catchment has stabilised, vegetation is occupying the basin around the lake, and the lake is less sensitive to changes (more stable) and sediments are thus able to preserve plant macrofossils. The lake is fully functioning and primary productivity has increased indicated by the increase of

diatoms in this lithozone (Fig. 3.3). The disappearance of plant macrofossils above approximately 1 m at ~2777 cal yr BP could be attributed to a slight deterioration of the climate and hence a concomitant drop in tree-line around the lake. The increased sedimentation rate to 0.71 mm/yr coincides approximately with the three layers of condensed organic bands, and the intensified MSR between 1063 and 942 cal yr BP overlaps the tightly spaced laminae at the top of the core from 0.18 to 0 m depth. These two events noted (increase of MSR to 0.71 mm/yr and 1.98 mm/yr) could be interpreted as increased storminess and intensification of the input of allochthonous sediment.

Chapter 4. Physical properties and palaeoenvironmental interpretations

4.0 Introduction

This chapter outlines the physical parameters that have been measured from the lake sediments. These include X-radiography, grey-scale measurements, magnetic susceptibility, and grain size. Each property has been introduced in a new section with background information about its particular function and how each one can contribute to palaeoenvironmental reconstruction on the basis of findings in previous studies. The methods are explained followed by results and a discussion.

4.1 X-radiography

4.1.1 Introduction and background

X-radiography began to be used in the field of palaeolimnology in the 1980s. Previously the method had been used mainly in tree-ring studies, geology, and marine sedimentology (Saarinen & Petterson, 2001). Early papers relating to the use of X-radiography on lake sediments in New Zealand are those of Lowe et al. (1981) and Lowe (1988). Various forms of information can now be extracted from X-ray images including enhanced laminae structures and composition, grey-scale generation, and the development of time series analyses applicable to regular laminae (Kemp & Pike, 2001). X-radiography is a high-resolution, fast and a non-destructive method that can be applied once the core is split and used as a long-term archive (Saarinen & Petterson, 2001).

The variations of sediment and densities of compacted layers down the core absorb different amounts of X-rays therefore emitting variations of "grey" in the X-radiograph (Tiljander et al., 2002). Sediments that are comprised of clastic material with minimal organic matter are able to 'absorb larger amounts of X-rays

and are represented by the pale grey/white bands in the X-radiograph. The darker layers in the X-ray image represent organic-rich sediments because this material has a lower affinity for X-rays (Tiljander et al., 2002).

Along with grey scale, X-radiography is commonly used to identify the abundance of laminae and their thicknesses, which can be measured via another image analysis tool. A perpendicular line is drawn from the sharp changes in grey scale and this function can help to identify distinct layers. The prominent boundaries between the layers make it easier for the program to identify the laminae with 95% reliability in comparison to estimates made using just the human eye (Saarinen & Petterson, 2001). Patterns of laminae and the distance/age between each have been used to infer cycles and possible climatic events (Saarinen & Petterson, 2001). The enhanced patterns of laminae can be used to correlate between multiple cores obtained from the same site and the most distinct layers can be used to connect cores to obtain a continuous record (Saarinen & Petterson, 2001).

The strong relationship between the physical proxies of the core such as grain size, magnetic susceptibility, and X-ray image analysis can be used to infer the input of terrigenous material into the lake that may be the result of disturbance in the catchment such as storms or earthquakes or more sustained climatic events (Mazzucchi et al., 2003).

4.1.2 Methods

X-ray images of the cores were captured using a portable veterinary X-ray imaging system provided by NIWA, Wellington. The model used was a Varian PaxScan 4030E digital receiver and an Ecotron EPX-F2800 X-ray source. ViVa 2.0 software was used to obtain and manipulate the images.

Before the X-ray can acquire images the machine needs to be brought up to the ideal voltage. This happens in a stepwise fashion to prolong the life of the instrument. Warming the machine up slowly in 10 kv intervals helps to identify the ideal voltage that suits the density of the cores. 50 kv was the optimum

voltage to gain a good resolution and to identify different bands within the cores of different densities. In the basal ~0.8 m of the cores the sediment is denser and required a higher voltage of 60 kv to capture these changes. The setting for mAs was stationary at 20 with all thrusts of both cores.

A 30 cm ruler was placed on the receiver with metal arrows indicating 10 cm intervals as a scale for the images. Two thrusts from the same core (e.g., 1115 T1 and 1115 T2) were placed parallel to each another on the receiver and lined up with the scale and metal arrowheads from 0–30 cm. The ViVa software was used to prepare the receiver and X-ray source, a dos meter was turned on to record collection of X-rays, and operators left the room to propagate the X-rays. Once the image was acquired, ViVa 2.0 was then used to manipulate the images to obtain the best resolution. Final images were saved and the process was repeated after moving cores up another 30 cm leaving metal arrowheads in place as markers for matching photos.

Images were cropped and 'stitched' to obtain total core length and converted to a 24-bit image. The total core image was imported into BMPix_PEAK, which is an automated program to identify layers, measure grey-scale, and count laminae. The BMPix_PEAK program was generated by Weber et al. (2010), which runs via Microsoft Excel, through a number of macros.

Once the image is imported the BMPix macro window appears along with the core (Fig. 4.0). The depth of the core is set on the left-hand side of the window from 0–561 cm and the line width (pixel) of the area being measured (red box surrounding image) is extended to 75. The "Go" button is then hit and the information is available in Excel for plotting. I then plotted depth vs "normalized gray" in a statistical coding program called R (discussed more in the section on grain size).

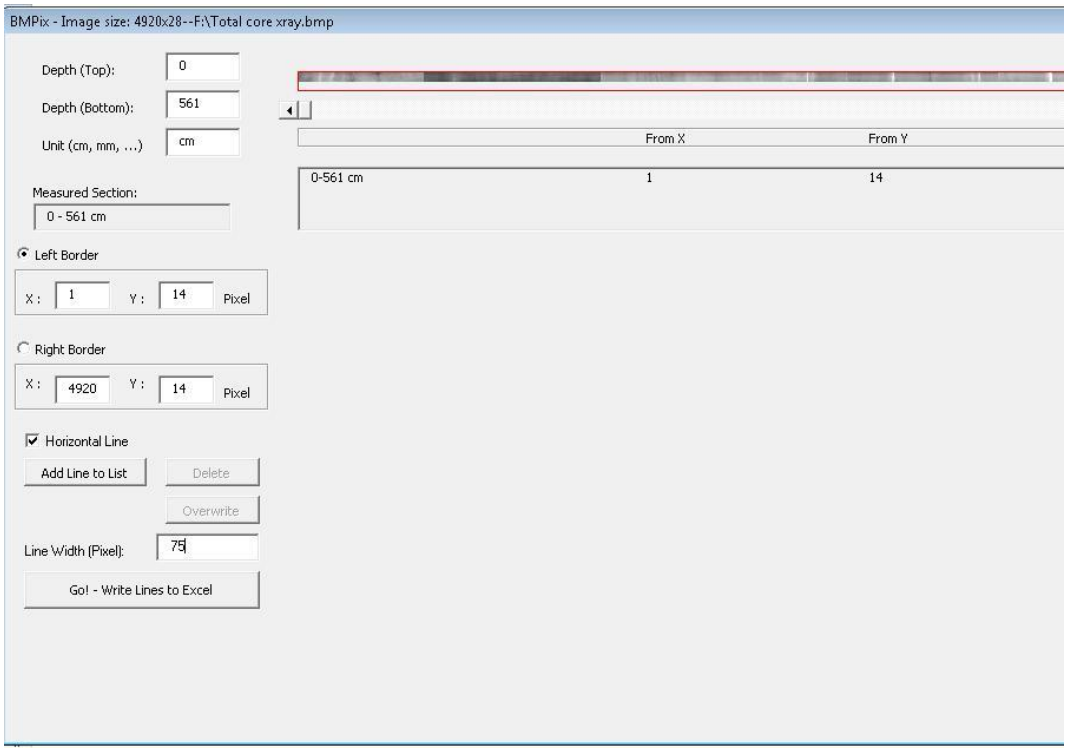

Figure 4.0 Example of BMPix pop up window that initiates image processing of the core.

4.1.3 Results

Grey-scale

Once the X-radiographs have been stitched together they can be used to interpret and enhance compositional changes down the core. The overall pattern shows a darker shade of grey with intermittent layers of light grey/white (Fig. 4.1). Normalized grey is also plotted in Fig. 4.1 and this attribute highlights any fluctuations in concert with the changes in colour of the X-ray images and gives a more visual impression. The grey-scale results are divided into 3 major zones based on changes observed and the chronology.

Zone 1: 5.6–5 m (~14,000 cal yr BP)

There appear to be minimal laminae excluding the two obvious macroscopic layers (~2 cm) of gravel, one at the base of the core (5.6 m) and one at approximately 5.4 m depth **(**~14,000 cal yr BP). The normalized grey shows two distinctive peaks coinciding with the gravel layers but otherwise very little change

is evident. Single granules are scattered throughout this section represented by the angular white-grey spots.

Zone 2: 5.0−3.5 m (13,932−11,000 cal yr BP)

At ~5 m depth, infrequent laminae start to appear and are present through to approximately ~11,000 cal yr BP at 3.3 m depth. The individual laminae in this section are ~1 cm in thickness and abundant. There are a few particularly thick layers (~2 mm) of interest located at 4.1 m or ~13,166 cal yr BP and 3.9 m or ~12,262 cal yr BP, respectively. These thicker layers are composed of gravel-sized particles bound by fine silt. There are frequent changes in normalized grey that are linked to the multiple laminae present in the X-ray images, with a few distinctive peaks corresponding to gravel layers at ~3.9 and 4.1 m. Other layers of interest included in this section are the dark grey/black segments between 4.2−4.3 m of approximately 1 cm in thickness.

Zone 3: 3.5−0 m (11,000 cal yr BP−~700 cal yr BP)

From ~11,000 cal yr BP through to the top of the core, the X-radiograph shows mainly massive sediments with the occasional denser layer manifest as white and interfingering dark-grey bands. The denser layers in this section are located between ~8700 and 5000 cal yr BP with a particularly distinct layer at ~5000 cal yr BP (~1.6 m). The normalized grey in this section is relatively 'flat', therefore enhancing the individual peaks of the minimal laminae present.

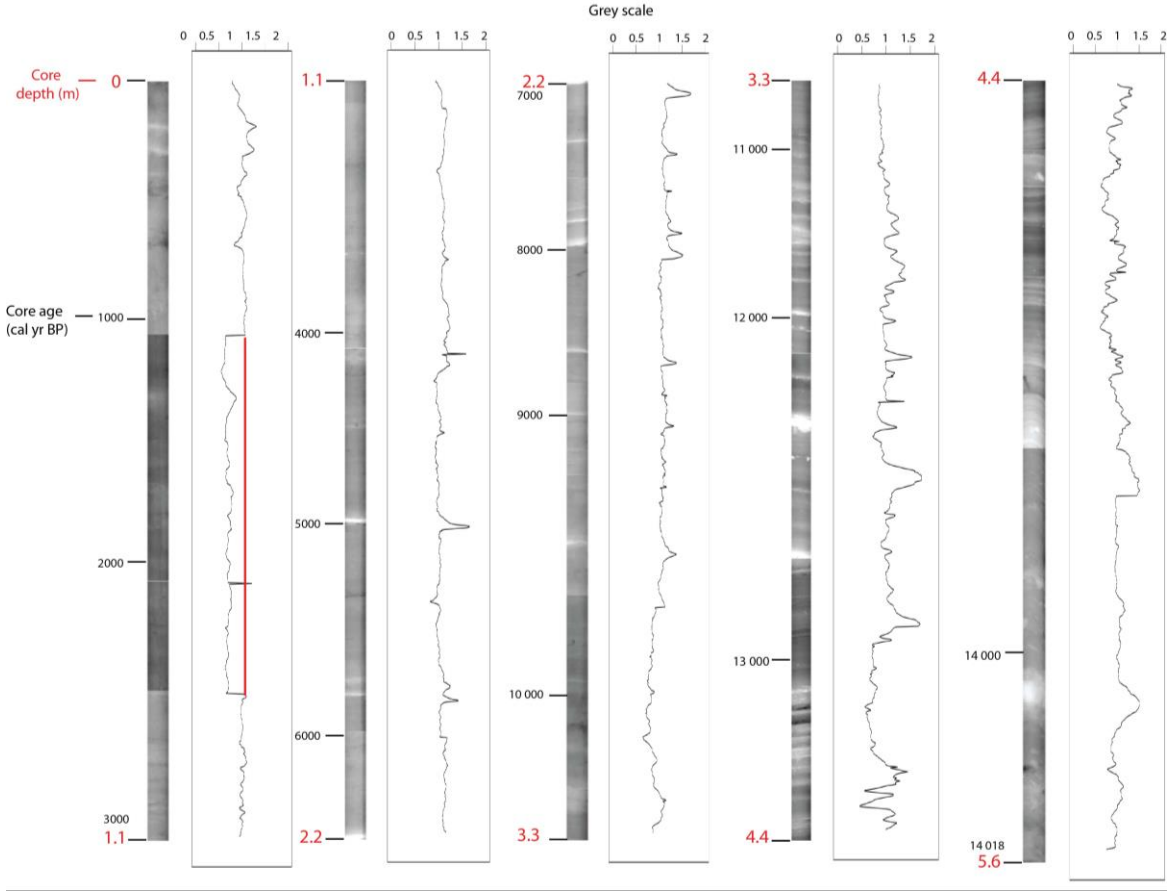

Figure 4.1 X-radiograph of the core from 0–5.6 m and chronology (in cal yrs BP) along the side. The "normalized grey" is plotted beside the X-radiograph showing the changes in density through the core. There is an artefact in the normalized grey where a different resolution was used to capture the X-radiograph and the vertical red line illustrates this with interpretation of where the values would be.

4.1.4 Lake history from X-radiography and grey-scale zones with some implications for palaeoenvironmental change

The X-radiography and grey-scale has been divided into three zones based on major changes in these parameters.

Zone 1: 5.6−5 m (~14,000 cal yr BP)

Lithozone 1 is a slightly lighter shade of grey in comparison to the remaining zones. There is only one lamination close to the top of this section. The two gravel layers are clearly visible as they appear denser than the surrounding sediment identified by the light grey/white colours at 5.4 and 5.2 m. The grey scale results shows two large peaks coinciding with these gravel layers and a reasonably flat image throughout the rest of this section. The gravel clasts (these may represent drop stones from the once-advanced glacier) are seen throughout as single white angular particles in the X-radiographs.

This zone represents the formation and early development and quite rapid infilling of the lake by coarse sediment (gravels) and fine grained material from the erosion of the surrounding bedrock brought on by the melting of a local cirque glacier. Prior to ~14,000 cal yr BP, temperatures were cold enough for glacier formation in the high altitude Tasman Mountains (Barrell, 2011); conditions started to warm and the local glacier began retreating and water infilled the pre-carved cirque basin, either from previous glacial cycles or the most recent local glacier advancment. Glacial melt transported gravel sized particles into the lake, or winter temperatures allowed the glacier to advance slightly and carry glacial drop stones into the lake at its terminus, or both. The gravel layers may be from more intensified melting or storm events that allowed the transportation of these relatively large particles.

The carbon content in this section is relatively low with values of 0.3 % (Chapter 5) at the bottom of the core and gradually increasing upward.The thin laminations at the base of the core could be attributed to seasonality influencing glacier retreat

and slight advances or stability during winter. The catchment is unstable and there is limited soil formation or organic matter.

Zone 2: 5.0−3.5 m (13,932−11,000 cal yr BP)

As seen in the X-radiograph (Fig.4.1), abundant and infrequent laminae appear in this zone. The background sedimentation is a darker shade of grey than that of zone 1. The laminae are mainly pale grey/white and some darker layers occur at 4.2 m and 4.3 m. There are two gravel layers in this section at 3.9 and 4.1 m. The grey scale changes from relatively flat to exceptionally wiggly, coinciding with abundant laminations identified by the X-radiograph.

The darker grey section in the X-radiographs of this part of the core suggests a higher organic matter content, possible soil formation in the catchment, and deposition of some soil-derived materials into the lake (such as demonstrated elsewhere by Tiljander et al., 2002). There is a high content of organic matter, reaching 15% (Chapter5) in this section, shown in the SEM micrographs that identify diatoms and some organic matter (Chapter 3) . The increased laminations in this zone could be interpreted in at least two ways: (1) the climate conditions were harsh and there were frequent storms flushing (or blowing) sediment into the lake from the surrounding catchment; or (2) the lake is still quite young at this stage and sensitive to slight changes in the catchment but the catchment itself is stabilizing and some of these layers could be autochthonous deposition as lake productivity increases seasonally. Micrographs obtained by SEM of the light yellow brown layers suggest an allochthonous input on the basis of the angularity of the inorganic particles and lack of diatoms (meaning limited in-lake productivity).

The two dark grey/black layers at 4.2 and 4.3 m are organic rich and these are the tangled moss and liverworts transported into the lake through heightened hydraulic transport or wind, possibly from storm events.

Zone 3: 3.3−0m (~11,000 cal yr BP−~700 cal yr BP)

Laminae almost disappear in this section and the grey-scale flattens out from ~11,000 cal yr BP. The laminations that are present are enhanced and 'protrude' as a large peak because of the surrounding flat grey-scale. The peaks coincide with the denser pale grey/white layers. There are some dark grey bands in the top 1 m of the core

The lake begins to stabilise from ~11,000 cal yr BP and organic matter decreases slightly in the sediments (on the basis of the slightly lighter colour of this zone in the X-radiograph). There is a decrease in organic carbon content in this section with a maximum of ~10% C (Chapter 5), and SEM micrographs show less organic matter (Chapter 3). The catchment stabilises because of vegetation cover, allowing soil formation, and together these factors reduce the amount of allochthonous sediment entering the lake. Conditions are stable and temperatures are relatively warm.

4.2 Magnetic susceptibility

4.2.1 Introduction and background

Magnetic susceptibility is the aptitude of a material to exert a magnetic moment of a specific strength once a magnetic field is applied. Once a magnetic field has been applied to the material, the observed measurement can help to classify its composition (Sandgren & Snowball, 2001). Magnetisation of lake sediments was first discovered in the 1920s. Current research of palaeomagnetism was developed in the 1960-1980s. There are several techniques that can be applied to obtain a magnetic susceptibility measurement and they are all non-destructive, relatively fast, and applicable to a whole/split core or bulk sediment samples (Nowaczyk, 2001).

Lacustrine sediment cores can provide a record of palaeomagnetic fluctuations through time and can be interpreted as (1) changes in catchment erosion, representing influxes of minerals from the surrounding rocks or cover beds or soils, (2) impact of an erosion event triggered by events such as storms or earthquakes, (3) a period of burning in the catchment (magnetic susceptibility increases in accordance with a burning event or shorty thereafter), (4) changes in peak runoff from streams entering a lake , (5) deposition of glacial debris from an active glacier, and (6) input of wind-blown minerals (Gedye et al., 2000; Sandgren & Snowball, 2001; Reynolds et al., 2004; McWethy et al., 2009; Balascio & Bradley, 2012). A strong magnetic field is applied to the sample to observe the behaviour. Minerals will be diamagnetic, paramagnetic or ferromagnetic. Diamagnetic minerals exert a negative to weak magnetism once a magnetic field has been applied, and minerals of this type include quartz, feldspars, and calcite. Paramagnetic minerals have a slightly more positive magnetism and include garnet, biotite, and carbonates. Ferromagnetic minerals produce a magnetic moment with or without an applied magnetism and tend to dilute other types of magnetism within the sample, and include magnetite (Sandgren & Snowball, 2001).

Magnetic susceptibility (MS) has become relatively common in palaeolimnological research because of the ease of data collection, the array of interpretations to suit the research aim, and the lack of destruction in comparison to other methods. A multi-proxy study by Balascio & Bradley (2012) found a relationship between organic matter and magnetic susceptibility in the lake sediments. Their results showed that when organic matter increased there was a decrease in magnetic susceptibility, and Balascio & Bradley (2012) inferred this decrease in MS to reflect, therefore, warm conditions. Vegetation flourished around the lake and soil formation was enhanced, stabilizing the catchment and limiting allochthonous input of organic matter. Cooler conditions are inferred from increased MS and thus low organic matter and concomitant increases in the input of inorganic clastic material. Various studies such as those of Ao (2010), Stephens et al. (2012), and Balascio & Bradley (2012), have found a strong relationship between grain size and MS. These three studies have interpreted an increase in magnetic susceptibility and grain size as a response to an influx of external sediment or heightened erosion rates. Ao (2010) stated that grain size and magnetic susceptibility fluctuations could be interpreted as glacial and interglacial cycles. The timing and impacts of initial human settlement in New Zealand has become increasingly important, and the "initial burning period" (burning typically was continued) is being used as a possible signal for the arrival of humans (e.g., Newnham et al., 1998b; McGlone & Wilmshurst, 1999). With the burning and removal of vegetation comes the increase of erosion, and McWethy et al. (2009) and Gedye et al. (2000) are among the many that have used vegetation changes and peaks in MS as proxies for fire records.

MS alone should be interpreted with some caution, as there are limitations to this method. Interpretations of the palaeomagnetic record are not so straight forward, as post-depositional processes can alter the mineral and not preserve the true signal. Post-depositional alteration can occur for certain minerals, such as magnetite, hence reducing the MS values attributable to this mineral. Alteration of magnetite can help to provide insight into geochemical changes within the lake through time (Sandgren & Snowball, 2001; Reynolds et al., 2008).

Adelaide Tarn is in a suitable position for a relatively undisturbed palaeomagnetic record. The lake is in an isolated catchment with one small inlet, and hence the source of the magnetic minerals are from the surrounding rock, cover deposits, soils, and potentially from wind-blown particles (Marx et al., 2009). The geology underlying Adelaide Tarn is a subset of the Greenland Group and has alternating sequences of sandstone and mudstone. The Greenland group has an abundance of quartz (35-50%), minor traces of plagioclase (6% or less) and rare mica, pyrite and ferromagnesian minerals (1% or less) (Laird, 1972; Roser et al., 1996). Fine-grained chlorite has also been observed which is formed at low to medium temperatures, suggesting a low-grade metamorphism, falling into the New Zealand Greenschist facies (Nathan, 1976). The mineral assemblage of the bedrock may help to interpret the magnetic susceptibility curve.

4.2.2 Methods

Magnetic susceptibility was the first method to be applied to the cores. There is minimal pre-treatment required and the cores could remain whole and in a wet state. An MS2 Barrington magnetic susceptibility meter was used to obtain measurements with a sensor type of M.S.1.C. This equipment was provided by Victoria University of Wellington. Before measurements could be taken, the magnetic susceptibility meter required a preheated phase of ~60 mins to allow for the calibration of its surroundings. The machine was programmed to SI units and then zeroed. The final preparation before obtaining a measurement of the sediment was to take a blank reading without the core, which takes into account the surrounding magnetism. One-metre thrusts of each core were consecutively pushed through the magnetic susceptibility loop with a measurement taken at 3 cm intervals. At the end of each ~ 1 m thrust, another blank reading was taken excluding the core to interpret the error of surrounding magnetism. Zeroing the blank measurements were required before the insertion of another ~1 m thrust.

All measurements were recorded along with blank readings for each thrust. The difference of the blank readings is important when interpreting the data (depending on the size of the change) and this difference between the start and the end blanks is subtracted from the measurements.

4.2.3 Results

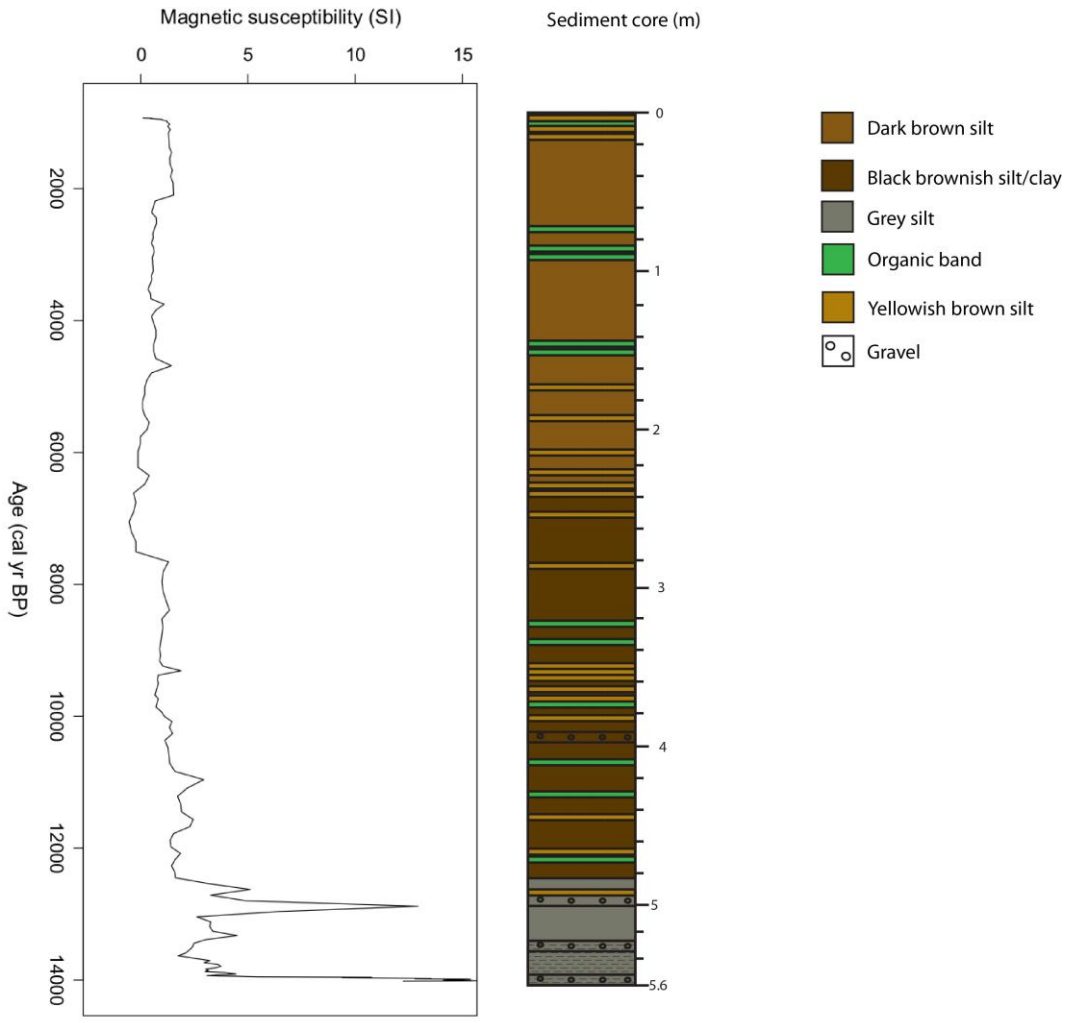

Figure 4.2 Magnetic susceptibility measurements (SI) plotted against age and the lithology of the core to show links between the distinct changes in each (refer to Appendix E for raw data).

Zone 1: 5.6–5 m (~14,000–12,500 cal yr BP)

Magnetic susceptibility is relatively high with measurements over 5 SI. There are two higher peaks of 15 and 12 SI located at the base of the core at ~14,000 and ~13,000 cal yr BP, respectively. These higher measurements of magnetic susceptibility directly coincide with lithozone 1 of the stratigraphic column, including the higher MS values that link to the gravel layers (Fig. 4.2).

Zone 2: 5–3 m (~12,500–7,600 cal yr BP)

The overall magnetic susceptibility measurements drop to between 2 to 5 SI with a few distinct peaks at ~11,600, 11,000 and 9,300 cal yr BP. In this section of the core, the measurements with higher values roughly coincide with the pale yellow/brown layers and organic bands. The gravel layer located at ~3.9 m in the stratigraphic column corresponds to a higher value of MS in this section (Fig. 4.2).

Zone 3: 3–0.7 m (~7,600–2,200 cal yr BP)

There is an abrupt drop of magnetic susceptibility at ~7,800 cal yr BP to negative values until ~6,000 cal yr BP. The magnetic susceptibility values steadily increase until ~2,200 cal yr BP.

The negative values overlap the transition from dark brown silt to pale brown silt in the sediments at 2.5 m. The increasing magnetic susceptibility until ~2,200 cal yr BP has two noticeable peaks that correspond to the organic-rich bands between 1 and 2 m.

Zone 4: 0.7–0 m (~2,200–~700 cal yr BP)

There is an abrupt increase to approximately 2 SI that is stable through to top of the core. Multiple light brown bands coincide with this increase.

4.2.4 Lake and catchment history based on magnetic susceptibility and some palaeoenvironmental implications

Here I present a synthesised version of the magnetic susceptibility results and they are separated into four zones based on major changes.

Zone 1: (~14,000 cal yr BP)

Magnetic susceptibility is heightened with measurements exceeding 5 SI. There are two higher values of 12 and 15 that roughly correspond to the gravel layers at

the base of the core and at 5.3 m. These high magnetic susceptibility (MS) measurements are only found in lithozone 1.

This signal of MS measurements supports the interpretation that the catchment at this time was bare and free of vegetation and only weakly developed soil, and so inorganic clastic material, carrying with it MS signatures of the surrounding bedrock, could be washed or blown into the newly formed lake. There is high MS and low to moderate percentage of organic carbon (0.3 to 4.0 %), which supports an interpretation that the sediments reperesent in-washing of allochthonous material. The gravel layers could also be derived alternatively from melting permafrost (if such permafrost existed) (Balascio & Bradley, 2012). Although mineral analysis has not been done on these sediments, the MS measurements can still give an indication of possible source of the magnetic minerals. The majority of the geology underlying Adelaide Tarn comprises quartz (35-50%) and plagioclase (~6%), which are both diamagnetic minerals and, in a large abundance, these will give high magnetic susceptibility measurements. Manganese oxides were identified in the sediments from lithozone 1 (in preparation for grain size analysis) which will produce a high MS signal. These minerals together will produce a high MS measurement in sediments deposited from an erosional phase of the catchment or from disturbance and erosion from abrupt events such as storms.

Zone 2: 5–3 m (12,500−7,600 cal yr BP)

The MS decreases to between 2 and 5 SI in lithozone 2. There are some higher peaks throughout this zone that coincide with condensed patches of pale yellow/brown layers and a higher peak with the gravel layer at 3.9 m (Fig. 4.2).

In this section the MS values are still relatively high in comparison to those obtained further up the core in lithozones 3 and 4. Increases in MS correspond with the pale yellow/brown bands. I infer that the climate becomes more stable and erosion in the catchment decreases, following the relationships described by Ao (2010). Spikes in MS values represent in-washing from erosional events. There is more organic matter in the sediments of this zone as the MS has

decreased from values in zone 1. Organic carbon reaches 15.0 % in this zone (Chapter 5). Forest vegetation has ascended in altitude (to just below the lake), representing warming conditions (Chapter 5), and has been able to occupy the catchment because of soil formation (Balascio & Bradley, 2012).

Zone 3: 3–0.7 m (7,600−2,200 cal yr BP)

Magnetic susceptibility decreases significantly to negative values from ~7,600 to 6,000 cal yr BP. This decline could be attributed to a further increase in organic matter and the stabilisation of lake productivity. The increase in diatoms evident in SEM micrographs supports this hypothesis: lake productivity is enhanced and primary productivity increases. After this abrupt decrease in MS the values steadily increase towards a higher value at ~2,200 cal yr BP. The gradual increase could be a reflection of increasing seasonality, possibly manifested as increased storminess in winter (and associated allochthonous input) and heightened productivity in summer. The forest assemblages are able to occupy the environment around the lake because of warming temperatures and increased stability of the catchment and faster soil formation. Tree-line was either on the perimeter of the basin or in the basin (dependant on soil formation within the catchment, wind and temperature).

Zone 4: 0.7–0 m (2,200 cal y BP − ~700 cal yr BP)

There is a sharp increase in MS at ~2,200 cal yr BP to 2 SI (Fig. 4.2), and the MS stays at this value upwards to the top of the core. Zones of pale yellow/brown layers correspond to this increase.

Here the climate appears to have ‘deteriorated’ slightly, cold sensitive taxa have moved out of the catchment, exposing soils and possibly bedrock to erosion (Chapter 5). Erosion events increased in frequency and influxes of sediment are captured in the lake sediment in the form of the MS peaks and pale yellow/brown layers (SEM micrographs show angular inorganic particles and few to no diatoms, Fig. 3.3). The close alpine shrub/forest ecotone around the lake at the present day may have developed at around this time (2200 cal yr BP to the top of the core).

4.3 Grain size analysis

4.3.1 Introduction and background

Grain size analysis has become important in interpreting palaeoenvironmental changes through time. Depending on the research aim, there are several ways grain size data can be interpreted. Grain size is an important physical factor when analysing lake sediments and can help to determine changes in patterns of other properties such as magnetic susceptibility. The changes in particle size in a lake sediment core can be used to infer (1) the source of the sediment, such as autochthonous or allochthonous, (2) the productivity of the lake at the time of deposition, (3) the energy required to transport the different sediment sizes, (4) palaeoenvironmental conditions, storm events, earthquakes, and (5) hydrology of the lake catchment (Last, 2001).

It is important to identify different modes within the grain size distributions because these help to determine the mechanism of transport and lake processes. Grain size alone is generally a direct indicator of landscape changes in response to climate and abrupt events such as storms (Last, 2001; Parris et al., 2009; Augustinus et al., 2011). In many lakes, autochthonous sediments in deeper waters are typically fine-grained (e.g. 3.9–6.3 μm); in-wash allochthonous events tend to deposit coarser grains (e.g. 2–64 mm), forming layers that interrupt these fine-grained sequences (Parris et al., 2009). Vegetation changes, soil formation, and glacierisation within the catchment, and external processes such as increased windiness and exotic dust flux, may also result in changes in sedimentation in lakes (Parris et al., 2009). Coupled with the coarse grain size transported from the lake catchment is local organic matter that adheres to these particles. It is important to note that if the study aim is directed at allochthonous input into the lake then samples need to be purified to remove the organic matter and aggregations of finer particles (Vaasma, 2008).

Numerous studies have utilized the grain size proxy in palaeolimnological research and it has proved to be a successful indicator of palaeoenvironmental

changes through time. Parris et al. (2009) undertook an extensive study of several lakes in North Hampshire and found a strong relationship of grain size in all records, i.e. cores from several lakes all showed similar patterns in grain size variations through time. This research was aimed to construct a storm record over the past 14,000 cal years from the observed grain size changes. Parris et al. (2009) found that at the start of the record ~14,000 cal yr BP there was a large in-wash of coarse sediment, which they infer reflect a shift to post-glacial conditions with an unstable and un-vegetated landscape. The lakes then stabilized as vegetation cover increased and there were episodic events adding allochthonous sediment into the lake (1400, 2100, 3000, 3900, 6800, 8200 and 11,500 cal yr BP). As stated above in the magnetic susceptibility section, Ao (2010), Balascio & Bradley (2012), and Stephens et al. (2012) all found relationships between magnetic susceptibility and grain size. Both proxies coinciding together can be interpreted as changes in the catchment landscape and erosional events. Page et al. (1994, 2010) also showed marked changes in sediment input and texture that relate to storm events in Holocene, Lake Tutira in eastern North Island. Page et al. (2010) provides a storm chronology since lake formation (7200 cal yr BP) and found 1400 layers that were made up of storm-derived material (dominated by allochthonous sediment).

The location and landforms around Adelaide Tarn make it ideal for obtaining a relatively undisturbed grain-size record. The stream entering the lake is contained entirely within the lake's surrounding catchment, hence no foreign sediment has been transported from vast distances by water (input from distal wind-blown sediment remains possible, however: Marx et al., 2009). The grain size data can fall into three categories: (1) normal sedimentation, (2) allochthonous input either via ice melt or from erosion resulting from relatively short-term events such as storms or earthquakes, and (3) wind-blown particles.

4.3.2 Methods

Pre-treatment of samples

A 0.5 mm spatula was used to take smear samples every centimetre down the core (~561 samples); smears were then placed into plastic vials for further analyses at the University of Waikato. The allocated sample was then placed into a glass jar using a spatula and left-over contents were rinsed with deionised water. Grain-size analysis required pre-treatment in order to remove any organic matter that would distort the data. To remove organic matter, 10 ml of 30% H_2O_2 was added to the sample and left for ~24 hours to digest. Samples were then added to a preheated (40° C) hot plate to catalyse the digestion reaction; after ~30 minutes they were taken off and left to cool. More H_2O_2 was required as the reaction was not complete, 5 additional millilitres were added and placed on the hotplate. An additional 10 ml of H_2O_2 were added and left over night to complete the final phase of reaction. The samples were put back on the hotplate one last time to remove excess H_2O_2 and 10 ml of distilled water were then added in preparation for particle-size analysis. A dispersing agent is needed to remove aggregates of clay and silt sized particles, and hence a pasteur pipette was used to add 5 drops of water-soluble calgon to disaggregate these flocs. Calgon requires ~12 hours to disperse the sediment; samples were then put in an ultrasonicator for 30 mins and were finally ready for particle-size analysis.

Particle-size analysis

The Malvern Mastersizer 2000 at the University of Waikato was used to obtain the grain size measurements. The Mastersizer uses laser diffraction to measure a size range of 0.02–2000 μm, which is ideal for lake sediments. The data are expressed as percentage per volume rather than a size per volume as larger particles would be overrepresented in the assemblage. A set marine standard operating procedure was chosen to represent the lake sediment samples in order to capture the range of particle types and densities. Various types of data are readily available to download from the Mastersizer software into Excel format. I chose percentage in each size category to represent the distributions of each sample

Statistical analysis – using "R"

The main aim of my grain size analysis was to determine the occurrence of in-washing events in the lake that may represent catchment disturbance. To achieve this aim I needed to identify the dominant modes and the changes in these through time. Modes are useful because they represent 'real' values in a grain size distribution rather than a statistical measure such as mean grain size that may not exist in reality (although mean grain sizes were also measured, along with other parameters). A statistical coding program called "R" (created by Ross Ihaka and Robert Gentleman from the University of Auckland in 1993) was used to identify common modes in all of the samples (Fig. 4.5). A package mixdist, engineered by Peter Macdonald (McMaster University, Ontario), was installed which runs through the R platform, and this package was used to locate the modes in the samples. Mixdist functions by statistically identifying polymodal distributions in a data set, whilst parameters such as means and standard deviations of the identified modes are manually constrained by the operator based on modes found (these values are called sigmas). Mixdist requires a specific coding framework in order to run the analyses (Macdonald & Green, 1988) (refer to Appendix A for mixdist script). Script or code is written into a new editing box (on the right of Fig. 4.3) and then this is run through the R console when the correct format is applied.

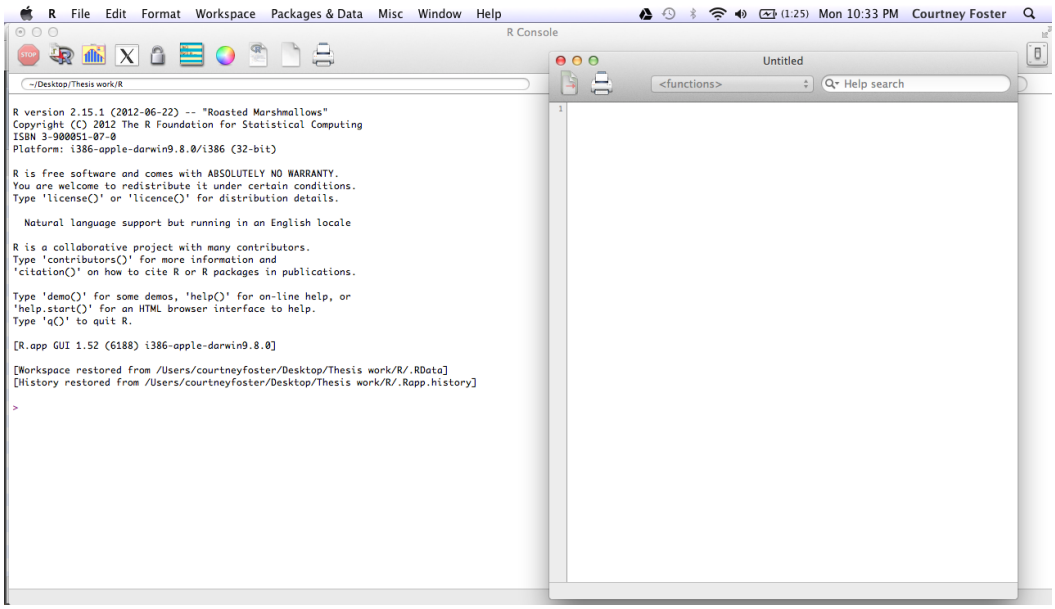

Figure 4.3 Example of the "R" platform; script window is located on the right and running the sequence occurs in the window on the left.

4.3.3 Results

Grain-size distribution and >32 μm fractions

Note: Grain size ranges used hereafter are as follows: clay, <3.9 μm; silt, 3.9–62 μm; sand 60–2000 μm; gravel >2 mm.

The grain size of the core is predominantly a mixture of ~45–50% clay and ~40–45% silt. Sand-size particles provide a very minor contribution to the overall composition and are generally no more than 5%. There are, however, fluctuations of sand throughout with some very substantial increases at depths of ~350 cm, 390 cm, 450 cm and one particularly sizeable increase at ~530 cm depth where concentration attains approximately 60%. From the base of the core (560 cm) to the top of the core, there is a very slight increase in clay with sand having an inverse relationship (Fig. 4.4). The silt-size fraction tends to remain constant throughout the core with a slight decrease where clay-sized particles overwhelm the samples.

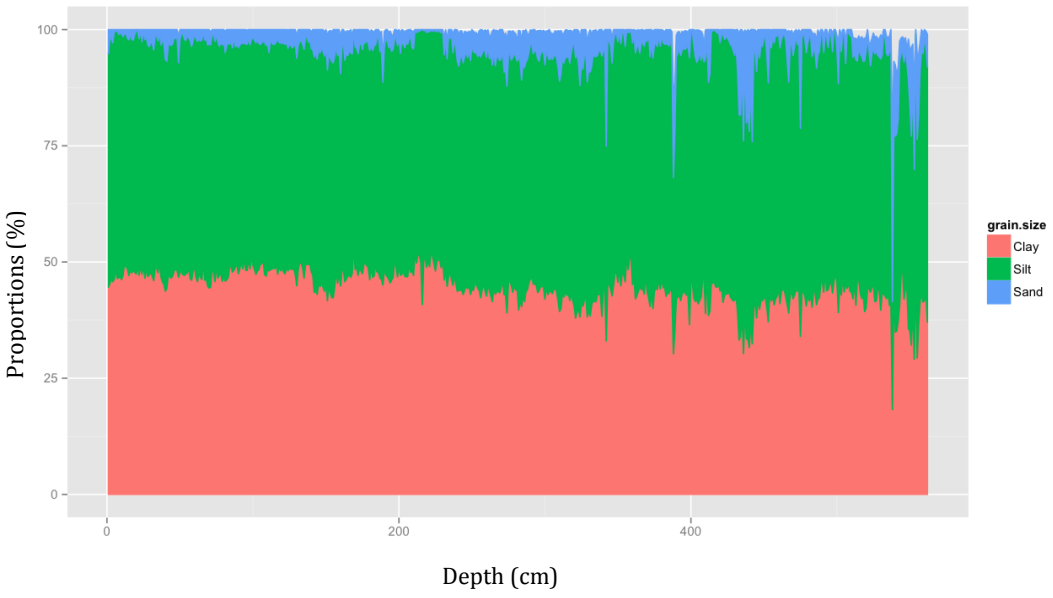

Figure 4.4 Fluctuations of clay, silt, and sand sized particles from 0 (left) to 5.6 m depth (right) (refer to Appendix D for raw data).

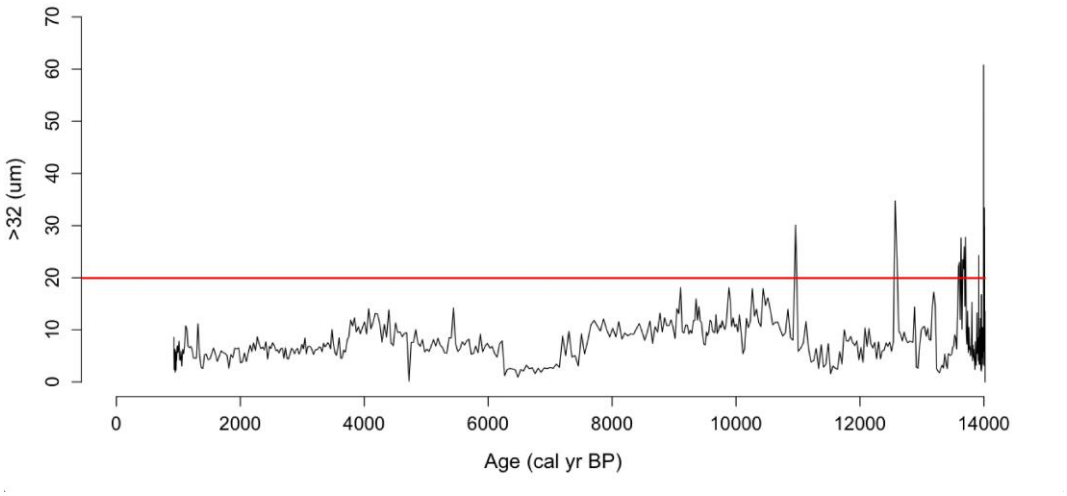

Figure 4.5 Fluctuations (in percent) of grain sizes >32 μm in diameter. The red line marks the 20% value. Where this value is exceeded, the sediments are inferred to have been washed (or blown) into the lake (following Augustinus et al., 2011).

Augustinus et al. (2011) used the >32 μm size fraction to represent the amount of allochthonous material entering a lake. In general, more than 20% of the total distribution that exceeds >32 μm is interpreted as terrestrial influx into the lake. I have plotted the >32 μm fraction of my samples through time taking note of areas that exceed 20% (Fig. 4.5). The results show that majority of this distribution falls below 20%. From >13,932 cal yr BP to 13,500 cal yr BP the >32 μm indicator is over 20% of the total proportion and ranges from 25 to 60% at the base of the core. There is a large proportion (35%) of >32 μm material at ~12,700 cal yr BP and after this the grain size distribution falls well below 10% until another large peak at ~11,000 cal yr BP (30%) (Fig. 4.5). From 11,000 cal yr BP through to 7800 cal yr BP there are intermittent increases over 10% that reach percentages up to 18%. From 7800 cal yr BP to the top of the core, all of the distribution is below 20%, but there are a few peaks at ~4000 cal yr BP that range between 10 and 15% and two just over 10% at the top of the core.

Identification of modes

Although there is a vast array of samples down the core, the majority of these showed similar distributions. A dominant mode was identified in all samples at ~8 μm and two sub-modes at 37 and 500 μm (Table 4.0). Representative size distributions were plotted against one other in R and these all showed the same pattern of modes with slight changes in sub-modes (Fig. 4.6).

As discussed in the methods section, the package Mixdist that runs through the R platform was used to track changes in the three modes down the core. The grain size unit is converted from microns to phi in order to construct a mixed distribution of the selected sample. A sample from 536 cm was chosen as an example to show changes in these modes. Here the dominant mode is >500 μm with sub-modes at 37 and 8 μm (Fig. 4.7)

Table 4.0 The three modes identified and their associated size ranges (all as μm).

Mode (μm)	Minimum size	Maximum size	Dominant size
Dominant mode	0.24	34	8
Sub-mode 1	33	62.5	37
Sub-mode 2	62.5	2000	500

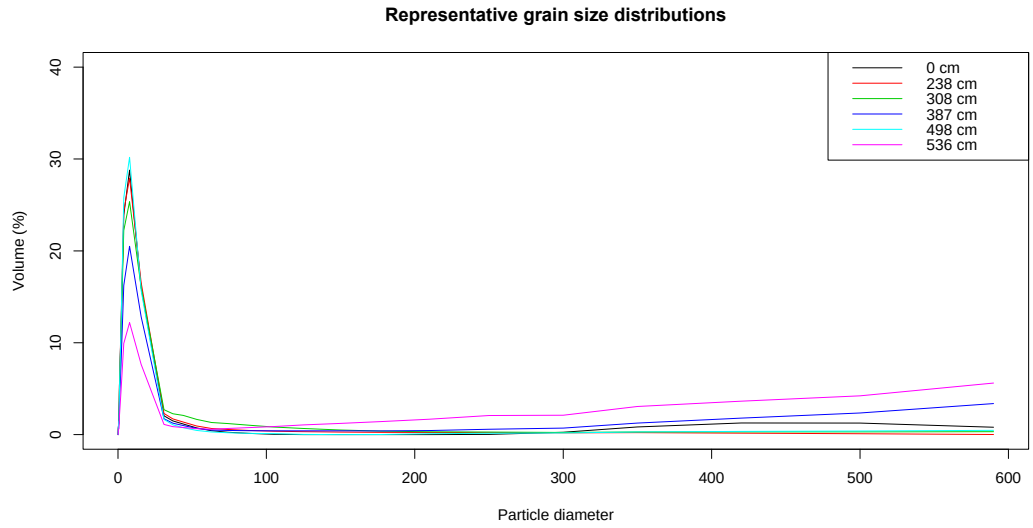

Figure 4.6 Representative grain size distributions from six samples that show polymodal patterns that are similar throughout the core. One dominant mode was found and two submodes.

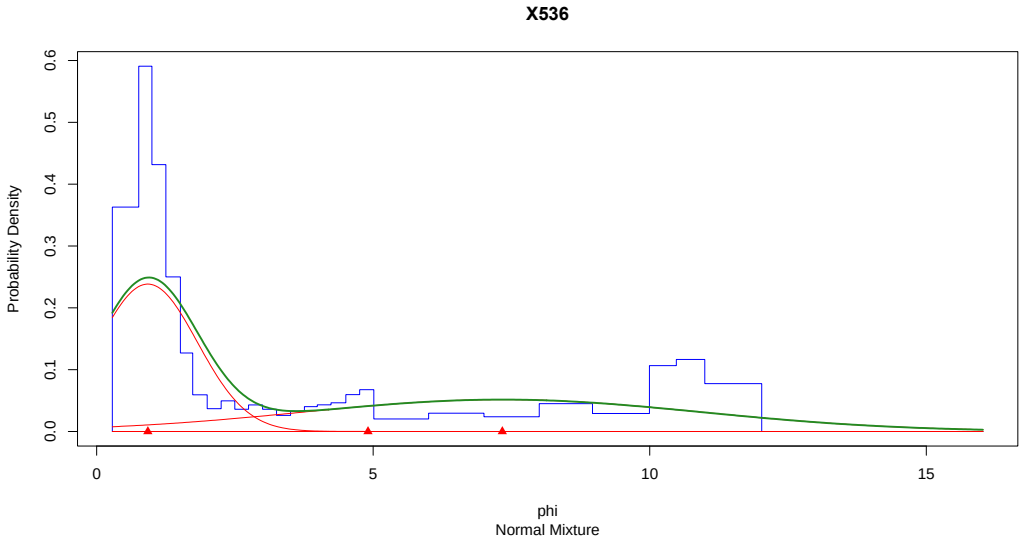

Figure 4.7 An example of the distributions of the three modes using sample 536 cm. Microns are converted to phi units and so the scale is the reverse of that shown in Fig. 4.8. There is a very large peak at ~1 phi (500 μm). The blue line is the particle size distribution, the red line is the identification of the three modes, and the green line is an overall smoothed curve of the polymodal distribution.

Physical core photos of representative layers show the colour changes and emphasise contacts of these layers (Fig. 4.8). The layers are described as gravel, organic bands (made up of tangled liverworts/mosses), and pale yellow brown clay layers. A number of these layers were chosen to characterise in terms of grain size distributions in order to determine their transport mechanism. Three samples each from the corresponding lithozones were also chosen to characterise the massive (non-bedded) sediments to compare with features of the layers. The mix distribution graphs have been plotted alongside photos of the massive (non-bedded) sediments and particular layers of interest (Fig. 4.8).

A) 536 cm - Gravel layer

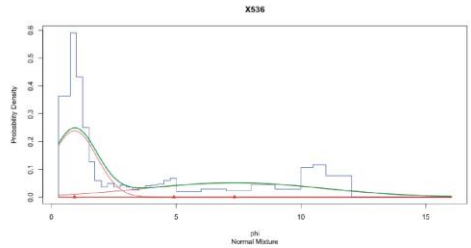

B) 388 cm - Gravel layer

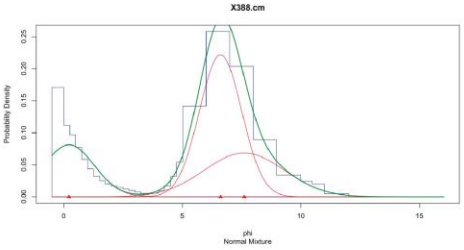

C) 339 cm - Organic band

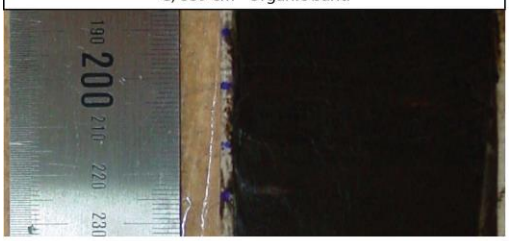

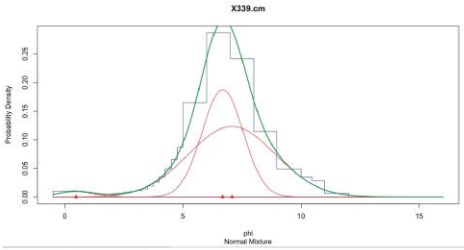

D) 83 cm - Organic band

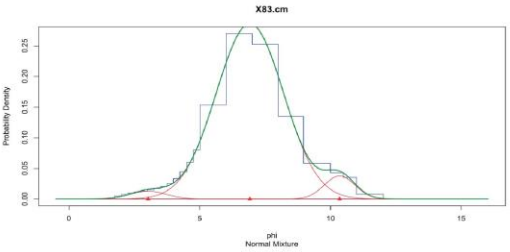

E) 409 cm - Light brown band

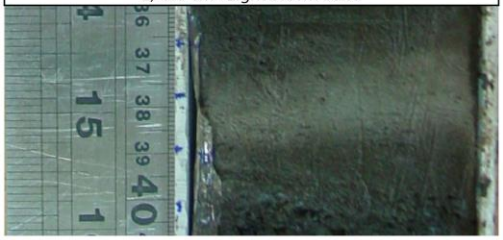

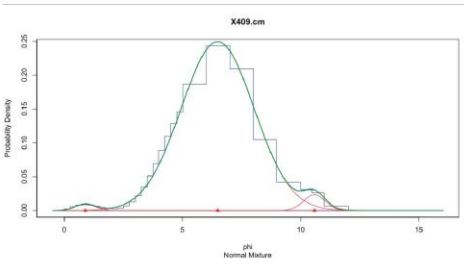

F) 169 cm - Light brown band

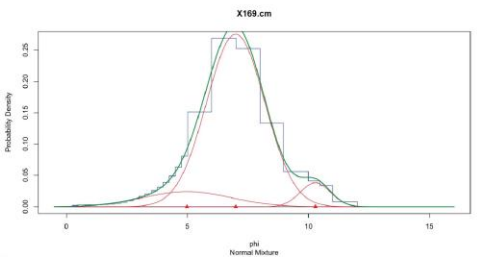

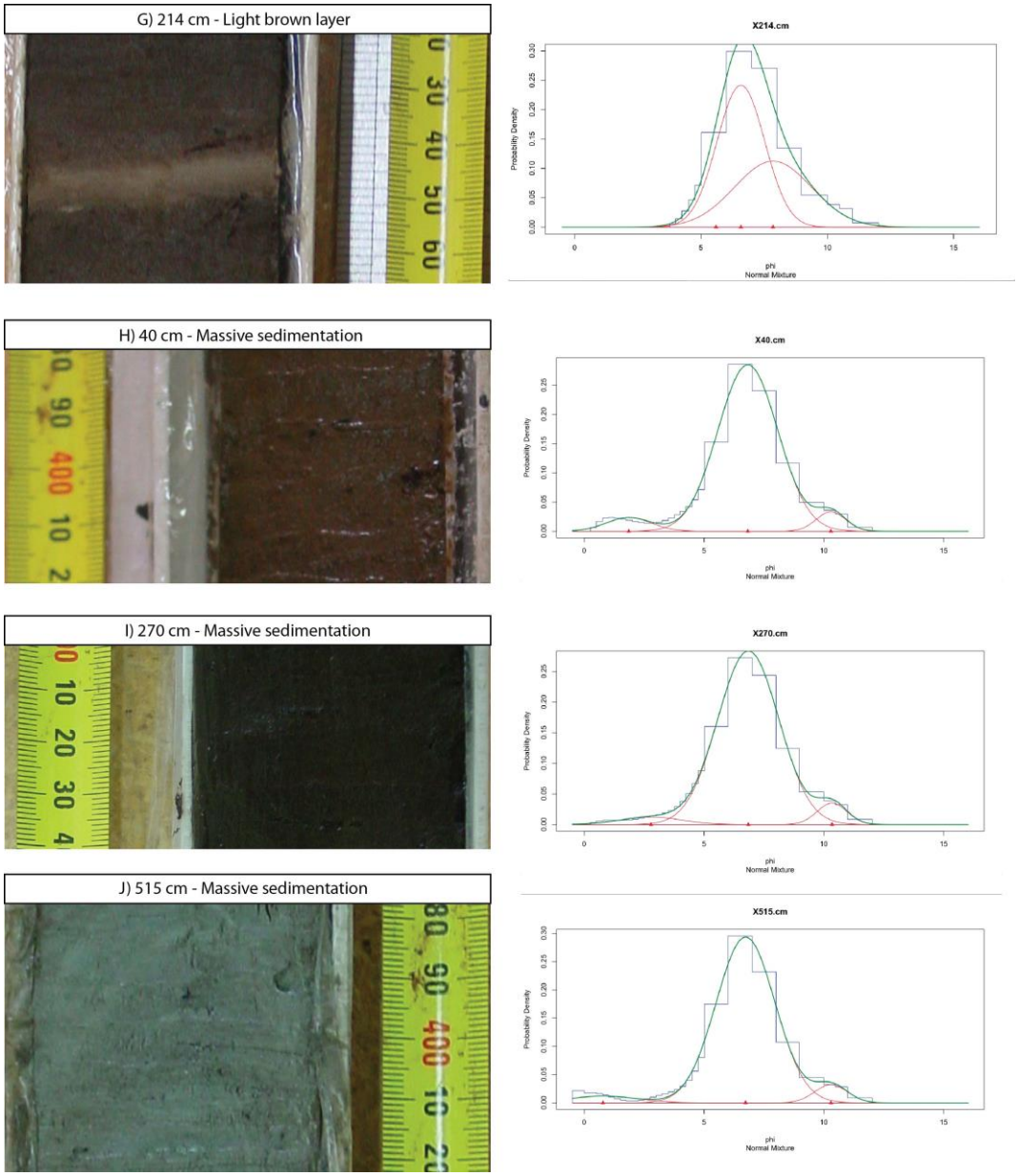

Figure 4.8 Physical photos of gravel layers (A and B), organic bands (C and D), light yellow brown layers (E, F and G) and examples from massive (non-bedded) sedimentation from lithozones 1, 2 and 3 (H, I and J). Alongside the photographs are the grain size mixed distributions associated with these layers.

Distribution of grain size in significant layers

The gravel layer chosen from 536 cm (Fig. 4.8A) is dominated by sediment larger than 500 μm and shows a very low and broad distribution over the two sub-modes (8 and 37 μm). The gravel layer at 338 cm is dominated by the primary mode, 8 μm, but also has a peak of gravel sized particles, >500 μm. This gravel layer is bound by a silt/clay matrix. The organic bands (Figs. 4.8C & D) comprise mainly fine silt with slight amounts in the other modes. The pale yellow/brown layers comprise mainly fine silt (8 μm) but show a shift in the sub modes to a slightly finer grain size. There is a small distribution of size over this finer mode but this mode is noticeable in the mix distribution graphs of layers from 169 cm (Fig. 4.8F), 409 cm (Fig. 4.8E), but not in 214 cm (Fig 4.8G).

Massive (non-bedded) samples characteristic of lithozone 1 (Fig. 4.8J) are dominated by fine clay/silts. The dominant mode is 8 μm and a small distribution over the finer modal grain size. There is also a small percentage of the total distribution of more than 500 μm. A sample characteristic of lithozone 2 (Fig. 4.8I) is much the same as that/those from lithozone 1 but only a very minor part is over 500 μm. A representative sample from lithozone 3 (Fig. 4.8H) is dominated by a mode of ~8 μm with two small peaks either side at >500 μm and one slightly below 8 μm; both of these peaks are slightly larger than those representative of lithozone 1.

4.3.4 Lake and catchment history based on changes in grain size and some palaeoenvironmental implications

In this section I discuss the overall grain size of the core and fluctuations in clay, silt and sand and possible palaeoclimate inferences are made. The polymodal distributions are examined and potential causal mechanisms are inferred based on the changes in the dominant grain size modes. Major changes are divided into three main zones coinciding with the three lithozones, from the base of the core to the top.

Zone 1: 5.6–4.8 m (~14,000 cal yr BP)

The overall composition is a mixture of clay, silt, and sand. Clay and silt dominate but there is a large amount of sand in comparison to sediments marking lithozones 2 and 3 further up the core. Distinct layers of sand occur at 5.6 and 5.3 m depth. On the contact of lithozone 1 and 2 there is a gravel layer that coincides with another sustained increase of sand to about 25% of the composition. Clay-size particles increase steadily into the next lithozone, silt remains constant, and sand gradually decreases. More than 20% of the grain size distribution is over 32 μm in this section.

The mix distribution graph for the gravel layer chosen from lithozone 1 (Fig. 4.8A) shows that the majority of the distribution is over 500 μm and this coarse size would require a high-energy mechanism to be transported and deposited in the lake. I suggest that melt-water from the retreating local glacier is a possible transport mechanism to account for the gravel, and hence warming conditions at this time are inferred. A record from Lake Pupuke (inAuckland) published by Augustinus et al. (2011) identified an erosional phase from ~14,000–13,000 cal yr BP. The erosional phase was suggested by the results that showed a large increase ($\geq$ 20%) in the total grain size distribution that is >32 $\mu m\ in\ diameter$ (32 microns was chosen as a threshold value to represent the amount of terrigenous input into the lake). This erosional phase identified by Augustinus et al. (2011) is roughly coincident with the > 32 μm proportions at this time in Adelaide Tarn

also (>20%). Bedrock (and possibly thin cover beds, e.g., colluvium and fine grained sediment eroded from glacial movements) are readily available for erosion and transportation into the lake. Gravel layers would have either been entrained in the glacier terminus as slight advancements (winter) or increased melting (summer). The gravel layers could have also entered the lake from storm events. The surrounding catchment is unstable and the lake itself was probably shallow and undeveloped.

Zone 2: 4.8–2.4 m (13,327–7709 cal yr BP)

In general, the grain size distributions of sediments of lithozone 2 are primarily dominated by clay and silt with a slight increase of sand (in comparison to the grain sizes of sediments of lithozone 1). There are a few fluctuations in sand throughout this zone and these include a large spike in sand at 3.8 m and this corresponds to a layer that also includes gravel. The light yellow/brown layer at 409 cm (Fig. 4.8e) has a slight increase in sand content. The grain sizes of layers chosen in Fig. 4.8 (which may not be representative of layers in other parts of the core) could be formed in one of two ways: (1) allochthonous sedimentation into the lake (SEM imaging suggests this), and (2) autochthonous sedimentation or normal in lake sedimentation (suggested by the mix distribution graphs).

The results suggest that at this time the glacier has been completely removed from the surrounding catchment and there is no glacial-till-derived in-wash into the lake. The catchment is stabilising, soil is beginning to form, and vegetation is able to occupy this new environment. The vegetation has stabilised the slopes and there is less in-wash into the lake. In comparison, the record from Lake Pupuke shows a decrease in percentage of grain sizes over 32 μm to 10% (rather than >20% in erosional phase) and this decrease is inferred as a warm moist phase (between 12,000 and 10,200 cal yr BP) with reduced sediment influx into the lake (Augustinus et al., 2011,2012). Adelaide Tarn shows the same similarity in grain size changes with the decrease in sand size particles and the proportion of grain size over 32 μm is much lower than 20%. There is a phase of higher peaks (10 to 15%) between 10,500 and 9000 cal yr BP where the lake is still sensitive to in-wash events but conditions are warming, as was suggested by Augustinus et al.

(2011) at Lake Pupuke. These peaks may roughly coincide with the yellow/brown layers throughout this section as they have slightly more sand content and from the SEM micrographs they are predominantly made up of angular sediment particles and thus could be attributable to small in-wash events. The lake is developing and primary productivity is able to flourish (Fig. 4.8F). There are some in-wash events indicated by the gravel layer (3.8 m) and increased sand contents (Fig. 4.4) that may relate to the distribution of the light brown layer such as 409 cm (Fig. 4.8E).

Zone 3: 2.4–0 m (7709 cal yr BP to ~700 cal yr BP)

This zone is dominated by clay and silt. The proportion of sand in this zone is less than 6% with two peaks that reach approximately 10% at depths of 1.5 m and 1.8 m. The representative pale yellow/brown layers (Figs. 4.8 F and G) in this section are dominated by clay and silt, suggesting enhancement of lake productivity.

The results suggest that the lake environment itself has become stable and is less sensitive to allochthonous in-washes from the catchment. The succession of vegetation in the catchment has advanced because of the optimum environmental conditions (Chapter 5). The tree-line has moved up the slopes of the basin to either the position seen today or a bit higher as warmer conditions prevailed (by 6,000 cal yr BP) and pushed out cold-tolerant taxa. By 2,200 cal yr BP the tree-line drops to the current position as climate degrades slightly (Chapter 5). There is a slight increase in sand content and this is attributed to increased erosion at approximately 1300 cal yr BP (0.49 cm depth), and this sand increase coincides with an increased proportion of clasts over 32 μm (Fig. 4.5). The organic bands of tangled liverworts and moss suggest that areas of saturation have developed around the lake (wetland areas, Chapter 1) and deposits from these have been washed into the lake during high rainfall events.

Aeolian dust

Aeolian dust could contribute to some of the grains in the sediment core as well, either from Australia or New Zealand. Grain size averages indicative of these origins are, 10–13 μm, 17–18 μm 23–24 μm, 25 μm as identified by Marx et al. (2009). These size ranges are from 4 phases identified from Marx et al. (2009) from deposits on Old Man Range in the southern South Island. The average grain size and identified modes along with mineral fingerprinting can be used to interpret wind strength from Australia and periods of aridity and heightened dust (Hesse, 1994; Marx et al., 2009). Adelaide Tarn is a potential locality for dust fall and preservation. Further work on particular size fractions and fingerprinting could be done here.

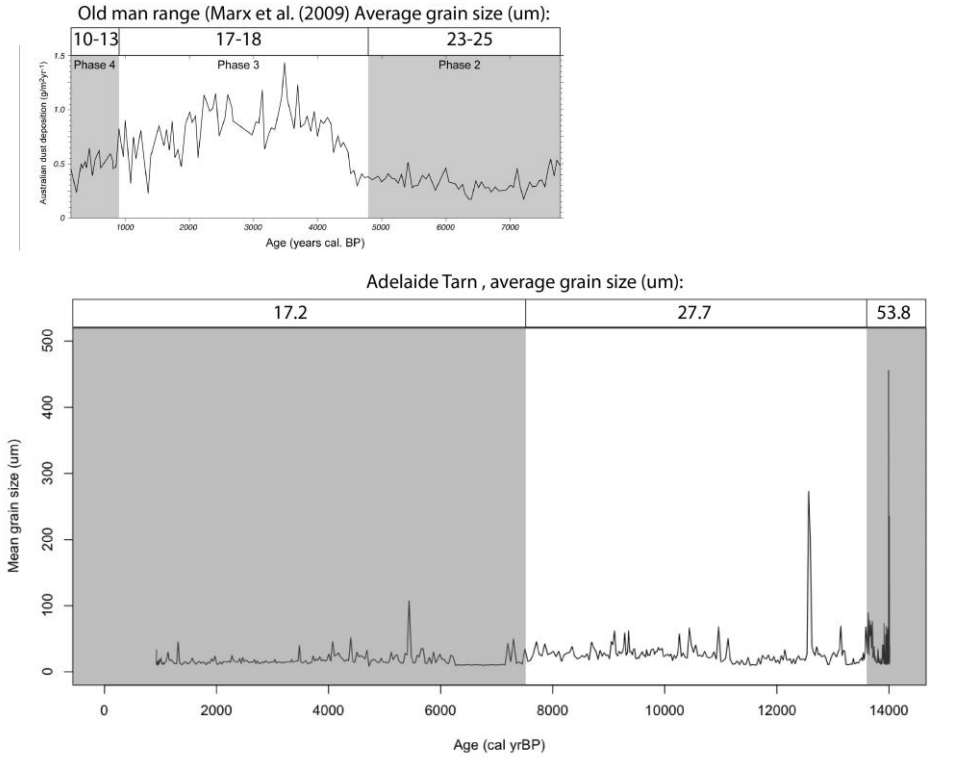

Figure 4.9 The top graph shows the three of the four phases of Australian dust deposition at Old Man Range (over the last ~7,000 cal years) and average grain size is located at the top of each phase (Marx et al., 2009). Adelaide Tarn results are plotted in the bottom graph with three main zones of grain size, and the average grain size in micrometres is reported at the top of each zone.

The Adelaide Tarn record extends to ~14,000 cal yr BP but does show broad overlap with the average grain sizes of the Old Man Range study (Fig. 4.11). Zone 1 of Adelaide Tarn has an average grain size of 17 μm which is much the same as that of Old Man Range phase 3 (~17 μm). At ~4800 cal yr BP, phase 2 of the Old Man Range study, shows an increase of average grain size to 23 to 25 μm, and Adelaide Tarn sediments also show this increase in size (27 μm) but a little prior to that of Old Man Range (Fig. 4.9). If these modes represent dust influx, then Adelaide Tarn appears to have a lead on dust deposition in comparison to that of Old Man Range. The Old Man Range is located south of Adelaide Tarn and this could explain the arrival of dust sized particles to Adelaide Tarn before that of Old Man Range. The belt of westerly wind flow could be slowly migrating southward in the New Zealand region over this time (which relates in part warming temperatures and increased aridity over Australia).

Chapter 5. Biological and chemical properties, and palaeoenvironmental interpretations

5.0 Introduction

In this chapter I outline the biological and chemical properties that have been analysed: these are plant macrofossils and carbon and nitrogen isotopes, respectively. The biological and chemical properties are split into two sections.

5.1 Plant macrofossils

5.1.1 Definition of a plant macrofossil

The definition of a macrofossil is plant material that can be seen by the naked eye or under a low-power microscope, unlike a microfossil. The magnification that might be required for a thorough identification is reasonably low and rarely exceeds x 500 (Grosse-Brauckmann, 1986). Plant macrofossils are whole or fragmented parts of plants such as leaves, stems, flowers, roots, fruit, and bark that are transported by wind or water (Greenwood, 1991). Macrofossils of lower plants such as liverworts, lichens, mosses, and algae can also be preserved under suitable conditions (Birks, 2001). Plant macrofossils are a direct imprint of their in-situ assemblage (taking into consideration the individual preservation levels of each species) and the environment that has allowed the growth of those particular species (Greenwood, 1991).

5.1.2 The use of plant macrofossil assemblages for palaeoenvironmental reconstruction

If plant macrofossils are found in a sediment core they can be potentially of great use in developing a comprehensive palaeoenvironmental record, and can confirm or support evidence from pollen-based reconstructions (e.g. Newnham et al., 1995; Velle et al., 2010). The stratigraphic position of the plant fragments is an

indication of the plant assemblages growing locally to the site as they are comparatively larger and heavier than pollen and are usually not transported far from their source plant (Birks & Birks, 2003). The composition of the floral assemblages can be used to infer the environmental conditions at the time of deposition. By studying modern analogues and working out their optimum habitat based on certain environmental conditions, we can assume the same for past plant assemblages and changes in these (Velle et al., 2010).

5.1.3 Taxonomic bias of fossil records

It is important to understand the causes of bias in plant macrofossil assemblages in order to make the best palaeoenvironmental interpretations and not rule out species that may have little to no abundance or overrepresentation. Not only does preservation of plant macrofossils vary between different plant species, but also different parts of the same plant may be preserved to varying degrees. Specific parts of plants require a certain type of structure that is dependent on its function. Strong lignified cells such as stems decay more slowly and are more readily preserved in comparison to other softer tissue organs such as the stamens of flowers (Greenwood, 1991). For this reason it can be difficult to identify a single fragment down to a species level as the distinguishable morphological features typically have degraded. The varying degrees of preservation among different species can influence the assemblage by either an over or underrepresentation of a particular species (Steart et al., 2009).

The physiochemistry of a leaf is the main driver of leaf decay rates and the physiochemistry includes the chemical make up of the leaf and its structure (Steart et al., 2009). Relevant chemical components of the leaf include (1) lignin to nitrogen ratio, (2) lignin and cellulose content, (3) lignin to manganese concentrations, and (4) nitrogen and potassium content. If the species has high lignin and low concentrations of nitrogen, phosphorus, and manganese (1, 2 and 3), the decay rate is much slower than species with the reverse composition. Plant materials with higher concentrations of nitrogen and phosphorus are more prone to microbial attack (Steart et al., 2009). Structural components of the leaf include cuticle thickness and hardness. The environment into which the fragments are

being deposited also has an influence on the rate of decay of all species, and environmental factors include temperature, nutrient availability, aerobic or anaerobic conditions, burial and water saturation. An anaerobic and fast burial allows a slower decay rate (Steart et al., 2009). Plant organs of the grass family have low lignification and will be poorly represented in fossil assemblages. Grass fragments decay faster than lignified materials and therefore cannot be identified to a species level if some have been preserved and these can only be grouped as *Poaceae* (McGlone, 2001). Different species can create bias of fossil assemblages through processes associated with abscission in relation to the rate of the shedding of leaves and seed mast years.

The varying degree of leaf retention between species can influence the fossil assemblage at the time of deposition by either over or underrepresentation. An example of varying retention times can be seen in the *Nothofagaceae* family where the leaf-fall production is the same between *Nothofagus menziesii* (silver beech) and *Nothofagus fusca* (red beech), but the tree retains the leaves for different time periods. The retention time on a red beech tree is approximately 12 months and a mature silver beech tree retains the same leaves for 3 to 5 years (Dawson, 1988; Sweetapple & Fraser, 1992). New Zealand *Nothofagus* species are known for their seed mast years where on average every 4 to 6 years they produce vast amounts of seeds, hence biasing the fossil assemblage for this time. Red and silver beeches have been found to have different mast years (Beggs, 1999). The size and nutritional value of red beech seeds are also more appealing to predators therefore promoting their underrepresentation in the fossil record and possible reduction of regeneration potential (Beggs, 1999).

5.1.4 Modern analogues of species found at Adelaide Tarn

This study uses an assemblage approach to interpret plant macrofossils, whereby past environments are inferred from modern biological assemblages and their known optimum habitats. A reference collection of modern analogues is used to identify the fossil material and the associated assemblages are then used to determine the environment or climate at the time of the deposition (Birks et al., 2010). In this section, photographs of reference species from the University of Waikato Herbarium were used to represent the species identified in the Adelaide Tarn sediment core (refer to Appendix B for UoW herbarium references species used). The present-day alpine herbs and shrubs observed around the lake are outlined also according to their optimum habitat parameters, although with exceptions of *Poaceae* and *Bryophytes*, these plants were not recognised in the assemblages (and hence not illustrated below). I have addressed the present-day environments of each species (optimum temperature, soil fertility, light dependence and aridity), altitudinal ranges and common associated species. The species identified are divided into (i) subalpine and (ii) alpine shrubs and herbs. The alpine shrubs and herbs are grouped together based on the two main environments observed around the lake at present. The work by Druce (1985) can also be used as an indicator of modern assemblages around Adelaide Tarn.

Subalpine species – Modern analogues of fossil species found in the core (leaves shown are ~7 to 15 mm in length)

Nothofagus fusca **(Red beech)**
Light dependence: High
Temp: Moderate temperatures
Aridity: Moderate
Soil fertility: Moderate
Altitudinal range: Sea level to <1000 m
Associated species: *Dracophyllum traversii, Phyllocladus alpinus, Coprosma sp. Libocedrus bidillii,* Mosses, liverworts and lichens. Simple forest type.
References: Dawson, 1988; Wardle, 1991

Nothofagus menziesii **(Silver beech)**
Light dependence: High
Temp: Mean Jan temp of 11°C (cold tolerant)
Aridity: High rainfall
Soil fertility: Low to moderate
Altitudinal range: Sea level to tree line (950-1250 m in South Island)
Associated species: *Dracophyllum traversii, Phyllocladus alpinus, Coprosma sp. Libocedrus bidillii,* Mosses, liverworts and lichens. Simple forest type.
References: Dawson, 1988; Wardle, 1991; Neuner & Bannister, 1995; Cullen et al., 2001

***Nothofagus solandri var. cliffortioides* (Mountain beech)**
Light dependence: High
Temp: Cold tolerant
Aridity: Tolerant of dry conditions
Soil fertility: Low
Altitudinal range: 500 m to >1250 m
Associated species: *Coprosma spp.* Species poor
References: Dawson, 1988; Neuner & Bannister, 1995; Cullen et al., 2001

***Libocedrus bidwillii* (Mountain cedar)**
Light dependence: High
Temp: Cold tolerant
Aridity: Moderate to high rianfall
Soil fertility: Moderate
Altitudinal range: 250 m to tree-line (1250 m)
Associated species: *Nothofagus* forest
References: Haase, 1986

***Phylocladus alpinus hook* (Mountain toatoa)**
Light dependence: Moderate to high
Temp: -1 to 10 ℃
Aridity: High rainfall
Soil fertility: Moderate
Altitudinal range: Lowland to 1500 m
Associated species: *Nothofagus* forest
References: Mark and Adams, 1973

***Dracophyllum longifolium* (Mountain neinei)**
Light dependence: Moderate
Temp: -1 to 10 ℃
Aridity: High rainfall (found in poorly drained soils and some peaty sites)
Soil fertility: Low to moderate
Altitudinal range: Low alpine to >1250 m
Associated species: *Nothofagus* forest, extends above tree-line into mixed snow tussock
References: Mark & Adams, 1973

Boggy environment

Empodisma spp. and *Chionochloa spp.* species were found in the wetter areas of the lower slopes around the lake, where these species require waterlogged and poorly drained areas to grow. Both species are cold tolerant (-1 to 10℃) and cover a wide range of altitudes, from sea level to low alpine (>1250 m) (Mark & Adams, 1976).

Alpine herbs within the cirque

Hebe spp., Coprosma spp., *Celmisia spp*., *Phormium cookianum*, *Astelia spp*., *Aciphylla spp*., and *Olearia colensoi* were all observed in the well-drained lower slopes of the cirque basin. These high alpine species can withstand temperatures ranging from -1 to 10 ℃, relatively dry and infertile soils, and frequent freeze-thaw days (Marks & Adams, 1973). The altitude ranges for these species are from 800 to 1500 m asl and they are found in high rainfall areas. *Phormium cookianum* and *Astelia spp.* can also be associated with poorly drained soils on the outer perimeters of boggy areas and can be found not far from tree-line.

5.1.5 Methods

Separation from sediment

To view the plant macrofossils, separation from the surrounding sediment by sieving was required. Firstly, 12 x 12 cm squares of 90 μm mesh were cut up for each of the 113 samples (every 5th centimetre down the core). A funnel was attached to a stand and clamp system to allow for ease of movement. The <90 μm fractions were caught in a container underneath the funnel and these were put aside for future pollen analysis to be undertaken for another study. Mesh was placed inside the funnel and the sample was placed on top of this. Small quantities of samples were rinsed through the mesh (with deionised water) to minimize clogging. Once the whole sample was rinsed through the mesh then the >90 μm fraction was put into a labelled container ready for plant macrofossil analysis.

Sorting and identification

The >90 μm fraction of each sample was viewed under a high-powered stereomicroscope with a camera set-up. Samples were placed onto a 5 x 5 mm grid transparent slide with 2-5 drops of water. Fragments of the same likeness were grouped together with possible identification along the way. A series of books, articles, and reference material from the University of Waikato Herbarium was used to identify the fossil fragments. Fragments or whole fossils of the same species were photographed and then put into glass vials labelled according to the core depth of the sample. All fragments that were identified were noted down along with their abundance and size. Professor Bruce Clarkson, a very senior botanist at the University of Waikato, helped with the final identification of the species.

Abundance scale

The plant macrofossil data were unable to be represented as per volume or area because of the range of sizes of fragments and the different levels of decay. There was a large abundance of small grass fragments (2−3 mm) of unknown species

within each of the samples and only 1−6 large leaf fragments (7−15 mm). The fragments were quantified by relative abundance but I had to take into consideration the size ranges and the larger abundance of grass fragments. Based on mass and size, I calculated that ~7−8 fragments of grass are the equivalent of one whole leaf so that the assemblage did not appear to be dominated by grass fragments. A scale from 1−5 was assigned so the data were plotted as relative abundances down the core. The numbers of the index represent their abundance: (1) rare, (2) some, (3) many, (4) common, and (5) abundant.

Plotting data

The data from each of the 113 samples, for the species identified, were plotted in "R" against the core chronology to view the changes in the species and to identify species assemblages.

5.1.6 Results

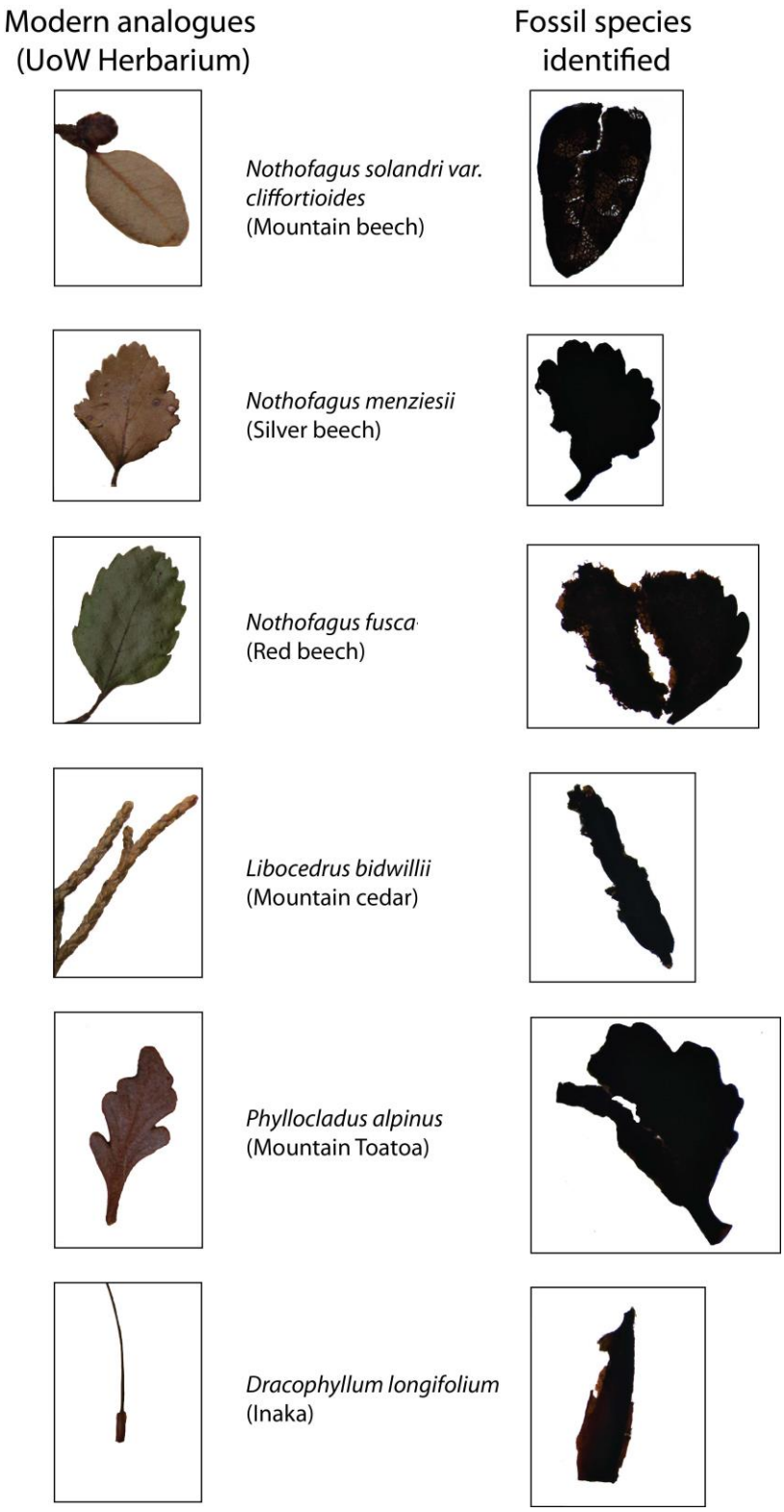

Figure 5.0 Fossil species identified in the core and the associated modern analogues used from the University of Waikato (UoW) Herbarium.

Identification and preservation

There were a number of well-preserved plant macrofossils in the core that were reasonably easy to identify based on reference material and journal articles (Fig. 5.0). Species of the *Nothofagus* family were easily identifiable because of the distinct toothed leaves and the unique venation pattern. *Libocedrus bidwillii* was relatively easy to recognise because of the tightly coiled leaf pattern, and when a leaf is broken off it has a distinct fibrous structure. The three *Phyllocladus alpinus* leaves that have been identified were difficult as they have a similar leaf morphology to that of *Nothofagus menziesii*.

There was also a large quantity of other plant macrofossils that had decayed more than others, or materials that were too small to identify. It was noticed that species of the *Poaceae* family were not well preserved and were only recognisable by the parallel ribbing in the very small fragments (2−3 mm) (Fig. 5.1A). The organic bands were comprised of tangled mosses and liverworts that appeared to have been preserved quite well (Fig. 5.1B).

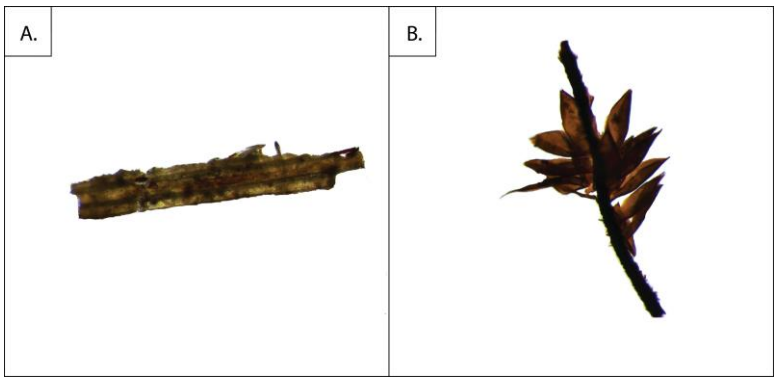

Figure 5.1 (A) A photograph of a piece of grass showing parallel ribbing, and (B) one of the many types of mosses/liverworts found in the organic layers (1–2 mm).

A number of very minute (<2 mm) leaves were found throughout the core and these are thought to be of the *Hebe* (or *Veronica*) genus. The minute *Hebe* leaves found are very well preserved and appear to be quite robust and reasonably firm.

The leaves all have a distinct serration on the perimeter of the leaf and these morphologies point towards the tip (Fig. 5.2).

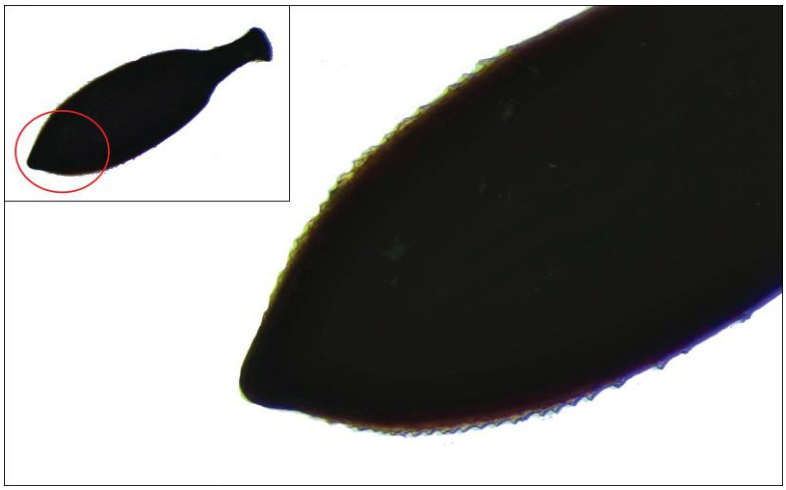

Figure 5.2 Photograph of one of the minute (<2 mm) leaves, identified here to be of the *Hebe* genus, with a close up of the distinctive serration.

There were very noticeable differences in the levels of preservation of the three *Nothofagus* species found. *N. menziesii* appeared to have the best preservation and the double toothed morphological feature of the leaf enabled it to be distinguishable from the rest of the *Nothofagus* species. The *N. menziesii* leaves were firm and mostly intact with little to no skeleton fossils. *N. fusca* leaves were far more fragile than the *N. menziesii* and they seemed a lot softer and easier to break. There were only three identifiable *N. fusca* leaves found in the entire core in comparison to the high numbers of *N. menziesii*. Leaves of *N. solandri var. cliffortioides* were identified mainly by the distinctive venation pattern and the oval shape of the leaf (no serrations, unlike the other two species). The fossil leaves of *N. solandri var. cliffortioides* were only seen in a skeletal form and hence suggesting a different level of decay and preservation to that of the other two *Nothofagus* species (Fig. 5.0).

Changes in relative abundance of the major species found

Nothofagus species were found to be the most dominant tree species throughout the core. *N. menziesii* was the most abundant of the three, with *N. fusca* and *N. solandri var. cliffortioides* relatively rare in comparison (Fig. 5.3). The assemblages also included many unidentifiable *Nothofagus* fragments that contributed to the overall dominance of this taxon over macrofossils of other tree species (refer to Appendix C for absolute abundance of plant macrofossils).

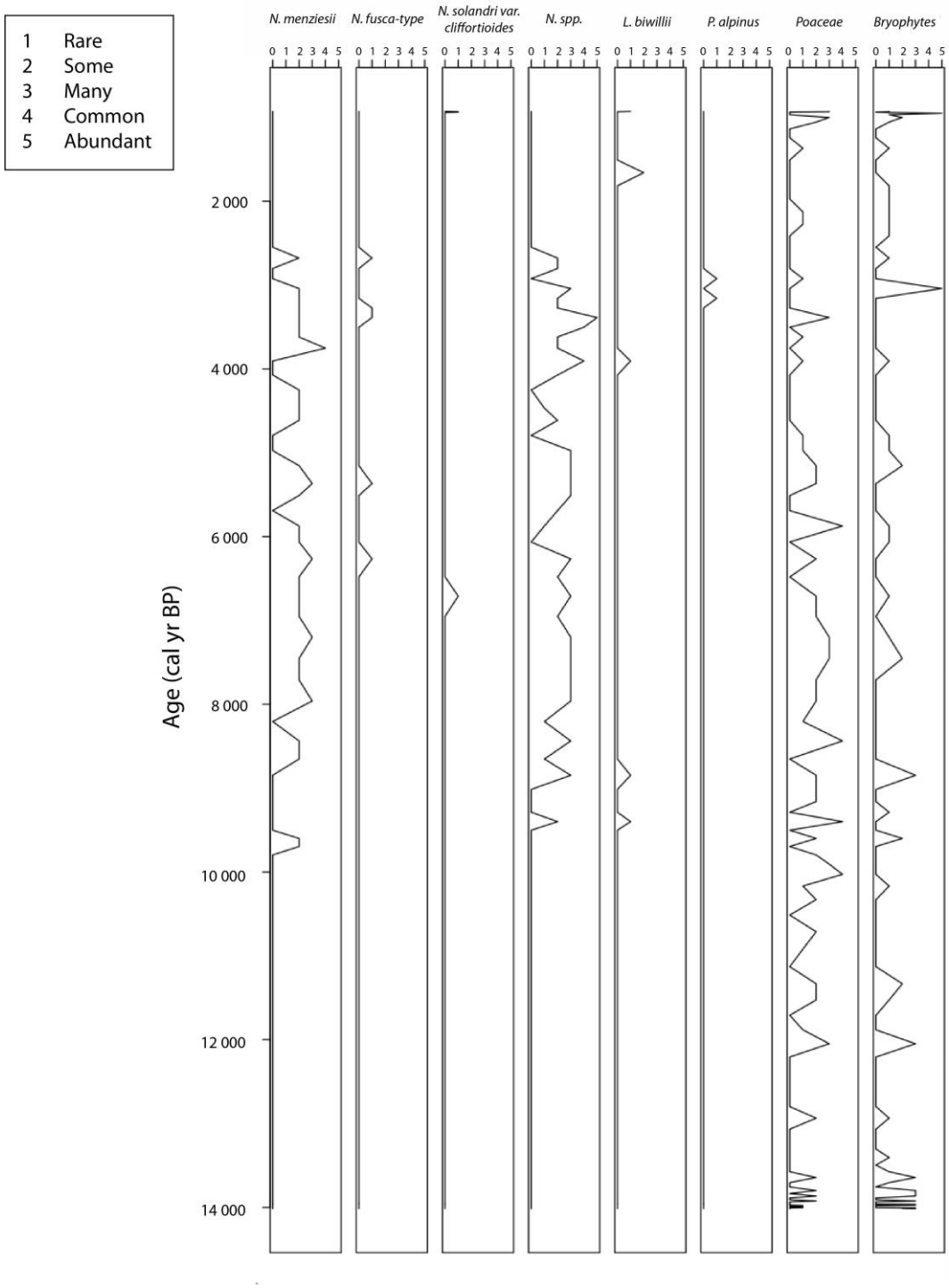

Figure 5.3 Graph showing the relative abundance of plant macrofossils of the major species identified throughout the core, and the changes of these since ~14,000 cal yr BP to the top of the core.

L. bidwillii and *P. alpinus* leaves were also relatively rare in comparison to *N. menziesii* leaves with only 5 and 2 leaves found, respectively. *Poaceae* and bryophytes (mosses and liverworts) sustained comparatively the same abundances throughout the core and were overall the major taxa.

The analysis of this record is subdivided into three distinctive zones based on major shifts in the plant macrofossil assemblages (Fig. 5.4, below).

Zone 1: ~14,000 cal yr BP to ~10,000 cal yr BP

There are absolutely no macrofossils from tree species in this zone, but there are abundant *Poaceae* and bryophyte remains. The *Poaceae* and bryophytes dominate this assemblage and range from 1 to 3 on the relative abundance index.

Zone 2: ~10,000 cal yr BP to ~2400 cal yr BP

Tree species abruptly appear at ~10,000 cal yr BP and at the same time there is a steady decline in grass species until 2400 cal yr BP. *Nothofagus spp*. dominate the assemblage and *N. menziesii* is the most abundant, ranging between 1 and 4. *N. fusca* appears at approximately 6200 cal yr BP and disappears again at 2400 cal yr BP. There is one *N. solandri var. cliffortioides* leaf located at approximately 6800 cal yr BP. *L. bidwillii* appears at 10,000 cal yr BP and disappears again from 8900−4000 cal yr BP.

Zone 3: ~2400 cal yr BP to ~700 cal yr BP

All tree species abruptly disappear in this section except for one leaf of *N. solandri var. cliffortioides* (at the top of the core) and two of *L. bidwillii* (located at ~2800 cal yr BP and in the topmost core sample). The assemblage has changed to be dominated by *Poaceae* and bryophytes.

5.1.7 Discussion – changes in vegetation assemblages through time and palaeoclimatic implications

The results in the three major zones are synthesised and inferences are made on the shifts in species assemblages with regard to changes in the catchment, preservation of different species, and changes in local climate.

Zone 1: ~14,000–10,000 cal yr BP

This zone includes the obvious formation and early development of the lake. Prior to ~14,000 years ago the lake had not formed but at that time or earlier there was very likely local glacier development induced by cool temperatures coincident with the early phase of the Antarctic Cold Reversal (ACR) chronozone between either ~14.6 and 12.8 cal. ka or ~14.1 and 12.4 cal. ka (Newnham et al., 2012; Lowe et al., 2013). However, approximately 14,000 years ago, the glacier began to retreat and in the process glacial till or other debris were washed into the pre-carved basin until ~13,337 cal years BP. The surrounding catchment was unstable and loose bedrock and detritus continued to be washed or blown into the basin as temperatures warmed through to ~10,000 cal yr BP. Because of catchment instability there was little to no soil formation for tree species to occupy. Grass and shrub species dominate the assemblages in this zone and they are indicative of cooler environments (Fig. 5.4). The lack of tree macrofossils could be attributed to a lag in the response time of the forest species, and therefore a delay in the ascent of the tree-line (see McGlone & Basher, 2012). If there were trees in the vicinity at the time then these may have been destroyed by the rapid sedimentation (in-washes of larger grain size, see Chapter 4) derived from the retreating glacier.

Zone 2: ~10,000−2400 cal yr BP

There is an abrupt shift from the grass and shrub assemblage to a tree-dominated assemblage. *Nothofagus menziesii* is far more evident than other tree species present in this zone. The structure of *N. menziesii* leaves allows for an increased

hardening prior to winter and therefore they are more frost tolerant and grow at higher altitudes (Neuner & Bannister, 1995). Other than two fragments of *L. bidwillii*, the forest diversity is relatively sparse which suggests that the temperature was still a bit too cold for other tree species to occupy the higher altitudes. *N. fusca* appears at ~6200 cal years BP which is an indication of warming temperatures allowing red beech to ascend in altitude. The lack of red beech from 10,000−6200 cal yr BP could also be attributed to the decay rates of the different *Nothofagus* species. The chemical structure of the leaves can determine the rate of decay and therefore affect the overall assemblage, as noted in the introduction. Leaves with higher nutrient to lignin ratios have a faster rate of decay in comparison with leaves that have higher amounts of lignin (Steart et al., 2009). The leaves of red beech have notably higher concentrations of nitrogen and phosphorus in comparison to those of silver and mountain beech (Heine, 1973). The higher decay rate of red beech leaves could mean that they are underrepresented in the lake sediments and, in fact, red beech may have been growing in close proximity to the lake. The potential underrepresentation problem means that I cannot rule this out.

The appearance of red beech suggests that the tree-line would have been higher than that of the present day and the forest has diversified with more light penetration allowing for a richer diversity (Fig. 5.4). Adelaide Tarn is 250 m higher than the present day altitudinal limit of *N. fusca* (1000 m) and, using the observed environmental lapse rate of 0.47˚C/100 m, produces a temperature of ~1.2˚C warmer than present day (R.M. Newnham pers. comm., 2013). This is a minimum as *N. Fusca* could have potentially grown at higher altitudes around the lake. There is one *L. bidwillii* leaf in the core at ~4,000 cal yr BP and *Phyllocladus alpinus* appears at approximately 2500 cal yr BP. The catchment is stabilising and there is some soil formation allowing for a species-rich environment with abundant grass and shrub species around the lake, and the tree-line is becoming more stable. The erosion indices of grain size and magnetic susceptibility both decrease during this period and these results suggest that there are better conditions within the lake to allow for the preservation of plant macrofossils (see Chapter 4).

Zone 3: ~2400 cal yr BP – ~700 cal yr BP

The shift of the species assemblage back to a *Poaceae*- and *bryophyte*- dominated assemblage is contrasted with the disappearance of the tree species apart from minor constituents of *L. bidwillii* and *N. solandri var. cliffortioides*. This change is consistent with observed vegetation patterns at the site today, implying that they became established during this zone. This zone is inferred to reflect a degradation of the climate and the tree-line is forced to descend because of slightly colder temperatures (Fig. 5.4). Tree macrofossils are usually unable to reach the lake because of the new position of the tree-line, which is similar to that of today. The occurrence of the mountain beech (*N. solandri*) in the sediments may be because it has less dense leaves than silver beech and hence could have been blown in by strong winds from nearby sites (cf. Dawson, 1988). The single occurrence of *N. solandri var. cliffortioides* is most likely an outlier. The presence of *L. bidwillii* may be because of remnant patches above the present-day tree-line. The shift to grass dominated species assemblage is because they are more tolerant of colder conditions than the local tree species.

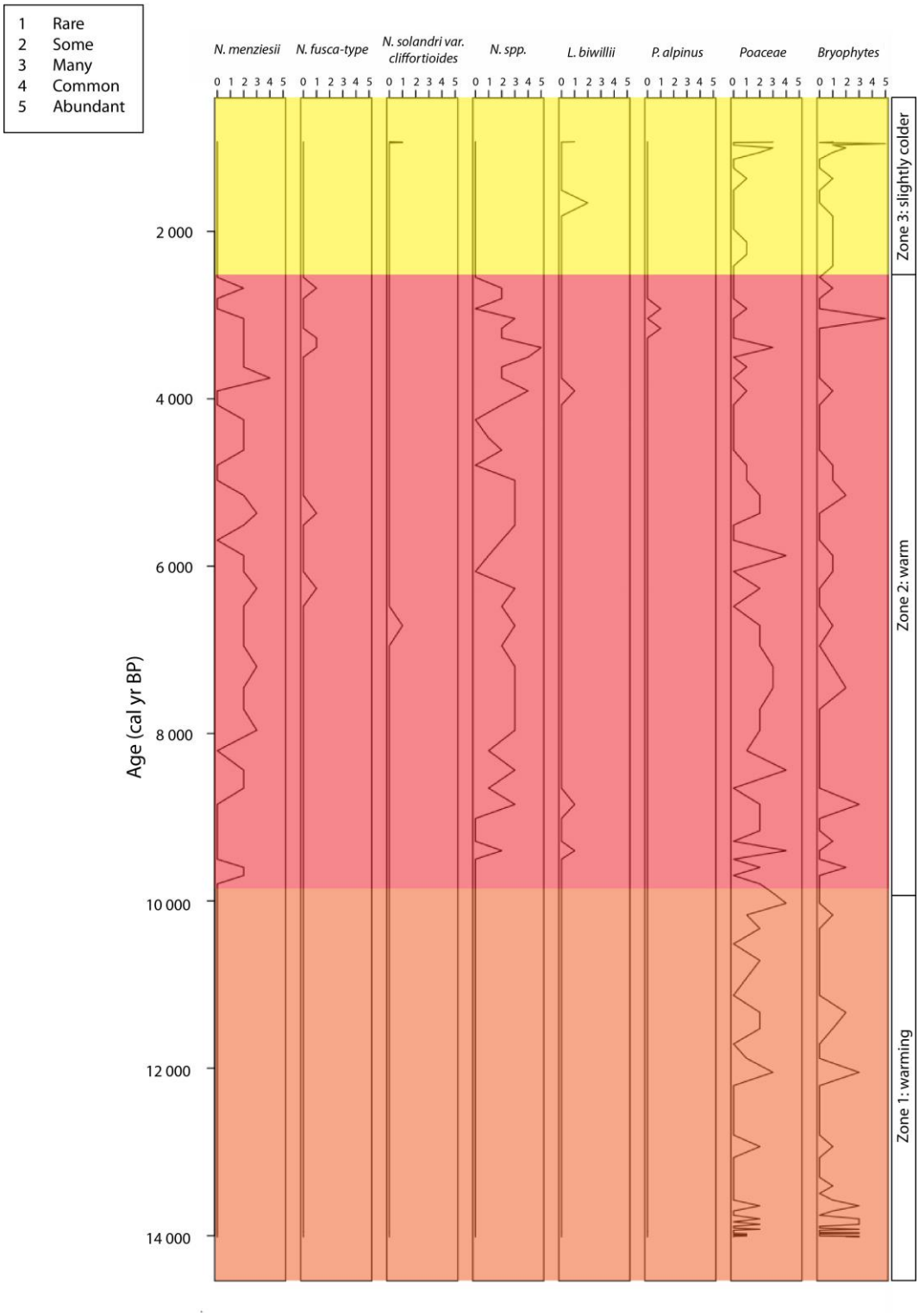

Figure 5.4 Plant macrofossil abundances throughout the core and the separation into three temperature zones based on major shifts in species assemblages.

5.2 Carbon

5.2.1 Introduction and background

The main source of organic matter entering a lake is derived from aquatic (in-lake) and the catchment vegetation. Aquatic species (non-vascular) are cellulose rich and have little-to-no lignin in comparison to vascular plants in the catchment such as grasses, shrubs and trees. When non-vascular and vascular plants are preserved within a lake they tend to hold these distinct signatures and it is possible to distinguish between the two in the sediments (Meyers & Teranes, 2001).

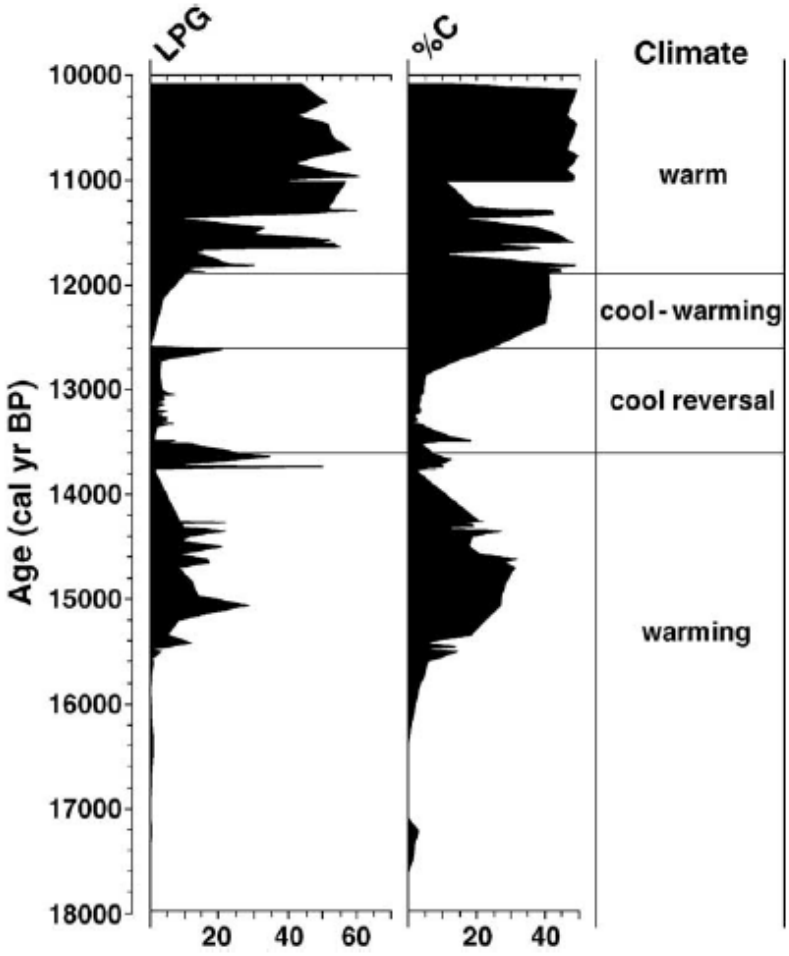

Figure 5.5 Lowland podocarp- to grass ratio (LPG) and carbon content (%) from montane Kaipo Bog in eastern North Island, and climatic conditions through time that influence in part the changes in these proxies (from Hajdas et al., 2006).

Carbon percentage was measured at Kaipo Bog and presented by Hajdas et al. (2006). During a cool period such as the cool reversal (from 13,600 to 12,600 cal yr BP) the carbon percentage was relatively low and increasing as the conditions warmed (12,600−11,900 cal yr BP) (Fig. 5.5) (Note that the timing of the cool episode has been revised subsequently to between 13,800 cal yr BP and 12,600 cal yr BP by Lowe et al., 2013.) In the cool warming interval (12,600−11,900 cal yr BP), podocarp species start to establish and become more prominent as the conditions progressively warm (Fig. 5.5). The warmer temperature allows for the expansion of warm taxa that are suited to this new temperature regime and this is also reflected in the increase in percentage carbon within the bog. Carbon content has become uniform from 11,900 cal yr BP through to 10,000 cal yr BP and is coincident with the sustained increase in podocarps (Hajdas et al., 2006) (Fig. 5.5). The increase in carbon percentage is attributed to higher levels of biological productivity in the bog and catchment. The Kaipo Bog carbon record is driven also by changes in substrate and hydrology and Hajdas et al. (2006) argue that the two are connected.

5.2.2 Methods

Carbon isotope samples were analysed from every 5th centimetre in the core. Samples 2−3 g in mass were taken from the initial 1 cm slice and air dried for 2−3 days depending on the density. The samples were weighed again and ranged in mass from 0.6−4.1 g. Each sample was then ground using a mortar and pestle and in between samples the mortar and pestle were cleaned with 70% ethanol, then detergent, and airbrushed to remove excess liquid and particles. Samples were then weighed (using high-precision scales) for analyses of carbon content, δ^{13}C (C % and δ^{13}C were analysed from the same sample) and δ^{15}N analysis. The samples had different weights depending on their position in the core and ranged from 9 to 60 mg (Fig. 5.6). The samples were then separately analysed for C and δ^{13}C together, and then δ^{15}N by Anjana Rajendram (Waikato Stable Isotope Unit, WSIU, at the University of Waikato) using the LECO TruSpec carbon/nitrogen determinator.

Figure 5.6 Weighing a sample for carbon isotope analysis.

5.2.3 Results

Zone 1: 5.6−4.8 m (~14,000 cal yr BP)

The carbon content is low to moderate in this zone, ranging from 0.3% at the base of the core to 8% at the transition of the next zone (lithozone 2). The percentage carbon is highly variable at the base of the core and gradually increases through time (Fig. 5.7). This section of relatively low to moderate C content coincides well with lithozone 1 (inorganic grey silt/clay).

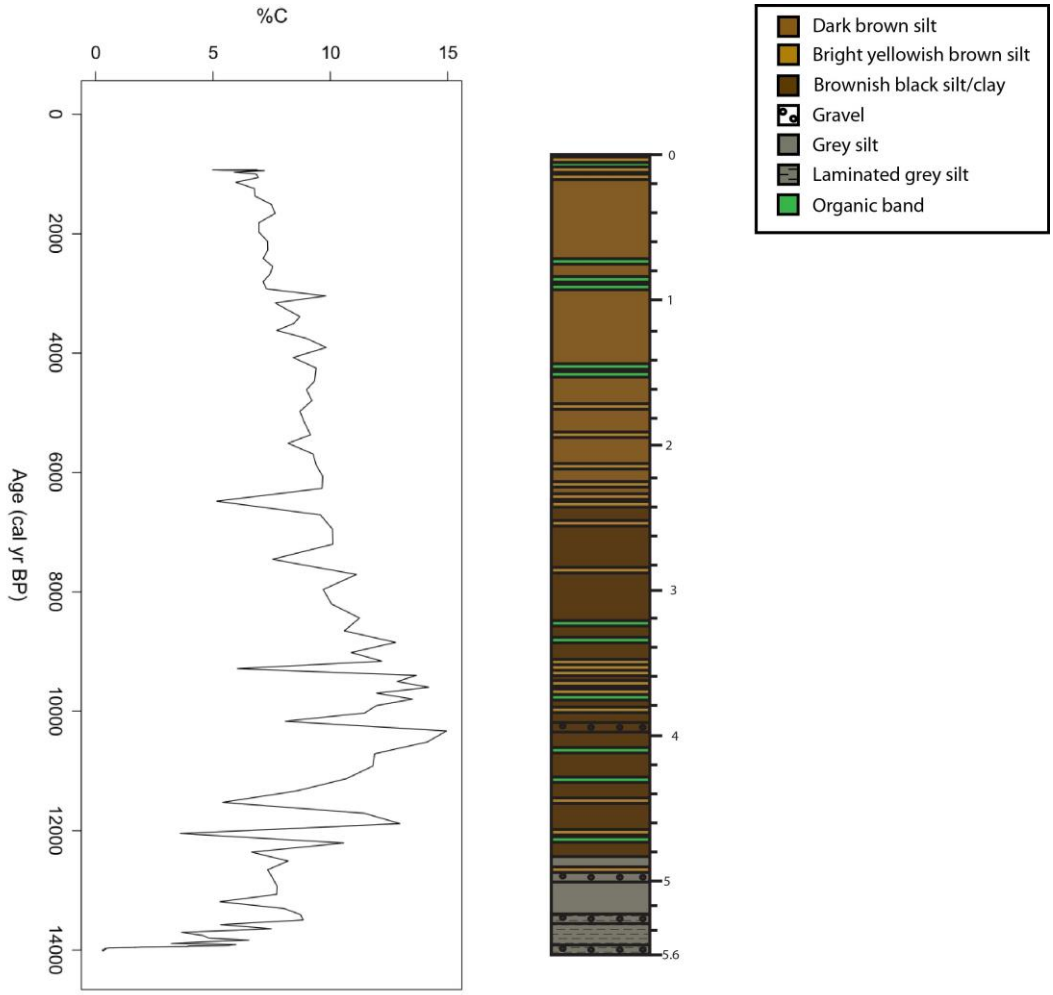

Figure 5.7 Changes in carbon content (%) through the core and showing marked changes with colour of lithozones.

Zone 2: 4.8−2.4 m (13,932−7709 cal yr BP)

In this zone the carbon content is very variable but in general increases and peaks at ~10,300 cal yr BP (15.0 %) and steadily decreases to the transition of the uppermost zone (zone 1). The marked decrease from 10 % carbon at 12,200 cal yr BP to 3 % carbon at ~12,000 cal yr BP is particularly noteworthy. The carbon content then increases to ~11 % around 11,800 cal yr BP (this zone of increased carbon overlaps the brownish black silt/clay of lithozone 2 (see Chapter 3). Another marked decrease occurs at 11,500 cal yr BP where carbon content drops to 5% (Fig. 5.7). The percentage carbon gradually drops from this point though time until an abrupt decline to ~8% carbon at the onset of the lithozone 3 at ~7709 cal yr BP.

Zone 3: 2.4−0 m (7709−~700 cal yr BP)

The carbon percentage has steadily decreased until the top of the core but is less variable than in the other two zones. Overall, there is a lower range in carbon (5−10%) than in the previous lithozone and this generally lower level of carbon is marked by the slight change in colour of the sediments to dark brown rather than the brownish black evident in lithozone 2. The lower values of carbon coincide with the top of the core (~5%) from 967 cal yr BP (Fig. 5.7).

5.2.4 Discussion – lake and catchment history

Zone 1: 5.6−4.8 m (~14,000 cal yr BP)

At the base of the core the percentage carbon ranges from 1% to 5% in the grey silt/clay lake sediments. The low carbon content is indicative of cool environmental conditions (coincident with the early part of the ACR) just prior to the formation of the lake and with little to no vegetation in the catchment yet (section 5.1.5). There are no trees in the vicinity of the lake basin from which remains could be transported and preserved and, if there were, the conditions of the young lake (not anoxic) did not allow for the preservation of these. The catchment was unstable and there would have been little to no soil formation to allow for the build up of other organic matter such as humus. Green & Lowe (1985) attributed low carbon in the basal sediments of Lake Maratoto (near Hamilton) to the soils in the catchment being low in carbon and little vegetation cover.

Zone 2: 4.8−2.4 m (13,932−7709 cal yr BP)

Zone 2 is representative of a warming climate, in which organic matter reaches the highest values for the entire core with a maximum of ~15 %. Formation of soils is promoted by an increasingly stable climate and is reflected by the increase in organic carbon content in the sediment. Organic matter has accumulated within the soils and been retained. Vegetation has developed around the lake margins and the tree-line has ascended (section 5.1.5). Humus and pollen that have been retained by the soils are now the main source of material being deposited into the lake rather than inorganic sediment particles that characterise the sediments of zone 1. Fragments of forest species, shrubs and herbs have been blown or washed into the lake, adding to the elevated carbon content in this zone, as high as ~15 % (section 5.1.5). The higher organic matter content can be seen by the darker colour of the sediments in lithozone 2, the darker grey shades (representing greater organic content) in the X-radiographs (Chapter 4), the abundance of plant macrofossils (described above), and the SEM micrographs (Chapter 3). The heightened carbon content in this zone and the ascending tree-line (marking

warming conditions) shows the same trend for the expansion of podocarps and the increasing carbon content from 12,600 to 10,000 cal yr BP at Kaipo Bog (Hajdas et al., 2006). The high content of carbon in the Adelaide Tarn sediments continues to ~7709 cal yr BP and the transition into zone 3.

Zone 3: 2.4−0 m (7709−700 cal yr BP)

In zone 3 there is a gradual decline in carbon content, but it is far less variable than in the previous two lithozones. The less variable results can be attributed to further stability of the catchment and less in-wash of terrestrial matter from soils and plant remains such as pollen, seeds and other plant material (plant macrofossils disappear at ~2400 cal yr BP, section 5.1.5). There is a distinct colour change as the sediments become dark brown rather than black/brown at ~2400 cal yr BP. The lake productivity in zone 3 is not so effectively "diluted" by the in-washing of allochthonous organic matter (section 5.1.5). Aquatic organisms have less carbon but a higher nitrogen ratio and this difference could explain the decrease in carbon in this section (this interpretation is speculative because total nitrogen content was not analysed) (cf. Meyers & Teranes, 2001). Hypothetically, the tree-line is forced to descend because of the slight climate deterioration and plant macrofossils are unable to reach the lake and therefore carbon contents decrease concomitantly in the lake sediments.

5.3 Carbon and nitrogen isotopes

5.3.1 Introduction and background

Assessing the carbon isotopic ($\delta^{13}C$) and nitrogen isotopic ($\delta^{15}N$) composition of bulk lake sediment samples can help in the interpretation of past lake productivity and give an indication of the source of organic matter entering the lake (Green and Lowe, 1994; Meyers & Teranes, 2001; Heyng et al., 2012). Where sites are characterised by particularly negative $\delta^{13}C$ (lacking allochthonous input), $\delta^{13}C$ alone can be used to interpret changes in lake productivity, as there is only one source (in-lake), not two (Heyng et al., 2012) (Fig. 5.8). Primary producers within the lake prefer to utilise ^{12}C from the dissolved inorganic carbon source (DIC) in their photosynthetic pathway. Removing ^{12}C from the DIC source consequently enriches the $\delta^{13}C$ pool. Assuming that this isotopic enrichment of DIC is more important than changes in the composition of atmospheric CO_2 (which exchanges with DIC) over the same period, increases in $\delta^{13}C$ of sedimentary organic matter may reflect changes in productivity (Meyers & Teranes, 2001; Leng & Marshall, 2004; Heyng et al., 2012). However, there are several limitations in such interpretations: (i) exchange with atmospheric CO_2 is neglected, and (ii) changes in overall productivity will increase the organic carbon percentage in the core, such that more depleted $\delta^{13}C$ values will correlate with increased productivity. Thus, for this approach to be valid, the $\delta^{13}C$ signature must be corrected for the contribution of allocthonous C sources. This is not possible here, and therefore such interpretations are beyond the scope of the present study.

A study undertaken by Striewski et al. (2009) saw a few marked changes in $\delta^{13}C$ throughout a core taken from Lake Pupuke in Auckland. In the top 22 cm of the core there was a shift to more positive $\delta^{13}C$ and Strieweski et al. (2009) attributed this shift to increased eutrophication of the lake where primary productivity has picked up, depleting ^{12}C from the DIC pool (brought on by anthropogenic influences). There are again more positive values of $\delta^{13}C$ further down the core but Striewski et al. (2009) interpreted these to be an influx of allochthonous organic matter input during cool periods. However, this study failed to account for

the natural variance of $\delta^{13}C$ (ca. -35 to -20 per mil) which exceeded the range of variance in their data. Furthermore, fluctuations of sedimentary $\delta^{15}N$ can give indications of the past oxygen concentrations of the lake especially during stratification, because N as NO_3^{2-} is quickly utilised as an electron acceptor under reducing conditions driving the enrichment of the residual N pool (Heyng et al., 2012). During anaerobic denitrification there is loss of nitrogen and associated fractionation. The remaining dissolved inorganic nitrogen (DIN) will be enriched in ^{15}N and the use of ^{14}N by primary producers enriches the ^{15}N organic matter (Heyng et al., 2012). $\delta^{15}N$ fractionates more than $\delta^{13}C$ and therefore produces a more coherent and stronger signal of the productivity. Fractionation of $\delta^{15}N$ is on average 3.4 per mil and 0.8 per mil for $\delta^{13}C$ (Hartland et al., 2011).

As previously discussed, the interpretation of bulk sedimentary $\delta^{13}C$ and $\delta^{15}N$ values are problematic because of the range of possible sources (and source signatures) and the natural variation inherent in them (Meyers & Teranes, 2001). There is also potential for diagenetic alteration of the sediments; for example, oxidation of organic matter by sulphate reduction and methanogenesis (Hollander & Smith, 2001). Broad changes in $\delta^{13}C$ can be ascribed to greater or lesser inputs of isotopically light substrates, such as filamentaceous algae, or more enriched materials such as allochthonous organic matter (Meyers & Teranes, 2001). Variations in N isotopes may be diagnostic of changes in in-lake processes such as denitrification, assuming that changes in atmospheric $\delta^{15}N$ over this period were not substantial (Heyng et al., 2006). McLauchlan et al. (2013) have shown that sedimentary $\delta^{15}N$ of N_2 over the Holocene declined globally from 15,000 cal yr BP to 7,056 cal yr BP at a rate of 0.25 kyr and from this point it has increased at a rate of 0.08 kyr. The natural range of variability for $\delta^{13}C$ in organic matter obtained from plants in C3 photosynthetic pathway is approximately -35 to -20 per mil (Leng & Marshall, 2004). Enzymatic processes act preferentially on ^{12}C, as with ^{14}N, and so sedimentary C has the potential to record changes in both production and within-lake processing of organic matter (respiration), where the fractionation of residual N and C isotopes exceeds the natural variation in the source signatures (Heaton 1986).

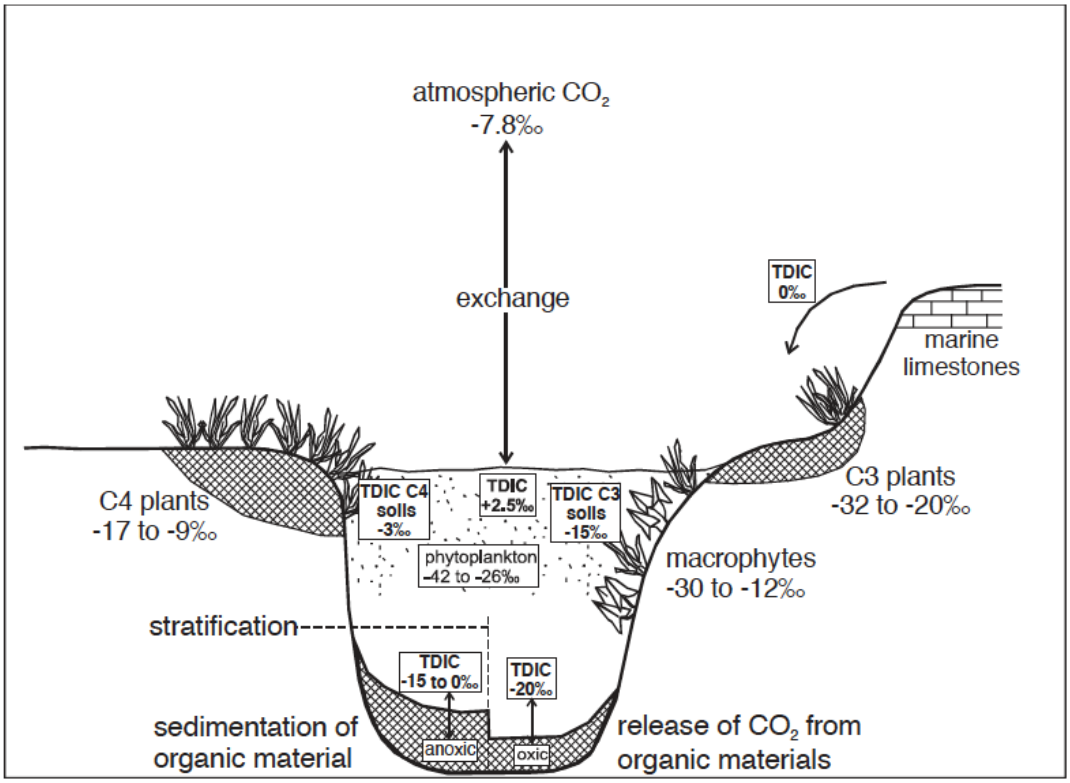

Figure 5.8 The average carbon isotope values entering a lake from a variety of sources. TDIC = total dissolved organic carbon. The dotted line represents a scenario of stratification and anoxic bottom waters. If anoxic then organic matter is more readily preserved and increases the amount in the sediment (from Leng & Marshall, 2004).

5.3.2 Methods

The methods for isotope analysis are stated in the methodology for preparation of carbon samples and measurement in Section 5.2.2.

5.3.3 Results

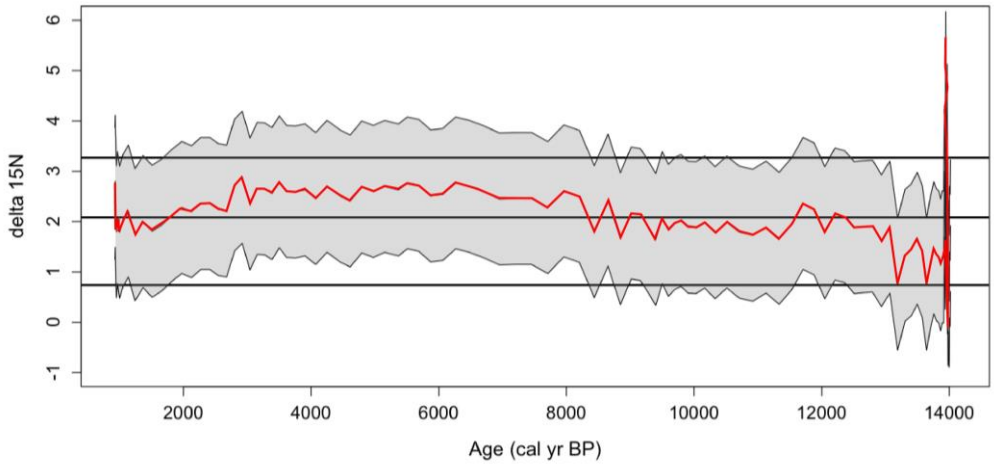

Figure 5.9 $\delta^{15}N$ values plotted in red against the calibrated ages of the sediments in Adelaide Tarn. The grey zones represent the ± 2 standard deviations uncertainty in the time series (refer to Appendix F for raw data).

The $\delta^{15}N$ results can be broken into two sections. From 13,932 cal yr BP onwards the $\delta^{15}N$ values exceed two standard deviations of the mean and are therefore true values as they are outside the natural variabilty range (Fig. 5.9). The $\delta^{15}N$ values from 13,932 to the top of the core are within the range of natural variability with a slight increase from 8000 through to 3000 cal yr BP (Fig. 5.9). Since trophic fractionation of $\delta^{15}N$ is of the order of 3.4 per mil, it is unlikely that these changes record profound shifts in the biogeochemistry of the lake system.

The $\delta^{13}C$ values (in red, Fig. 5.10), can also be separated into two major zones. From 13,932 cal yr BP onwards there is the same spike as $\delta^{15}N$ and they also exceed the upper standard deviations. The remaining $\delta^{13}C$ values are well within the range of natural variability (within upper and lower standard deviations).

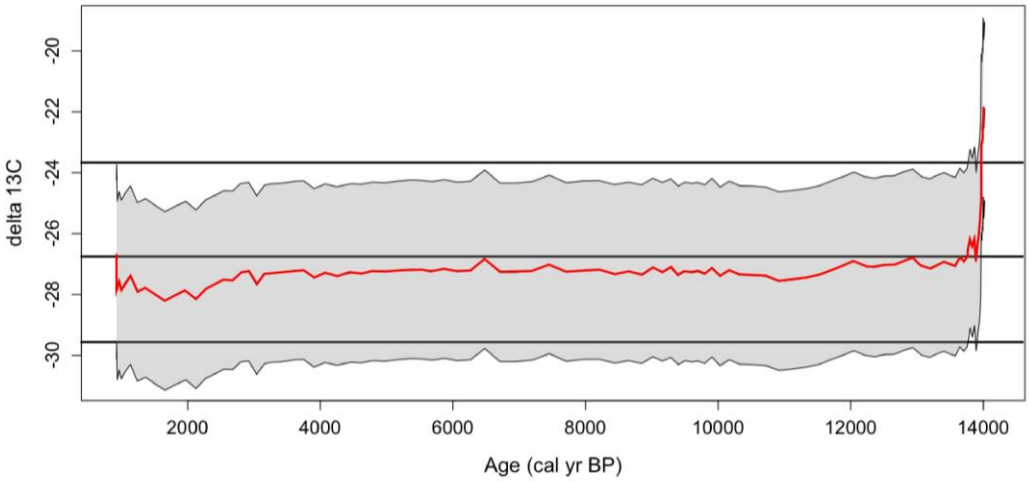

Figure 5.10 $\delta^{13}C$ values plotted in red against age of sediments and 2 standard deviations on either side (black wiggles). The middle black line is the average $\delta^{13}C$ value (-26.03 per mil) and the black lines above and below are the standard deviations (2σ), 2.93 per mil on either side of the mean.

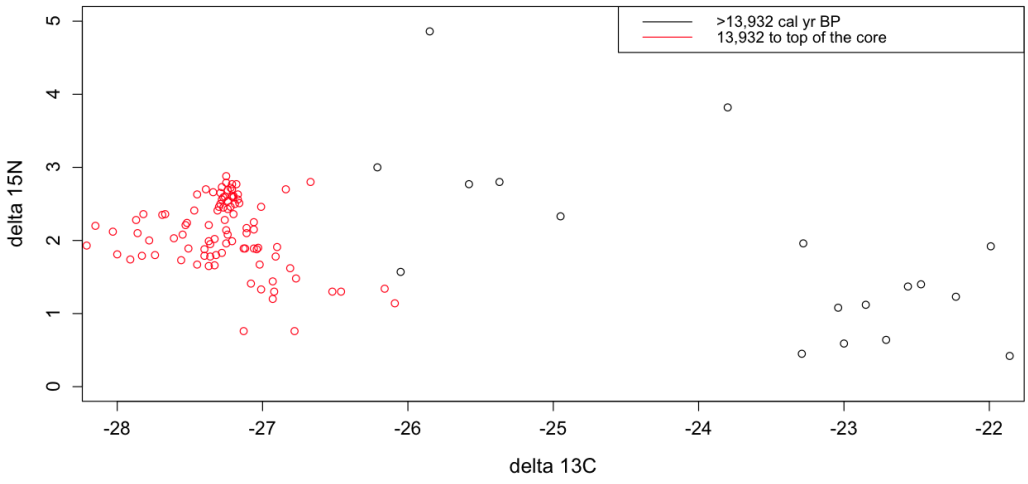

Figure 5.11 Is a representation of the two major populations is the $\delta^{13}C$ and $\delta^{15}N$ values and shows the distinct shift after 13,932 cal yr BP.

The population prior to 13,932 cal yr BP has more positive $\delta^{13}C$ values and the population after 13,932 cal yr BP shifts to more negative $\delta^{13}C$ values and middle range $\delta^{15}N$ (2-3 per mil) (Fig. 5.11).

5.3.4 Discussion

The large peaks in $\delta^{13}C$ and $\delta^{15}N$ values from before 13,932 cal yr BP onwards are prior or close to the initial stability (onset of primary production) of the lake. The results suggest that at the point where both isotopes reach values consistent with a terrestrial carbon source (13,932 cal yr BP) possibly associated with the onset of primary production within the lake (Fig. 5.11). Overall, these results imply a stabilisation of in-lake processes throughout the mid-to-late Holocene. The values of $\delta^{13}C$ from 13,932 cal yr BP to the top of the core are in the range of natural variability and, because of the lower fractionation (0.8 per mil) of this isotope, possible changes in primary production/respiration are not enhanced as much as those for $\delta^{15}N$ (3.4 per mil) which is more suitable for inferring changes in the redox status of the water body (Hartland et al., 2011). The slight increase of $\delta^{15}N$ from 8000 to 3000 cal yr BP may suggests a gradual increase of denitrification of the lake, or a natural change in the delivery of nitrate in the inflowing waters. The Adelaide Tarn $\delta^{15}N$ record (Fig. 5.9) shows the inverse of the broad global trend of $\delta^{15}N$ changes for lake sediments identified by McLauchlan et al. (2013): $\delta^{15}N$ declined globally from 15,000 cal yr BP to 7,056 cal yr BP and then increased.

Chapter 6. Synthesis: palaeoenvironmental changes since ~14,000 cal yr BP at Adelaide Tarn and comparison with other New Zealand climate records

6.0 Introduction

This chapter is a synthesis firstly of the stratigraphy and the physical, biological and chemical proxies measured on the 5.6-m long sediment core taken from the low-alpine lake, Adelaide Tarn, and their interpretation with regard to the history of the lake and its catchment. The Adelaide Tarn palaeoenvironmental record is summarised as a climate event stratigraphy (AT-CES) dating between about 14,000 cal yr BP and about 940 to >700 cal yr BP. This record is then compared with various records from a range of terrestrial archives (speleothems, peats, and lakes) at various latitudes and altitudes in New Zealand that span the last ~14,000 cal years. The findings from this research at AT contribute to climate records that are particularly lacking in the North-west Nelson region.

6.1 The Adelaide Tarn climate event stratigraphy (AT-CES)

6.1.1 Synthesis

The properties included in the synthesis are stratigraphy (including an age model attained using a spline function developed from a set of 15 ^{14}C ages, 14 of which were obtained from plant macrofossils), lithology, magnetic susceptibility, grain size (the proportion of grains >32 μm in diameter is chosen to represent this parameter), plant macrofossils, organic carbon content, and two isotopes ($\delta^{13}C$, $\delta^{15}N$). The aim is to identify relationships between all of the proxies measured. The stratigraphic zones assigned on the basis of changes evident in each property through the core record (from chapters 3, 4 and 5) have been summarised in Fig. 6.0. Grain size measurements were taken at highest resolution (every 1 cm down

the core) and other properties are lower in resolution, ranging between every 3 cm (magnetic susceptibility) and every 5 cm down the core (plant macrofossils, carbon content, and isotopes). Four broad climatic zones marking changes were identified (Fig. 6.1).

6.1.2 Stratigraphy and lithozones

The Adelaide Tarn sediment record begins at ~14,000 cal yr BP with 0.8 m of inorganic grey silts (lithozone 1) accumulating at a rate of 1.31 mm/yr which is relatively fast in comparison to those for the rest of the core. Relatively uniform, well sorted, fine grained grey sediment (with three gravel layers) comprising inorganic angular particles, with no diatoms, are indicative of glacio-fluvial outwash from a retreating local glacier (cf. Turney et al., 2003; Vandergoes et al., 2008; McGlone & Basher, 2012). The present geomorphology of the Adelaide Tarn catchment comprises a classical cirque (amphitheatre-shaped) basin formed from scouring by glacial ice during a recent glacial advance (or previous glacial advance) before ~14,000 cal yr BP. Quaternary glaciogeomorphology in the Tasman Mountains indicates that there were glaciers in the vicinity of Adelaide Tarn during past glacials and that the latest remnant glaciers had disappeared by ~14,000 cal yr BP (Barrell, 2011). This timing is consistent with that of the Adelaide Tarn basal sediments that are dated to ~14,000 cal yr BP.

Lithozone 2 comprises brownish black organic silt and clay with intermittent light yellow/brown laminae. Lithozone 2, aged between ~13,932 cal yr BP and ~7709 cal yr BP, is 2.4 m thick and the mean sedimentation rate decreases up the core ranging between 0.20 and 0.38 mm/yr. The transition from inorganic grey silts of lithozone 1 to these organic brownish black silts/clays is indicative of cool to warming conditions, and the increasing stability of the catchment is indicated by the decrease in sedimentation rate (cf. Vandergoes et al., 2008). Diatoms become evident in this zone (identified via the SEM micrographs) and angular inorganic particles decrease in abundance. The light yellow/brown layers are characterised by a slight increase in sand, a dominance of angular inorganic sediment particles, and lack of diatoms. In general, these features of the lithozone 2 sediments suggest that the catchment has become more stable and is acclimatising to the new,

warmer climatic regime. The catchment is still not fully vegetated and is sensitive to erosional events, forming the light yellow/brown layers that may be attributable to in-washing of sediment from storm or earthquake events. At 7709 cal yr BP the brownish black sediments transition into lithozone 3.

Lithozone 3 comprises dark brown organic silt and persists until the top of the core at 0 m. The sedimentation rate is relatively uniform (ranging between 0.26–0.40 mm/yr) in this zone until mean sedimentations rates increase to 0.71 mm/yr and to 1.98 mm/yr from 3622–3566 cal yr BP and 1063–942 cal yr BP, respectively. Diatoms become more abundant and have a richer species assemblage (identified via SEM micrographs) and these characteristics suggest that primary productivity within the lake has increased since ~7709 cal yr BP (see Table 3.0).

6.1.3 Summary of properties

This section comprises a summary of the properties (proxies) measured (excluding the stratigraphic lithozones) throughout the core. It is divided into four zones, which become inferred climate events for the Adelaide Tarn record in the next section (section 6.1.4).

Zone 1: ~14,000 cal yr BP

Grain size, magnetic susceptibility, and isotopes ($\delta^{15}N$ and $\delta^{13}C$) are all at a maximum at approximately 14,000 cal yr BP, hence all fit into a narrow zone (Fig. 6.0). The >32 μm grain size fraction, chosen to represent fluctuation of terrigenous input into the lake (following Augustinus et al., 2011), comprises 20–60% of the total proportion of >32μm in the basal sediments of the core. Magnetic susceptibility is 12–15 SI, $\delta^{15}N$ reaches 5 ‰, and $\delta^{13}C$ is the most positive in this zone reaching -22 ‰. This zone is also marked by low to only moderate organic carbon content, which ranges between 0.3 and 4% (Fig. 6.0). There are very few plant macrofossils preserved in this zone, the only ones identified being a few fragments of *Poaceae* species.

Zone 2: 13,932–10,000 cal yr BP

The base of zone 2 is marked by a sharp change in the >32 μm grain size parameter, magnetic susceptibility, and isotope measurements. The percentage of grain size >32 μm decreases dramatically to ≤10%, magnetic susceptibility values drop to 2–5 SI, $\delta^{15}N$ concentration drops to between 1 and 2 ‰ and $\delta^{13}C$ becomes more negative, ranging between -26 and -28 ‰ (Fig. 6.0). Carbon content steadily increases through this time period (reaching a maximum of 15%) and plant macrofossil assemblages are still dominated by *Poaceae* species (Fig. 6.0).

Zone 3: 10,000–2400 calyr BP

From 10,000 to 2400 cal yr BP, organic carbon content decrease, magnetic susceptibility values decrease, $\delta^{13}C$ remains essentially the same, and $\delta^{15}N$ gradually increases in concentration towards 2400 cal yr BP (Fig. 6.0). Magnetic susceptibility values become very low, the >32 μm grain size parameter remains approximately the same as in zone 2 but with some marked spikes ranging from 10 to 15% (of >32 μm material). $\delta^{15}N$ shows a steady increase to 3 ‰. The plant macrofossil assemblage shifts to *Nothofagus* (primarily dominated by *N. menziesii*with some *N. fusca*) dominated with minor constituents of *L. bidwillii* and *P. alpinus*. The carbon content starts gradually declining in percentage (reaching a low of 5%) from ~10,000 cal yr BP (Fig. 6.0).

Zone 4: 2400–~700 cal yr BP

From 2400 cal yr BP, magnetic susceptibility increases to 2 to 3 SI and the plant macrofossil assemblages shift to *Poaceae* dominated and tree species disappear except for one leaf of *N. solandri var. cliffortioides*. The remaining proxies are roughly the same as in zone 3.

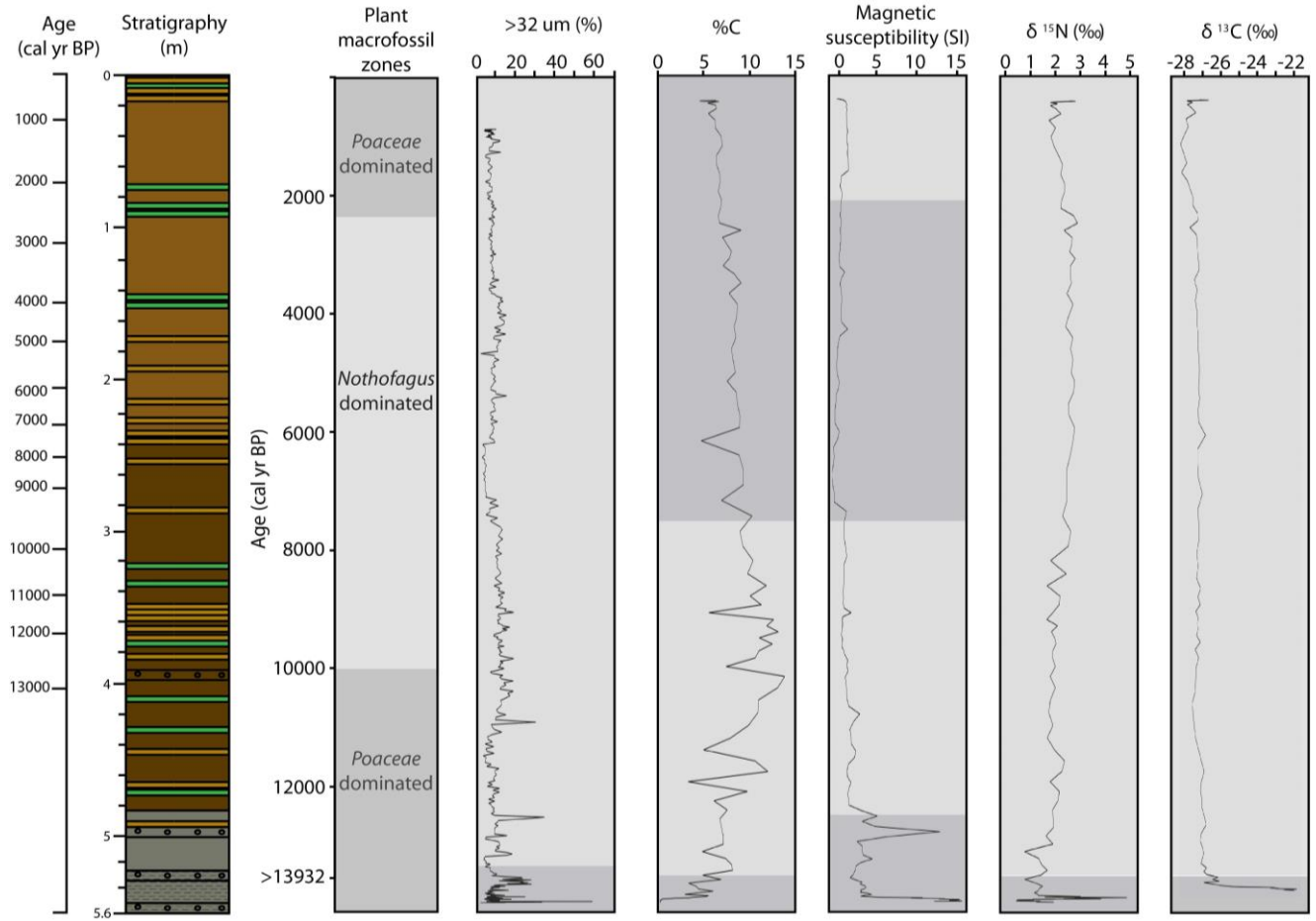

Figure 6.0 Synthesis of stratigraphy, physical, chemical and biological proxies measured from Adelaide Tarn sediments. Core depth is given in metres and modelled ages are in cal yr BP. Note that the age-scale for the six grey boxes at right has been made uniformly linear. The different shades of grey represent different zones identified according to changes in the proxies represented (discussed in chapters 3 to 5).

6.1.4 Palaeoenvironmental implications and inferred climate events

In Fig. 6.1, palaeoenvironmental conditions have been inferred as four broad zones based on the interlocking proxies, and are referred to as the Adelaide Tarn climate event stratigraphy (AT-CES, far right column). Summaries of inferred past environments of Adelaide Tarn are also given in Fig. 6.1, and these are based on zones identified from changes in each of the proxies measured (Fig. 6.0).

Grain size and magnetic susceptibility are inferred to be related to erosional events in the catchment where there is a concomitant increase in grain size in the lake sediments and an influx of magnetic minerals (from the underlying bedrock) deposited in the lake basin. A high energy hydraulic transport mechanism is required for the deposition of large grains and associated minerals into the lake. A decrease in these two proxies suggests that the catchment (and lake) have become more stable. $\delta^{15}N$ and $\delta^{13}C$ isotopes give information on the changes in lake productivity and source of organic matter in the lake and the catchment. Plant macrofossils and carbon content record signals of catchment stability, temperature changes and net precipitation.

AT climate event 1: ~14,000 cal yr BP

Soon after the initial formation of the lake at ~14,000 cal yr BP, coincident in time with the early part of the ACR, the proxies all point to cool conditions becoming warmer by ~14,000 cal yr BP. A substantial erosion event, causing in-wash of terrigenous materials, is indicated by the >32 μm grain-size fraction exceeding 20% and by large MS values, took place soon after the lake developed. Most likely a local cirque glacier in the basin began retreating and meltwater discharge added fluvioglacial sediment into the basin. Both isotopes show relatively high values (very positive or less negative; Fig. 6.0), which are indicative of addition into the lake with the surrounding in-wash of terrigenous material rather than as primary productivity within the lake. The low to only moderate carbon content and very small amounts of plant macrofossils (which are

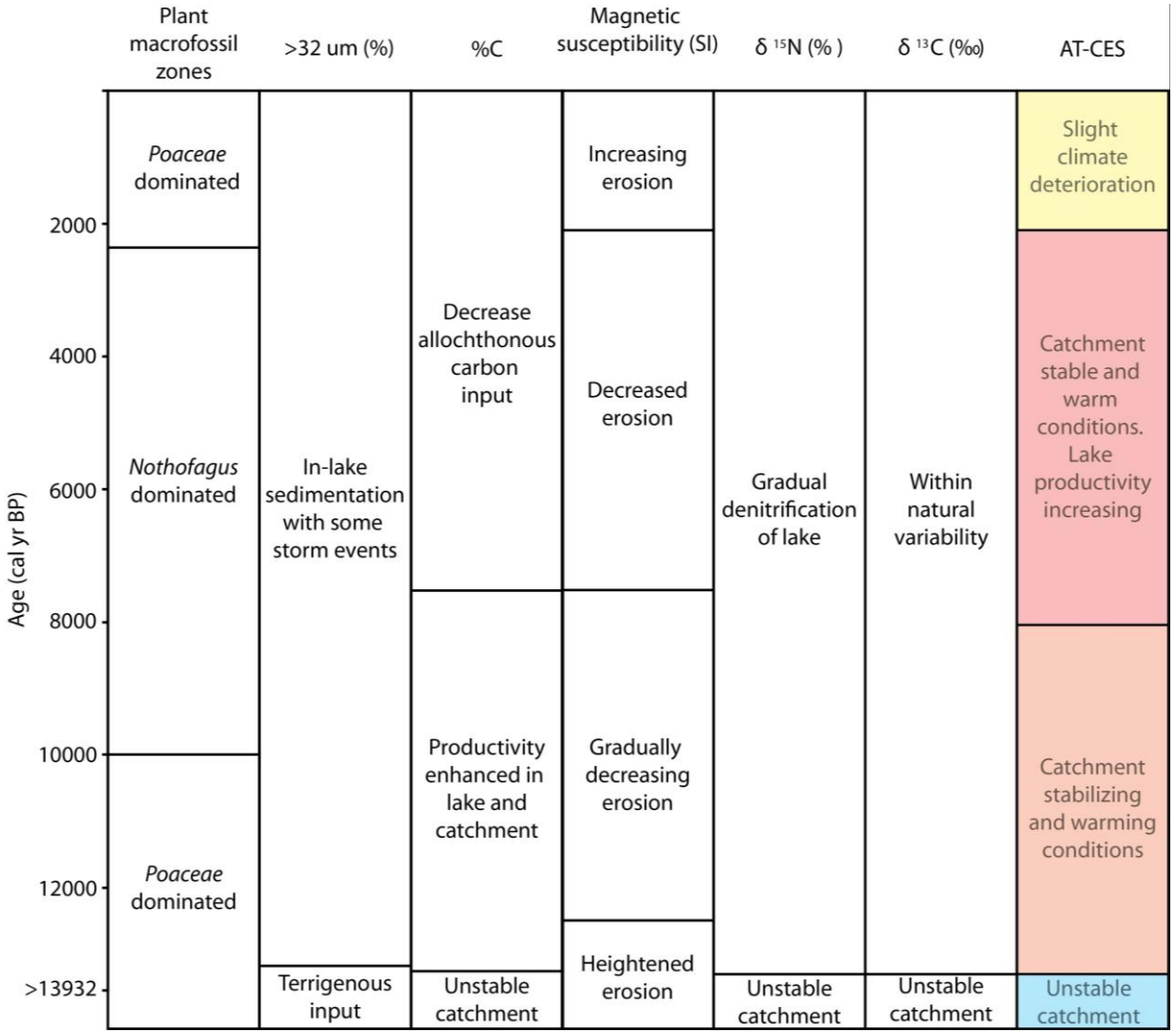

Figure 6.1 Summary of past environments of Adelaide Tarn based on zones identified from changes in each of the proxies measured. Palaeoenvironmental conditions have been inferred as four broad zones based on the interlocking proxies, and are referred to as the Adelaide Tarn climate event stratigraphy (AT-CES) in the column at far right.

dominated by *Poaceae* species) suggest that conditions were unstable and the environment was not optimal for tree species to inhabit (Fig. 6.1). If tree species were present then the developing hydrological system of the lake would suggest that preservation of the plant macrofossil leaves would be inadequate.

AT climate event 2: ~13,932–10,000 cal yr BP

This zone marks a decrease in grain size and magnetic susceptibility and these changes suggest that the catchment is stabilizing and there is less erosion. The $\delta^{15}N$ values drop abruptly and $\delta^{13}C$ becomes more negative, and these changes are consistent with the onset of primary production within the lake along with the appearance of diatoms (Fig. 6.1). The organic carbon content steadily increases and this could mean that soil is forming in the vicinity of the lake and allowing for the accumulation of organic matter such as humus, pollen and plant fragments. Plant macrofossils become more abundant but are still dominated by *Poaceae,* which is a more robust and cold-tolerant species than species representative of forests. There is no indication of tree species yet, but I infer that the climate conditions are warming during this phase (Fig. 6.1). The tree-line may take longer to respond and ascend in altitude.

AT climate event 3: ~10,000–2400 cal yr BP

Magnetic susceptibility measurements become very low and the >32 μm grain-size fraction is approximately 10% except for a series of small peaks of around 10 to 15%. These small peaks of grain-size may suggest additions of allochthonous material (comprising angular sediment particles and no diatoms, as shown by SEM micrographs) into the lake that could be attributed local storm events. The plant macrofossil assemblage becomes dominated by tree species, mainly *Nothofagus menziesii* and assemblage associated species including *L. bidwillii* and *P. alpinus*. The shift to a tree-dominated assemblage indicates the movement of the tree-line closer to the lake to allow for the transport (by wind or water) and preservation of the fossils within the lake sediments. *N. fusca* macrofossils appear

at approximately 6400 cal yr BP, and this sudden appearance could be for one of two (or more) reasons: (1) temperatures have become warmer to allow for optimum environmental conditions for *N. fusca* trees to inhabit higher altitudes than normal, or (2) the higher degradation levels of the *N.fusca* leaves has meant that it is not present or is underrepresented in the assemblage prior to 6400 cal yr BP. I therefore cannot rule out unequivocally the presence of this species prior to 6400 cal yr BP, or infer that the climate has warmed more since 6400 to allow for the appearance of *N. fusca*. The presence of *N. fusca* suggests that this zone was ~1.2˚C warmer on average than present day (see Chapter 5).

The organic carbon content in the sediments deceases towards the top of the core from ~10,000 cal yr BP (Fig. 6.1). The decreasing carbon content could be associated to the increasing stability of the catchment whilst more diverse floral assemblages occupy the basin. Erosion has decreased and therefore less allochthonous in-wash sediment is entering the lake and the carbon entrained in the soils from humus and pollen accumulation is hence not adding to the lake's carbon reservoir. $\delta^{15}N$ increases slightly, which suggests slight denitrification of the lake and an increase of lake productivity from organisms up-taking ^{12}N and enriching the sediments with $\delta^{15}N$. Overall for this zone, the climate is warm, primary productivity has increased within the lake, and the catchment has further stabilised (Fig. 6.1).

AT climate event 4: 2400–~700 cal yr BP

The climate deteriorates from ~2400 cal yr BP and this deterioraion is inferred from the changes in plant macrofossils and increase in magnetic susceptibility. At 2400 cal yr BP, tree species disappear (except one leaf of *N. solandri var. cliffortioides*) and the assemblage becomes dominated by *Poaceae*, a cold tolerant species. The increase of magnetic susceptibility could be an indication of a slightly less stable catchment, and allowing for the removal of soil and possibly bedrock into the lake.

6.1.5 Adelaide Tarn pollen record

Ignacio Jara of Victoria University of Wellington, under the supervision by Prof Rewi Newnham, constructed the Adelaide Tarn pollen record and here I will present the climatic zones that he has identified from the changes in pollen assemblages. The four climatic zones that separate the pollen record are based on a palaeo-vegetation index where the abundance of rimu pollen is divided by the abundance of *Nothofagus*. High values show the dominance of rimu over *Nothofagus*, representing mild conditions. Low values of the palaeo-vegetation index represent cold conditions.

The Adelaide Tarn record gave the opportunity of analysing plant macrofossils as well as pollen. Pollen is easily transported and in large quantities and can represent a more regional climate and provide insights into non-local vegetation development, whereas plant macrofossils may be a more reliable indicator of the vegetation composition at or near the sampling site (e.g. Newnham et al., 1995). Plant macrofossils are not transported as easily and represent a more local in-situ palaeoenvironment, hence their importance in inferring tree-line positions which is becoming increasingly important in the context of climate change (McGlone & Basher, 2012). There are far fewer plant macrofossils in comparison to pollen so they may not show the true representation of the assemblage and therefore it is ideal to analyse both.

The Adelaide Tarn plant macrofossil record shows warming from 14,000 to 10,000 cal yr BP and sustained conditions of relative warmth from 10,000 cal yr BP through to 2400 cal yr BP in the macrofossil record until all tree species disappear. The pollen record shows sustained warming temperatures from 14,000 cal yr BP through to ~5800 cal yr BP but this period is punctuated by a slightly cooler event from 9200 to 8300 cal yr BP. Both records show a deterioration of climate from 2400 cal yr BP to the top of the record but the pollen signal indicating the start of a deteriorating climate occurs at 5800 cal yr BP, about 3000 cal years before that inferred from the macrofossil assemblages (Fig. 6.2).

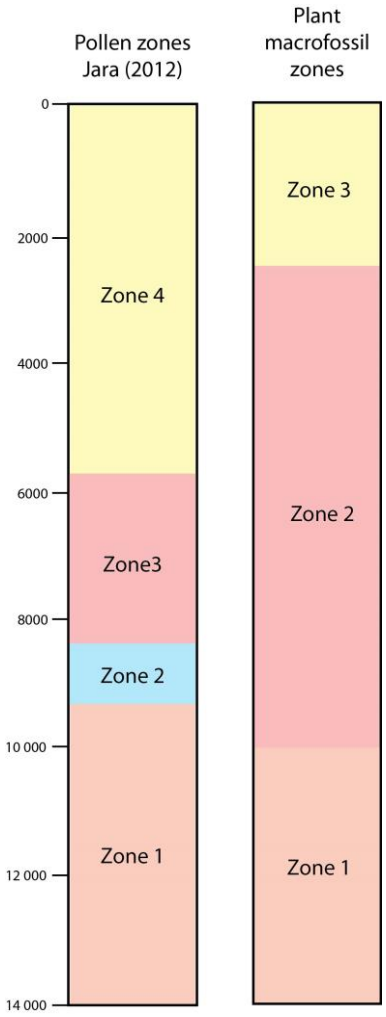

Figure 6.2 Pollen zones of Ignacio Jara (based on personal communications and Jara et al., 2012) from Adelaide Tarn (at left) in comparison with the zones derived here (at right) using plant macrofossil assemblages (Chapter 5). Pollen zones are characterised as follows: zone 1, increasing abundance of rimu; zone 2, increase in *Nothofagus* species; zone 3, increase in rimu; and zone 4, decreasing abundances of rimu. Plant macrofossil zones are characterised as follows: zone 1, *Poaceae* dominated; zone 2, *Nothofagus* dominated; and zone 3, *Poaceae* dominated.

6.2 Comparison of AT-CES with New Zealand records spanning the last 14,000 years

The AT-CES is compared with chosen records from various latitudes, altitudes and types of records and proxies that span ~14,000 years (Table 6.0). The last 14,000 years of the NZ-CES stratotype will also be examined (Barrell et al., 2013). By comparing the AT-CES with other records across New Zealand enables me to identify how the AT-CES fits in or otherwise with climatic changes recognised elsewhere in the late-glacial and Holocene. Because there are few records spanning the last ~14,000 cal years in the same region as Adelaide Tarn, I have chosen various records from both the North and South Islands. I recognise that these records may be offset in some way temporally from the changes established from Adelaide Tarn because of different resolutions and because a range of proxies were used in their construction (see discussions about such comparisons in Barrell et al., 2005, 2013; and Alloway et al., 2007).

Table 6.0 New Zealand records spanning the last ~14,000 years selected to compare with the AT-CES.

Name of record	Location	Type of proxy	Reference
NZ-CES	Three reference locations (stratotypes)	Pollen	Barrell et al. (2013)
Lake Tutira	Hawke's Bay	Changes in lithology	Page et al. (2010)
Lake Maratoto	Central Waikato	Changes in lithology including growth of peat in adjacent bog; pollen	Green & Lowe (1985); Wilmshurst et al. (2007)
Cass	Central South Island	Pollen	Wilmshurst et al. (2007)
Cropp Valley	Southern Alps (south west of Cass)	Pollen	McGlone & Basher (2012)
North-west South Island	North-west South Island	Speleothems	Williams et al. (2010)
Kettle Bog	Cass Basin, South Island	Pollen and plant macrofossils	McGlone et al. (2004)

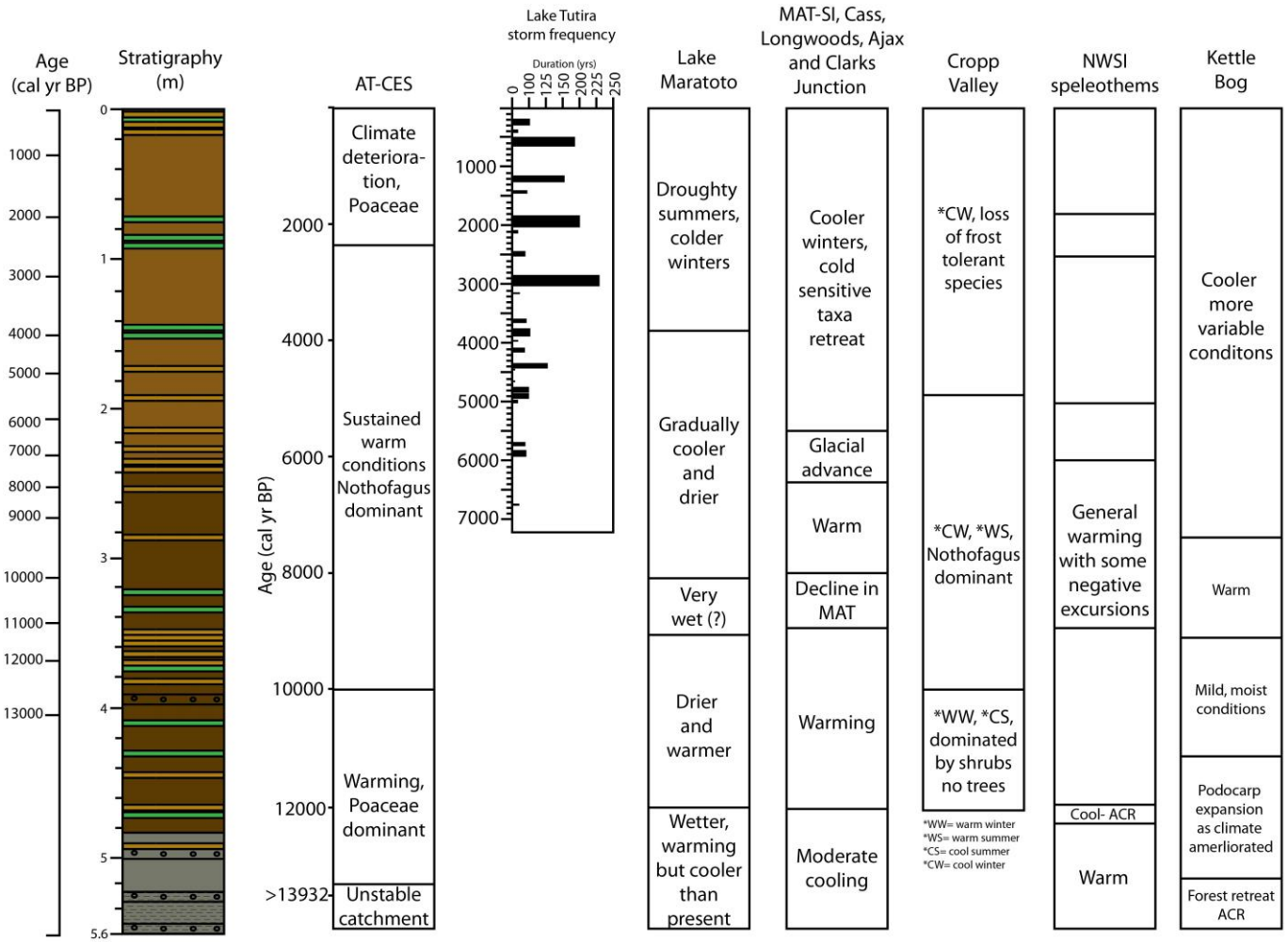

Figure 6.3 Summary of selected records for comparison of AT-CES. MAT= mean annual temperature; NWSI = North-west South Island (see text). Note age scale for AT-CES and other records has been made uniformly linear.

6.2.1 NZ-CES

The New Zealand climate event stratigraphy spans the period 30,000 to 8,000 cal yr BP and on this basis only part of the record (~14,000–8000 cal yr BP) is relevant to the Adelaide Tarn record. There does not seem to be any clear overlap of the two records (Fig. 6.4).

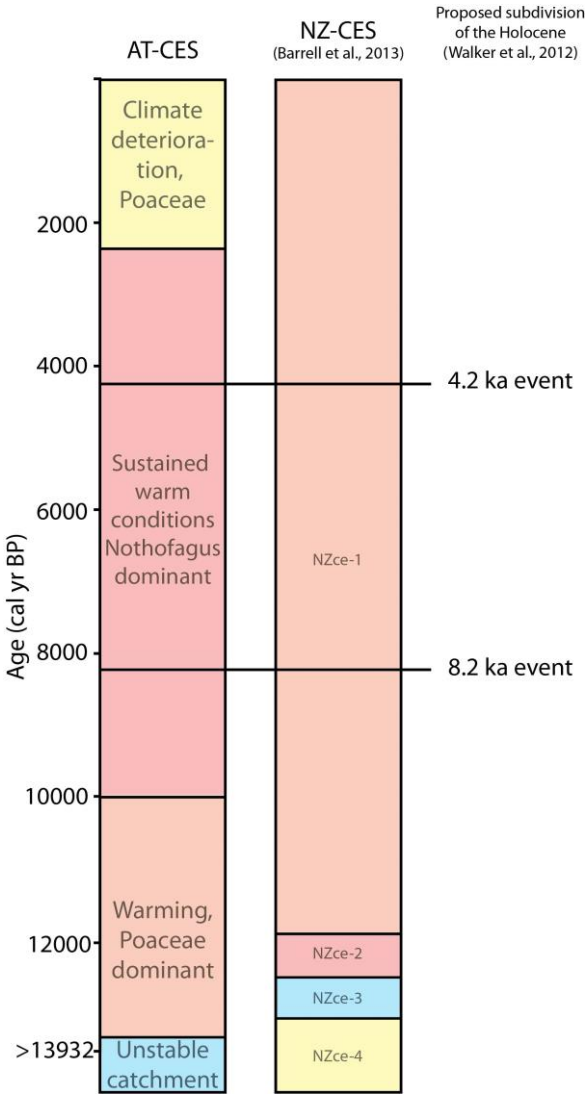

Figure 6.4 Comparison of the AT-CES with the New Zealand climate event stratigraphy spanning the last ~14,000 years (Barrel et al., 2013). The start of the Holocene is defined at the boundary of NZce-2 and -1 (Walker et al., 2009). The two cool events that Walker et al. (2012) have proposed to subdivide the Holocene into three units (Early, Middle, Late) are shown alongside the NZ-CES record.

The boundaries are indicative of the general timing of these events and are not definitive ages. Timing of the start and end of events can differ between localities according to latitude (e.g. Carter et al., 2008; Newnham et al., 2012; Lowe et al., 2013). The Holocene Epoch remains undifferentiated at this time. Walker et al. (2012) proposed the Holocene is subdivided into the Early Holocene to Middle Holocene (boundary defined by the 8.2 ka event) and the Middle to Late Holocene (boundary defined by the 4.2 ka event) (Fig. 6.3). The 8.2 ka event is a period of abrupt cooling that has been identified in various records overseas but only one possible identification has been made in New Zealand, that of Augustinus et al. (2008). The 4.2 ka event shows abrupt cooling and aridity in multiple localities globally but has not yet been recognised in New Zealand (Walker et al., 2012). The lack of evidence for these events in the Adelaide Tarn record does not currently support the tripartite subdivision of the Holocene as proposed by Walker et al. (2012).

6.2.2 Lake Tutira

Lake Tutira is located in the the Hawke's Bay region, eastern North Island, and is situated approximately 200 m asl. Page et al. (2010) constructed a mid-Holocene storm frequency record since ~7200 cal yr BP. The storm deposits are defined by beds grading from coarse sediment to clay and an organic carbon content of <2%. The storm events have increased in duration and intensity since ~3000 cal yr BP (Fig. 6.3). However, it is recognised that Lake Tutira is an eastern North Island site primarily influenced by the La Nina phase of the ENSO cycle that increases tropical storms over the eastern North Island. The intensification and intensity of ENSO events has increased over the last ~600 years in southern Ecuador (Moy et al., 2002). These records of ENSO events together could be the reason for the slight climate deterioration (forcing tree species to ascend) that is seen in the AT-CES

6.2.3 Lake Maratoto

Lake Maratoto is located in the Waikato lowlands near Hamilton airport and is the parastratotype for the Pleistocene/Holocene boundary (Walker et al., 2009; Barrell et al., 2013). Changes in sediment characteristics were used to infer changes in the lake and the catchment. The wetter, warmer but cooler than present phase of Maratoto (>12,000 cal yr BP) is roughly coincident with that of Adelaide Tarn. Climate conditions at Adelaide Tarn are warming but the appearance of tree species does not occur until 10,000 cal yr BP and this could mean that the optimum temperatures for the tree-line to ascend are not yet reached. The drier and warmer phase of Maratoto until 8000 cal yr BP roughly overlaps the warm conditions of Adelaide Tarn. The cooler and drier phase of Maratoto from ~8000 to ~4000 cal yr BP is not mimicked by the Adelaide Tarn record (Fig. 6.3). Both records show climate deterioration for the past few thousand years, indicated by the change in vegetation at Adelaide Tarn from ~2500 cal yr BP.

6.2.4 Mean annual temperatures, South Island

Wilmshurst et al. (2007) developed two methods for estimating mean annual temperatures (MATs) using a temperature transfer function and modern analogue method from pollen records throughout New Zealand. They constructed the MATs spanning 18,000 years from several localities. Here I focus only on the southern localities: Cass, Ajax, Longwoods and Clarks Junction (Lake Maratoto was also studied by Wilmshurst et al., 2007). The combined southern records showed similar patterns of change in MAT and the overall pattern can be seen in Fig. 6.3 (column 5). Firstly, the combined southern records suggest cooling until ~12,000 cal yr BP, but such cooling is not evident in the Adelaide Tarn record. This could be because Adelaide Tarn was too young to capture this cooling event which is roughly coincident with the ACR. Glaciers had also been completely removed from the Tasman Mountains by ~14,000 years therefore during the initial development of the lake it may not have picked up this sensitive change in climate regime. The southern records show warm mean annual temperatures from 12,000 through to 5500 cal yr BP with a peak at 11,500 to 9000 cal yr BP. This warm

period is coincident with that of Adelaide Tarn although the AT-CES shows sustained warm temperatures right through to 2400 cal yr BP. The warm period of the southern sites is punctuated by a cool period from 9000 to 8000 cal yr BP and ends with a glacial re-advancement (Southern Alps) at ~5500 cal yr B. Neither of these cool episodes are captured in the Adelaide Tarn record; they could be an indication of local climates in the areas where temperatures were reconstructured by Wilmshurst et al. (2007), and possibly slightly cooler winters where the cold sensitive taxa have retreated (Wilmshurt et al., 2007). The mean annual temperature recorded in the southern sites decreases between 4000 and 3000 cal yr BP to current mean annual temperatures and this deterioration is consistent with a deterioration at Adelaide Tarn from about 2400 cal yr BP (Fig. 6.3).

6.2.5 Cropp Valley

McGlone and Basher (2012) undertook research on the change in tree-line from Cropp Valley located in the western Southern Alps. The present-day tree-line at Cropp Valley is at 1000 m asl and the regional tree-line is between 1150 and 1200 m. The Cropp Valley tree-line is lower because of the cold air drainage from the surrounding Southern Alps. In the Cropp Valley record from 12,000 to 10,000 cal yr BP, no tree species are found in the pollen assemblage and it is dominated by shrubs, grasses and small trees. The tree-line is low and the current alpine forest was absent and this feature is seen in the Adelaide Tarn record also with the dominance of grass and absence of tree species (Fig. 6.3). The climatic conditions inferred by McGlone and Basher (2012) during this time are warm winters and cool summers which explains the lack of tree species including *L. Bidwillii*. From ~10,000 cal yr BP, both records show the spread of *Nothofagus* forest to approximately 5000 cal yr BP at the Cropp Valley site and ~2400 cal yr BP for Adelaide Tarn (Fig. 6.3). McGlone & Basher (2012) infer this time period as having colder winters and shorter but warmer summers. At the Cropp Valley site from ~5000 cal yr BP, the forest species are marked by the disappearance of frost-tolerant taxa as the winters become cooler and this could explain the minimal presence of *N. Fusca* in the Adelaide Tarn record as it is a frost-sensitive species and *N. menziesii* dominates because of its frost-tolerant hardening character. The alpine trees at the Cropp Valley site overtake the grasses and shrubs because of warmer summers but this change is not seen in the AT-CES because it is at a higher altitude.

6.2.6 North-west South Island (NWSI) speleothems

Williams et al. (2010) constructed a $\delta^{18}O$ record to represent the North-west South Island. From ~14,100 cal yr ago (ages based on U-series), the $\delta^{18}O$ values became more positive which is indicative of warming conditions. At approximately 12,200 to 12,000 cal yr ago a negative excursion in the $\delta^{18}O$ values occurred and this is roughly the same age as the ACR (see also Helstrom et al., 1998). The warming is coincident with that of Adelaide Tarn but the AT record has not been

able to capture the ACR because of the development of the lake at this time and the removal of local glaciers. From 12,000 cal yr ago, the NWSI speleothem record becomes more negative compared with values of the present day but is punctuated by several short-lived negative shifts of $\delta^{18}O$ values (negative phases are represented by single black lines in the NWSI record in Fig. 6.3). The positive values of $\delta^{18}O$ suggest warming through the Holocene and this is consistent with that of Adelaide Tarn. There is no evidence of climate deterioration in the NWSI $\delta^{18}O$ record.

6.2.7 Kettle Bog

The pollen and plant macrofossil record constructed by McGlone et al. (2004) shows a marked retreat in forest species about the time of the ACR and again the AT-CES is unable to capture this event. From 13,600 cal yr BP podocarps expanded at Kettle Bog as the climate ameliorated before the Holocene. The podocarp species replace shrubs and the climate remains warm through to 7500 cal yr BP. The warming phase of Kettle Bog is consistent with that of Adelaide Tarn. From 7500 cal yr BP at Kettle Bog, there is a marked transition from podocarp species into *Nothofagus* species and this is inferred to be a response to cooler more variable conditions (Mcglone et al., 2004). The AT-CES also shows this more variable climate with the disappearance of tree-species and the shift to *Poaceae* dominated assemblages from ~2400 cal yr BP. The shift to *Nothofagus* species at Kettle Bog could be indicative of the lower altitude of this site (<700 m), meaning therefore they are able to inhabit this environment, unlike at the higher altitudes of Adelaide Tarn.

6.2.8 Summary of comparisons

In general, the AT-CES is consistent with climate records chosen for comparison. Records from Kettle Bog, and the southern sites used to reconstruct MATs, show a cool phase the overlaps the ACR but this is not preserved within the relatively young Adelaide Tarn record. There are at least two possibilities for this: (1) Adelaide Tarn was developing as a lake during this time, and the basal sediments

are indicative of a very unstable catchment, and so it would be difficult to preserve any impact of the ACR, and (2) the glaciers in the locality of the lake have retreated by ~14,000 years and the unstable catchment has not been able to adapt fast enough to preserve changes within vegetation. In general, all records indicate warming conditions from around the start of the Holocene or a bit later. All records (excluding speleothems) show a cooling and variability of climate through to present day (including increased storm periods, Page et al. 2010), decrease in MAT (Wilmshurt et al., 2007), decrease or removal of cold sensitive taxa (AT-CES, Green & Lowe, 1985; McGlone et al., 2004; Wilmshurt et al., 2007; McGlone & Basher, 2012) (Fig. 6.3).

The record that shows the strongest relationship with that of Adelaide Tarn is the record from Cropp Valley constructed by McGlone & Basher (2012). The vegetation history shows the same shifts in assemblages from the start of each record. Both records show the dominance of grass and shrub species and the absence of trees though to 10,000 cal yr BP. From 10,000 cal yr BP there is the expansion of Nothofagus followed by the removal of frost-tolerant species. McGlone & Basher (2012) concluded that during the later part of the late glacial and the early Holocene, cool summers, warm winters and generally drier-than-present conditions prevailed in New Zealand. Summers shortened but became warmer, while winters lengthened and cooled in the course of the Holocene. As a consequence, apparently contradictory trends emerged in the mid-to-late Holocene as exemplified by the Cropp Valley assemblages: lowland forests changed character, losing frost-sensitive components as winters became cooler, while alpine trees began to replace previous low-growing shrublands in response to warmer summers.

6.3 Potential ENSO and possible southward migration of westerly winds

6.3.1 ENSO

Moy et al. (2002) found that warm ENSO events became more frequent over the Holocene and then steadily declined from ~1200 cal yr BP. A long-term scale of ENSO activity also overlies this, alternating between highs and lows every ~2000 years.

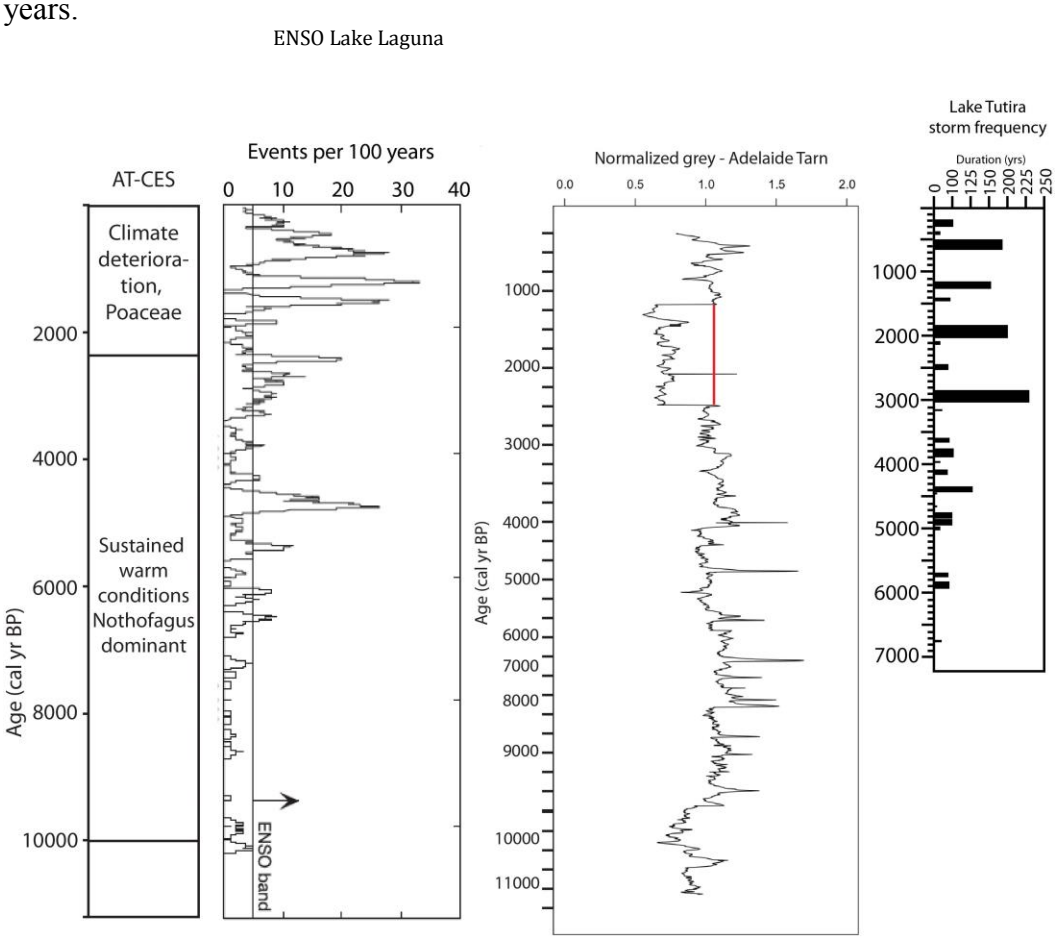

Figure 6.5 The AT-CES and grey scale measurements in comparison with ENSO activity over the last 12,000 cal years from Moy et al. (2002) and with storm events from Lake Tutira (Page et al., 2010). Note that the drop in grey scale, marked here by the red vertical bar, is an artefact due to a different resolution used in that part of the core when taking X-radiograph and the red line is an interpretation of where the values would be.

The ENSO record is from Laguna Pallcacocha in southern Ecuador and in the core were multiple light-coloured, inorganic clastic laminae similar to those of Adelaide Tarn. The light-coloured laminae of Laguna Pallcacocha were inferred to be deposited during increased ENSO events. Moy et al. (2002) Suggested ENSO increased from 7000 cal yr BP with more frequent intensification from 1800 cal yr BP and then decreased from 1200 cal yr BP (Fig. 6.5). The grey scale record for the sediments of Adelaide Tarn represents changes in density up the core and the marked peaks represent denser, more clastic sediments (shown by SEM analysis). The Adelaide Tarn grey scale record shows a broadly similar trend to that of ENSO activity from Laguna Pallcacocha with slightly lower values at 10,000 cal yr BP. The larger peaks in grey scale show a good relationship with frequency of ENSO events per 100 yr. The Lake Tutira storm event shows increase duration of events from 7000 cal yr BP and all records show a slight decrease from ~1000 cal yr BP. The increase in ENSO events per 100 years from ~2000 overlaps the climate deterioration phase of the AT-CES and could be a possible cause of this.

6.3.2 Potential southward migration of westerly winds

As mentioned in Chapter 4, a component of the Adelaide Tarn grain size record could represent aeolian dust derived either from local New Zealand or Australian sources. Although fingerprinting of these indicative size fractions (Fig. 6.6) has not been undertaken to define a source, Adelaide Tarn could be a potential locality to identify dust and therefore infer changes in south westerly wind patterns through time. The mean grain size for Adelaide Tarn (AT) sediments is plotted along with mean grain size for each of the lithozones and in comparison to the record of dust flux at Old Man Range (OMR) (derived by Marx et al., 2009). It is interesting to note that the mean grain size for sediments oflithozone 2 of AT (27.7 μm) is similar to the mean grain size for phase 2 of the OMR record (23-25 μm), but the timings differ in that the 27.7 μm size persists at AT until ~7500 cal yr BP (when the mean grain size drops to 17.2 μm) whereas in the OMR record the phase 2 sediments marked by the 23-25 μm mean grain size persist until ~4700 cal yr BP (Fig. 6.6). The mean grain size of sediments of lithozone 1 (17.2 μm) is the same as that of the sediments of phase 3 of OMR (17-18 μm).

Temperatures are generally warming during this period (13,000 cal yr BP through to 2400 cal yr BP) and the westerly wind belt is moving south, therefore seemingly depositing aeolian dust into Adelaide Tarn prior to deposition onto Old Man Range. It is recognised that further work is needed to make further inferences but this is an interesting find.

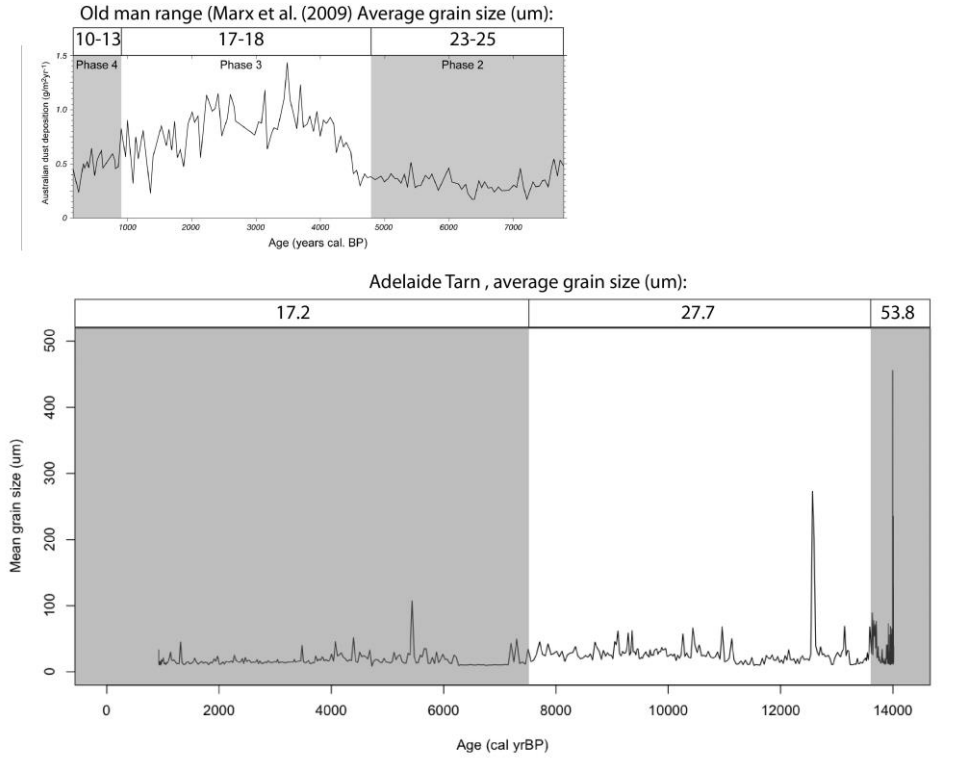

Figure 6.6 The top graph is Australian dust flux into Old Man Range with three major phases identified by the changes in mean grain size (Marx et al., 2009). The bottom graph represents the Adelaide Tarn zones and associated mean grain sizes (from right to left are lithozones 1, 2 and 3).

Chapter 7. Conclusions

7.0 Summary of main conclusions

This is the first study undertaken at Adelaide Tarn (AT). Given the paucity of climatic records spanning the Holocene in central New Zealand, the AT-CES builds on and supports previous work. This study also presents a plant macrofossil record in support of the detailed pollen record constructed by Ignacio Jara (Victoria University of Wellington). Studies of plant macrofossils spanning the last 14,000 years are limited in New Zealand and the AT record identifies the importance of analysing pollen and plant macrofossils in tandem where possible. Because of the increasing interest in reconstructing past tree-line positions with respect to temperature, the AT-CES can further support these types of studies, in particular that of McGlone & Basher (2012).

The principal aim of this research was to reconstruct the history of Adelaide Tarn and its catchment from the time of initial sediment accumulation ~14,000 cal yr BP) through to the top of the core (younger than 926 cal yr BP and pre-~700 cal yr BP) and to develop a dated palaeoclimate and environmental change record using analyses of physical, biological and chemical properties preserved within the sediments. To aid in the achievement of this aim the following objectives were completed:

(1) A stratigraphic framework was constructed along with a chronology developed from 15 radiocarbon dates, 14 of which were on in-situ plant macrofossil remains. Within the stratigraphy of the core are three major changes in sediment described (from base to top of core) as lithozones 1, 2 and 3. Lithozone 1, from 5.6–4.8 m depth, comprises inorganic grey silts with a Munsell colour of 5Y 6/1 and these basal sediments are estimated to be a little older than ~13,932 cal yr BP, the oldest ^{14}C age obtained at a depth of 5.0 m. Lithozone 2 consists of organic brownish black (10YR 2/3) silt and clay and is located between 4.8 and 2.3 m in the sediment core, spanning the period ~13,932 to 7709 cal yr BP. Lithozone 3 comprises dark brown (10YR 3/4) organic-rich silt

between 2.3 m depth and the core top, spanning an age range from ~7709 cal yr BP through to a little older than ~700 cal yr BP. This age of the topmost sediments is estimated from the ^{14}C date of 942 cal yr BP at 13 cm depth together with palynological data that shows the topmost sediments pre-date both European adventives (i.e. before ~1840 AD) and Polynesian deforestation signals that typically date to around ~700 cal yr ago (e.g. Newnham et al., 1998b; McGlone & Wilmshurst, 1999; Wilmshurst et al., 2007). Several yellowish/brown (10YR 6/8) laminae are found throughout lithozones 2 and 3, and one layer occurs in lithozone 1.

(2) A range of physical, biological and chemical analyses were undertaken from the properties preserved in the lake sediments.

Physical components

- X-radiography and grey-scale analyses identified three zones roughly in coincidence with the three lithozones. The X-radiography helped to determine the approximate organic content of the three zones based on the colour changes which represent clastic inorganic sediment of lithozone 1 (pale grey) versus non-clastic organic sediments of lithozones 2 and 3 (dark grey). The organic contents were confirmed by subsequent carbon analyses (described below). Grey scale analyses showed the presence of laminae throughout the core very clearly, allowing sections with abundant laminae to be identified (lithozone 2, decreasing in abundance in lithozone 3). These laminae tend to contain a higher proportion of sand than the non-laminated sediments, and may represent inwashing of catchment materials in storm events.

Four zones were identified from the magnetic susceptibility record and these were interpreted, from base to top of core, as (i) an enhanced period of catchment erosion and hence lake deposition from ~14,000 to –12,500 cal yr BP; (ii) decreasing catchment erosion and generally stable catchment from ~12,500 to ~7600 cal yr BP; (iii) a phase of catchment stability from ~7600 to ~2200 cal yr BP; and (iv) a slight increase in erosion from 2200 cal yr BP to the top of the core. Three zones were identified from the high-resolution grain-size records that are

roughly coincident with the three lithozones. Grain-size zones are interpreted as (i) heightened terrigenous input early in the lake's development at ~14,000 cal yr BP); (ii) stabilising catchment as sand size steadily decreases up the core, with the laminae in this section from ~13,932 to 7709 cal yr BP being interpreted as possible storm events or catchment responses to intense rainfall (these laminae are dominated by angular inorganic particles shown in SEM micrographs); and (iii) essentially a very stable catchment from ~7709 cal yr Bp to the top of the core at a little before ~700 cal yr BP..

Biological components

- Three major zones were identified in the sediments from the in-situ plant macrofossil assemblages and these were interpreted as follows. (i) From ~14,000 to ~10,000 cal yr BP the assemblage is dominated by *Poaceae* species. Although *Poaceae* species are a cold tolerant family, this zone is interpreted to represent warming conditions as indicated by the glacio-fluvial sediment in-wash from a retreating local glacier. (ii) From ~10,000 to 2400 cal yr BP the assemblage comprises predominantly tree species and this change at ~10,000 cal yr BP suggests that conditions are warm enough to allow for trees and that the tree-line has ascended. The assemblage consists of primarily of *N. menziessii* with minor constituents of *N. fusca* (appearing at ~6400 cal yr BP), *L. bidwillii* and *P. alpinus*. (iii) At ~2400 cal yr BP the sediments contain a *Poaceae*-dominated assemblages and macrofossils from tree species descend.

Chemical components

- The organic carbon content of the sediments of the three lithozones are as follows. Lithozone 1 has low to moderate carbon content, between 0.3 and 4%. Lithozone 2 has the highest level of organic carbon, reaching 15% at ~10,000 cal yr BP. Lithozone 3 shows moderate to high levels of organic carbon, from 4 to 10%. Both of the stable isotopes measured ($\delta^{15}N$ and $\delta^{13}C$) have heightened (more positive/less negative) values from ~14,000 cal yr BP at the base of the core, and then both decrease abruptly at the onset of lake productivity at 13,932 cal yr BP (Fig. 6.0). $\delta^{15}N$ is just outside the natural variability of this isotope and is

suggested that this is slight denitrification of the lake from 8000 to 3000 cal yr BP.

(3) The lake and catchment history has been constructed based on the zones identified for each proxy and the overall inferred palaeoenvionments for these zones, the AT climate events, have been interpreted spanning the past ~14,000 cal years (Fig. 6.1).

- **AT climate event 1** from ~14,000 cal yr BP is inferred as a period of marked catchment instability. Enhanced erosion and concomitant rapid deposition of inorganic clastic sediments in the lake are suggested by coarse grain sizes, high magnetic susceptibility values, $\delta^{15}N$ and $\delta^{13}C$ values, and lack of forest vegetation in the catchment on the basis of pollen and plant macrofossil records (Figs. 6.0 and 6.1).

- **AT climate event 2** is from ~13,932 to ~10,000 cal yr BP and is inferred as a period of warming on the basis of the decrease in allocthonous input (grain size and magnetic susceptibility data; Fig. 6.0) and a more stable catchment. The plant macrofossils are dominated by *Poaceae* but the forest species are unable to occupy this environment.

- **AT climate event 3** is from ~10,000 to ~2400 cal yr BP and shows a marked shift from *Poaceae*-dominated assemblages to *Nothofagus* dominated assemblages at ~10,000 cal yr BP (Fig. 6.0). Erosional events and associated in-washing of detritus are reduced generally. Abundant laminae in this zone, however, dominated by angular inorganic particles (SEM micrographs), possibly represent the input of sediment from storm events. The isotopic analyses suggest that the lake was productive from ~10,000 cal yr BP. This zone is inferred to be one of sustained warmer temperatures; the presence of *N. fusca* suggests that mean annual temperatures were at least ~1.2˚C warmer than those of the present day (see Chapter 5).

- **AT climate event 4** from ~2400 cal BP to ~700 cal yr BP is marked by a shift to *Poaceae*-dominated plant assemblages and the complete disappearance of tree species. This zone is thus inferred to represent a period of relatively minor climate deterioration which, nevertheless, has forced the colder tolerant species to descend (Fig. 6.1).

(4) The Adelaide Tarn climate event stratigraphy (AT-CES), summarised in Fig. 6.1, was then compared to various records across New Zealand (including the NZ-CES of Barrell et al., 2013). The AT-CES was compared to records from Lake Tutira (Page et al., 2012), Lake Maratoto (Green & Lowe, 1985), southern mean annual temperature records derived from palynology (Wilmshurt et al., 2007), Cropp Valley palynology (McGlone & Basher, 2012), North-west South Island speleothems (Williams et al., 2010) and Kettle Bog palynology (McGlone et al., 2004). From these comparisons it was found that the record from Cropp Valley (McGlone & Basher, 2012) has the strongest relationship with the AT-CES: similar vegetational changes, from grass and shrub dominated in the late-glacial to the expansion of *Nothofagus* in the early Holocene and the final zone in the late Holocene where the disappearance of frost sensitive species occurred.

Possible inputs of distal aeolian dust into Adelaide Tarn were also considered (Fig. 6.6) and the implications for the southward migration of westerlies during the Holocene were examined. Likely storm events identified in the AT record (as laminae), and their significance, were compared with ENSO events as described by Page et al. (2010) and Moy et al. (2002).

7.1 Recommendations for further work

- Further SEM work on different samples to further define the three lithozones, and on the yellowish/brown laminae to make a more reliable interpretation of these layers and understand the possible mechanism involved in their deposition.

- Obtain radiocarbon dates for the bottom of the core and possibly the top of the core to improve the chronology of these sections. Another possible chronological tool would be to detect and identify cryptotephras (if present) in the core.

- Undertake a more extensive plant macrofossil analysis focusing on areas of particular interest: (1) refine boundaries of assemblage shifts, and (2) sampling at a higher resolution (e.g. in between the 5 cm-intervals analysed for this research).

- Undertake XRF and XRD analyses of samples within each of the lithozones and of the yellow/brown laminae to try to 'fingerprint' the source of these sediments. Fingerprint the mean sediment sizes identified from Marx et al. (2009) to help infer changes in the positions of the westerly wind belt during the lateglacial and the Holocene (and aridity of Australia).

- Undertake a range of analyses on diatoms, chironomids, lipids, pigments and other proxies (as summarised in Table 2.0).

References

Alloway, B. V., Lowe, D. J., Barrel, D. J., Newnham, R. M., Almond, P. C., Augustinus, P. C., et al. (2007). Towards a climate event stratigraphy for New Zealand over the past 30 000 years (NZ-INTIMATE project). *Journal of Quaternary Science, 22*(1), 9-35.

Anderson, N. J. (1995). Using the past to predict the future: lake sediments and the modelling of limnological disturbance. *Ecological Modelling, 78*, 149-172.

Ao, H. (2010). Mineral-magnetic signal of long-term climatic variation in Pleistocene fluvio-lacustrine sediments, Nihewan Basin (North China). *Journal of Asian Earth Sciences, 39*, 692-700.

Augustinus, P., Bleakley, N., Deng, Y., Shane, P., & Cochran, U. (2008). Rapid change in early Holocene environments inferred from Lake Pupuke, Auckland City, New Zealand. *Journal of Quaternary Science, 23*(5), 435-447.

Augustinus, P., Cochran, U., Kattel, G., D'Costa, D., & Shane, P. (2011). Late Quaternary paleolimnology of Onepoto maar, Auckland, New Zealand: Implications for the drivers of regional paleoclimate. *Quaternary International, 253*, 18-31.

Augustinus, P., Cochran, U., Kattel, G., D'Costa, D., & Shane, P. (2012). Late Quaternary paleolimnology of Onepoto maar, Auckland, New Zealand: Implications for the drivers of regional paleoclimate. *Quaternary International, 253*, 18-31.

Balascio, N. L., & Bradley, R. S. (2012). Evaluating Holocene climate change in northern Norway using sediment records from two contrasting lake systems. *Journal of Paleolimnology, 48*, 259-273.

Barrell, D. J. (2011). Quaternary Glaciers of New Zealand. In J. Ehlers, P. L. Gibbard, & P. D. Hughes (Eds.), *Developments in Quaternary Science: Quaternary glaciations - extent and chronology* (Vol. 15, pp. 1047-1064). Amsterdam: Elsevier.

Barrell, D. J., Alloway, B. V., Schulmeister, J., & Newnham, R. M. (2005). *Towards a climate event stratigraphy for New Zealand over the past 30,000 years.* New Zealand: Institute of Geological and Nuclear Sciences.

Barrell, D. J., Almond, P. C., Vandergoes, M. J., Lowe, D. J., Newnham, R. M., & INTIMATE members. (2013). A composite pollen-based stratotype for inter-regional evaluation of climatic events in New Zealand over the past 30,000 years (NZ-INTIMATE project). *Quaternary Science Reviews*, In press.

Barrell, D. J., Anderson, B. G., & Denton, G. H. (2011). *Glacial geomorphology of the central South Island, New Zealand.* GNS Monograph 27, Geological & Nuclear Science, Lower Hutt, New Zealand.

Battarbee, R. W. (2000). Palaeolimnological approaches to climate change, with special regard to the biological record. *Quaternary Science Reviews, 19*, 107-124.

Battarbee, R. W., & Bennion, H. (2011). Palaeolimnology and its developing role in assessing the history and extent of human impact on lake ecosystems. *Journal of Paleolimnology, 45*, 399-404.

Beggs, J. R. (1999). Comparison of the quality of red and silver beech (Nothofagus) seeds in Nelson Lakes National Park, New Zealand. *New Zealand Journal of Botany, 37*, 495-501.

Birks, H. B., Heiri, O., Seppa, H., & Bjune, A. E. (2010). Strengths and weaknesses of quantitative climate reconstructions based on Late-Quaternary biological proxies. *The Open Ecology Journal, 3*, 68-110.

Birks, H. H. (2001). Plant macrofossils. In J. P. Smol, H. B. Birks, & W. M. Last (Eds.), *Tracking Environmental Change Using Lake Sediments: Terrestrial, Algal, and Siliceous Indicators* (Vol. 3, pp. 49-74). Dordrecht: Kluwer Academic Publishers.

Birks, H. H., & Birks, H. B. (2003). Reconstructing Holocene climates from pollen and plant macrofossils. In A. Mackay, R. Battarbee, J. Birks, & F. Oldfield (Eds.), *Global change in the Holocene* (pp. 342-357). London: Arnold Hodder Headline Group.

Bjorck, S., & Wohlfarth, B. (2001). ^{14}C chronostratigraphic techniques in paleolimnology. In W. M. Last, & J. P. Smol (Eds.), *Tracking Environmental Change Using Lake Sediments: Basin Analysis, Coring, and Chronological Techniques* (Vol. 1, pp. 205-245). Dordrecht: Kluwer Academic Publishers.

Blockley, S. P., Lane, C. S., Hardiman, M., Rasmussen, S. O., Seierstad, I. K., Steffensen, J. P., et al. (2012). Synchronisation of palaeoenvironmental records over the last 60,000 years, and an extended INTIMATE event stratigraphy to 48,000 b2k. *Quaternary Science Reviews, 36*, 2-10.

Bostock, H. C., Barrows, T. T., Carter, L., Chase, Z., Cortese, G., Dunbar, G. B., et al. (2013). A review of the Australian-New Zealand sector of the Southern Ocean over the last 30 Ka (Aus-INTIMATE project). *Quaternary Science Reviews*, In press.

Brook, M. S., Kirkbride, M. P., & Brock, B. W. (2006). Cirque development in a steadily uplifting range: rates of erosion and long-term morphometric change in alpine cirques in the Ben Ohau Range, New Zealand. *Earth Surface Processes and Landforms, 31*, 1167-1175.

Carter, J. A., & Lian, O. B. (2000). Palaeoenvironmental reconstruction from the last interglacial using phytolith analysis, southeastern North Island, New Zealand. *Journal of Quaternary Science, 15*(7), 733-743.

Carter, L., Manighetti, B., Ganssen, G., & Northcote, L. (2008). Southwest Pacific modulation of abrupt climate change during the Antarctic Cold Reversal–Younger Dryas. *Palaeogeography, Palaeoclimatology, Palaeoecology, 260*, 284-298.

Clarkson, B. R., McGlone, M. S., Lowe, D. J., & Clarkson, B. D. (1995). Macrofossils and pollen representing forests of the pre-Taupo volcanic eruption (c. 1850 yr BP) era at Pureora and Benneydale, central North Island, New Zealand. *Journal of The Royal Society of New Zealand, 25*(2), 263-281.

Cohen, A. S. (2003). *Paleolimnology; the history and evolution of lake sytems.* New York: Oxford University Press.

Cullen, L. E., Stewart, G. H., Duncan, R. P., & Palmer, J. G. (2001). Disturbance and Climate Warming Influences on New Zealand Nothofagus Tree-Line Population Dynamics. *Journal of Ecology, 89*, 1061-1071.

Dawson, J. W. (1988). *Forest vines to snow tussocks: the story of New Zealand plants.* Wellington: Victoria University Press.

Deevey, E. S. (1955). Paleolimnology of the upper swamp deposit, Pyramid Valley. *Records of the Canterbury Museum (New Zealand), 6*, 291-344.

Drake, H., & Burrows, C. J. (1980). The influx of potential macrofossils into Lady Lake, north Westland, New Zealand. *New Zealand Journal of Botany, 18*(2), 257-274.

Druce, A. P. (1985). *Higher plants (lycopods, ferns, gymnosperms, flowering plants) of Snowden RA., N.W. Nelson, 3500-6089 ft (1060-1850 m).* Unpublished field notes, DSIR, Botany Division.

Evans, I. S., & Cox, N. (1974). Geomorphometry and the operational definition of cirques. *Royal Geographical Society, 6*(2), 150-153.

Finsinger, W., & Wagner-Cremer, F. (2009). Stomatal-based inference models for reconstruction of atmospheric CO_2 concentration: a method assessment using a calibration and validation approach. *The Holocene, 19*, 757-764.

Folk, R. L. (1968). *Petrology of Sedimentary Rocks.* Austin, Texas: Hemphill Publishing Company (Drawer M).

Gasiorowski, M. (2008). Depostion rate of lake sediments under different alternative stable states. *Geochronometria, 32*, 29-35.

Gedye, S. J., Jones, R. T., Tinner, W., Ammann, B., & Oldfield, F. (2000). The use of mineral magnetism in the reconstruction of fire history: a case study from Lago di Origlio, Swiss Alps. *Palaeogeography, Palaeoclimatology, Palaeoecology, 164*, 101-110.

Glew, J. R., Smol, J. P., & Last, W. M. (2001). Sediment core collection and extrusion. In W. M. Last, & J. P. Smol (Eds.), *Tracking Environmental Change Using Lake Sediments: Basin Analysis, Coring, and Chronological Techniques* (Vol. 1, pp. 73-105). Dordrecht: Kluwer Academic Publishers.

Gomez, B., Carter, L., Orpin, A. R., Cobb, K. M., Page, M. J., Trustrum, N. A., et al. (2011). ENSO/SAM interactions during the middle and late Holocene. *The Holocene*, 1-8.

Gordon, J. E. (2001). The corries of the Cairngorm Mountains. *Scottish Geographical Journal, 117*(1), 49-62.

Green, J. D., & Lowe, D. J. (1985). Stratigraphy and development of c. 17 000 year old Lake Maratoto, North Island, New Zealand, with some inferences about postglacial climatic change. *New Zealand Journal of Geology and Geophysics, 28*(4), 675-699.

Green, J. D., & Lowe, D. J. (1992). Palaeolimnology in New Zealand. *Quaternary Australasia, 10*(2), 25-34.

Green, J. D., & Lowe, D. J. (1994). Origins and development. Lake Rotoroa: Change in an Urban Lake. *NIWA Ecosystems Publication, 9*, 13-23.

Greenwood, D. R. (1991). The taphonomy of plant macrofossils. In S. K. Donovan (Ed.), *The processes of fossilization* (pp. 141-169). New York: Columbia University Press.

Grosse-Brauckmann, G. (1986). Analysis of vegetative plant macrofossils. In B. E. Berglund (Ed.), *Handbook of Holocene Palaeoecology and Palaeohydrology* (pp. 591-618). Chichester: John Wiley & Sons.

Haase, P. (1986). A study of a *Libocedrus bidwillii* population at Pegleg Flat, Arthur's Pass, New Zealand. *New Zealand Journal of Ecology, 9*, 153-156.

Hajdas, I., Lowe, D. J., Newnham, R. M., & Bonani, G. (2006). Timing of the late-glacial climate reversal in the Southern Hemisphere using high-resolution radiocarbon chronology for Kaipo bog, New Zealand. *Quaternary Research, 65*, 340-345.

Hartland, A., Fenwick, G. D., & Bury, S. J. (2011). Tracing sewage-derived organic matter into a shallow groundwater food web using stable isotope and fluorescence signatures. *Marine and Freshwater Research, 62*, 119-129.

Heaton, T. H. (1986). Isotopic studies of nitrogen pollution in the hydrosphere and atmosphere: a review. *Chemical Geology, 59*, 87-102.

Heine, M. (1973). A comparison of nutrients in leaves and litter of Red, Silver and Mountain Beech. *Mauri Ora*, 55-60.

Hellstrom, J., McCulloch, M., & Stone, J. (1998). A detailed 31,000-year record of climate and vegetation change, from the isotope geochemistry of two New Zealand speleotherms. *Quaternary Research, 50*, 167-178.

Hesse, P. P. (1994). The record of continental dust from Australia in Tasman Sea sediments. *Quaternary Science Reviews, 13*, 257-272.

Heyng, A. M., Mayr, C., Lucke, A., Striewski, B., Wastegard, S., & Wissel, H. (2012). Environmental changes in northern New Zealand since the Middle Holocene inferred from stable isotope records ($\delta^{15}N$, $\delta^{13}C$) of Lake Pupuke. *Journal of Paleolimnology, 48*, 351-366.

Hogg, A. G., Fifield, L., Turney, C. S., Palmer, J., Galbraith, R., & Baillie, M. G. (2006). Dating ancient wood by high sensitivity liquid scintillation counting and accelerator mass spectrometry - Pushing the boundaries. *Quaternary Geochronology, 1*, 241-248.

Hollander, D. J., & Smith, M. A. (2001). Microbially mediated carbon cycling as a control on the delta ^{13}C of sedimentary carbon in eutrophic Lake Mendota (USA): New models for interpreting isotopic excursions in the sedimentary record. *Geochimica et Cosmochimica Acta, 65*, 4321-4337.

Jara, I. A., Newnham, R. M., Vandergoes , M. J., Foster, C. R., Lowe, D. J., Moreno, P., et al. (2012). Stratigraphy and palynology of a c. 14,000 yr-long lake sediment record from Adelaide Tarn, northwest Nelson, and some paleoclimatic implications. In A. Pittari, & R. Hansen (Ed.), *Geosciences 2012 Conference. 134A.* Hamilton, New Zealand: Geoscience Society of New Zealand.

Jeter, H. W. (2000). Determining the ages of recent sediments using measurements of trace radioactivity. *Terra et Aqua, 78*, 21-28.

Jongens, R. (2006). Structure of the Buller and Takaka Terrane rocks adjacent to the Anatoki Fault, northwest Nelson, New Zealand. *New Zealand Journal of Geology and Geophysics, 49*(4), 443-461.

Kemp, A. E., Dean, J., Pearce, R. B., & Pike, J. (2001). Recognition and analysis of bedding and sediment fabric features. In *Tracking Environmental Change using Lake Sediments: Physical and Geochemical Methods* (Vol. 2, pp. 7-22). Dordrecht: Kluwer Academic Publishers.

Korhola, A., Olander, H., & Blom, T. (2000). Cladoceran and chironomid assemblages as quantitative indicators of water depth in subarctic Fennoscandian lakes. *Journal of Paleolimnology, 24*, 43-54.

Laird, M. G. (1972). Sedimentology of the Greenland Group in the Paparoa Range, West Coast, South Island. *New Zealand Journal, 15*(3), 372-393.

Last, W. M. (2001). Textural analysis of lake sediments. In W. M. Last, & J. P. Smol (Eds.), *Tracking Environmental Change Using Lake Sediments: Physical and Geochemical Methods* (Vol. 2, pp. 41-81). Dordrecht: Kluwer Academic Publishers.

Leathwick, J. R., Wilson, G., & Stephens, R. T. (2002). *Climate Surfaces for New Zealand.* Landcare Research Contract Report: LC9798/126, Landcare Research, Biodiversity and Conservation Division, Hamilton.

Lee, J. A., Flower, R. J., Ryves, D., Vologina, E., & Strum, M. (1998). Identifying sedimentation patterns in Lake Baikal using whole core and surface scanning magnetic susceptibility. *Journal of Paleolimnology, 20*, 187-202.

Lees, C. M. (1986). Late quaternary palynology of the southern Ruahine Range North Island, New Zealand. *New Zealand Journal of Botany, 24*(2), 315-329.

Leng, M. J., & Marshall, J. D. (2004). Palaeoclimate interpretation of stable isotope data from lake sediment archives. *Quaternary Science Reviews, 23*, 811-831.

Li, X., Rapson, G. L., & Flenley, J. R. (2008). Holocene vegetational and climatic history, Sponge Swamp, Haast, south-western New Zealand. *Quaternary International, 184*, 129-138.

Lowe, D. J. (1988). Stratigraphy, age, composition, and correlation of late Quaternary tephras interbedded with organic sediments in Waikato lakes, North Island, New Zealand. *New Zealand Journal of Geology and Geophysics, 31*(2), 125-165.

Lowe, D. J., & Green, J. D. (1992). Lakes. In J. M. Soons, & M. J. Selby (Eds.), *Landforms of New Zealand. Second Edition.* Auckland: Longman Paul.

Lowe, D. J., Blaauw, M., Hogg, A. G., & Newnham, R. M. (2013). Ages of 24 widespread tephras erupted since 30,000 years ago in New Zealand, with re-evaluation of the timing and palaeoclimatic implications of the Lateglacial cool episode recorded at Kaipo bog. *Quaternary Science Reviews*.

Lowe, D. J., Green, J. D., Northcote, T. G., & Hall, K. J. (1997). Holocene fluctuations of a meromictic lake in southern British Columbia. *Quaternary Research, 48*, 100-113.

Lowe, D. J., Hogg, A. G., & Hendy, C. H. (1981). Detection of thin tephra deposits in peat and organic lake sediments by rapid X-radiography and X-ray fluorescence techniques. *Proceedings of Tephra Workshop, 30th June–1st July, 1980. VUW Geology Dept.*

Lowe, D. J., Shane, P. A., Alloway, B. V., & Newnham, R. M. (2008). Fingerprints and age models for widespread New Zealand tephra marker beds erupted since 30,000 years ago: a framework for NZ-INTIMATE. *Quaternary Science Reviews, 27*, 95-126.

Lowe, J. J., Rasmussen, S. O., Bjorck, S., Hoek, W. Z., Steffensen, J. P., Walker, M. J., et al. (2008). Synchronisation of palaeoenvironmental events in the North Atlantic region during the Last Termination: a revised protocol recommended by the INTIMATE group. *Quaternary Science Reviews, 27*, 6-17.

Macdonald, P. D., & Green, P. E. (1988). *User's Guide to Program MIX: An Interactive Program for Fitting Mixtures of Distributions.* Ichthus Data Systems.

Mark, A. F., & Adams, N. M. (1973). *New Zealand Alpine Plants.* Wellington: A.H. & A.W. Reed.

Marra, M., & Laschen, R. A. (2004). Late Quaternary paleoecology from fossil beetle communities in the Awatere Valley, South Island, New Zealand. *Journal of Biogeography, 31*, 571-586.

Marx, S. K., McGowan, H. A., & Kamber, B. S. (2009). Long-range dust transport from eastern Australia: A proxy for Holocene aridity and ENSO-type climate variability. *Earth and Planetary Science Letters, 282*, 167-177.

Mauquoy, D., Hughes, P. D., & van Geel, B. (2010). A protocol for plant macrofossil analysis of peat deposits. *Mires and Peat, 7*, 1-5.

Mazzucchi, D., Spooner, I. S., Gilbert, R., & Osborn, G. (2003). Reconstruction of Holcene climate using multiproxy analysis of sediments from Pyramid Lake, British Columbia, Canada. *Arctic, Antarctic, and Alpine Research, 35*(4), 520-529.

McCarthy, A., Mackintosh, A., Rieser, U., & Fink, D. (2008). Mountain glacier chronology from Boulder Lake, New Zealand, indicates MIS 4 and MIS 2 ice advances of similar extent. *Arctic, Antarctic, and Alpine Research, 40*(4), 695-708.

McGlone, M. S. (2001). The origin of the indigenous grasslands of southeastern South Island in relation to pre-human woody ecosystems. *New Zealand Journal of Ecology, 25*(1), 1-15.

McGlone, M. S. (2002). A Holocene and latest Pleistocene pollen record from Lake Poukawa, Hawke's Bay, New Zealand. *Global and Planetary Change, 33*, 283-299.

McGlone, M. S., & Basher, L. (2012). Holocene vegetation change at treeline, Cropp Valley, Southern Alps, New Zealand. *Terra Australis, 34*, 343-358.

McGlone, M. S., & Wilmshurst, J. M. (1999). A Holocene record of climate, vegetation change and peat bog development, east Otago, South Island, New Zealand. *Journal of Quaternary Science, 14*(3), 239-254.

McGlone, M. S., & Wilmshurst, J. M. (1999). Dating initial Maori environmental impact in New Zealand. *Quaternary International, 59*, 17-26.

McGlone, M. S., Hall, G. M., & Wlimshurst, J. M. (2011). Seasonality in the early Holocene: Extending fossil-based estimates with a forest ecosystem process model. *The Holocene, 21*(4), 517-526.

McGlone, M. S., Turney, C. S., & Wilmshurst, J. M. (2004). Late-glacial and Holocene vegetation and climatic history of the Cass Basin, central South Island, New Zealand. *Quaternary Research, 62*, 267-279.

McLauchlan, K. K., Williams, J. J., Craine, J. M., & Jeffers, E. S. (2013). Changes in global nitrogen cycling during the Holocene epoch. *Nature, 495*, 352-356.

McWethy, D. B., Whitlock, C., Wilmshurst, J. M., McGlone, M. S., & Li, X. (2009). Rapid deforestation of South Island, New Zealand, by early Polynesian fires. *The Holocene, 19*(6), 883-897.

Meyers, P. A., & Teranes, J. L. (2001). Sediment organic matter. In *Tracking Environmental Change Using Lake Sediments: Physical and Geochemical Methods* (Vol. 2, pp. 239-270). Dordrecht: Kluwer Academic Publishers.

Mildenhall, D. C., Cochran, U. A., & Cook, R. A. (2006). Reconnaissance sediment and microfossil analyses of a laminated short piston core from Lake Tekapo, South Island, New Zealand. *New Zealand Journal of Geology and Geophysics, 49*, 463-476.

Moreno, P. I., Francois, J. P., Moy, C. M., & Villa-Martinez, R. (2010). Covariability of the southern westerlies and atmospheric CO_2 during the Holocene. *Geology, 38*, 727-730.

Moy, C. M., Seltzer, G. O., Rodbell, D. T., & Anderson, D. M. (2002). Variability of El Nino/Southern Oscillation activity at millennial timescales during the Holocene epoch. *Nature, 420*, 162-165.

Myrbo, A., & Wright, H. E. (2008). *An introduction to Lingstone and Bolivia Coring Equipment.* Minneapolis, MN : National Lacustrine Core Facility, University of Minnesota.

Nathan, S. (1976). Geochemistry of the Greenland Group (early Ordovician), New Zealand. *New Zealand Journal of Geology and Geophysics, 19*(5), 683-706.

Neukom, R., & Gergis, J. (2011). Southern Hemisphere high-resolution palaeoclimate records of the last 2000 years. *The Holocene, 22*(5), 501-524.

Neuner, G., & Bannister, P. (1995). Frost resistance and susceptibility to ice formation during natural hardening in relation to leaf anatomy in three evergreen tree species from New Zealand. *Tree Physiology, 15*, 371-377.

Newnham, R. M., & Lowe, D. J. (1991). Holocene vegetation and volcanic activity, Auckland Isthmus, New Zealand. *Journal of Quaternary Science, 6*, 177-193.

Newnham, R. M., & Lowe, D. J. (2000). Fine-resolution pollen record of late-glacial climate reversal from New Zealand. *Geology, 28*, 759-762.

Newnham, R. M., de Lange, P. J., & Lowe, D. J. (1995). Holocene vegetation, climate and history of a raised bog complex, northern New Zealand based on palynology, plant macrofossils and tephrochronology. *The Holocene, 5*(3), 267-282.

Newnham, R. M., Lowe, D. J., & Matthews, B. W. (1998a). A late-Holocene and prehistoric record of environmental change from Lake Waikaremoana, New Zealand. *The Holocene, 8*(4), 443-454.

Newnham, R. M., Lowe, D. J., & Williams, P. W. (1999). Quaternary environmental change in New Zealand: a review. *Progress in Physical Geography, 23*(4), 567-610.

Newnham, R. M., Lowe, D. J., Green, J. D., Turner, G. M., Harper, M. A., McGlone, M. S., et al. (2004). A discontinuous ca. 80 ka record of Late Quaternary environmental change from Lake Omapere, Northland, New Zealand. *Palaeogeography, Palaeoclimatology, Palaeoecology, 207*, 165-198.

Newnham, R. M., Lowe, D. J., McGlone, M. S., Wilmshurst, J. M., & Higham, T. F. (1998b). The Kaharoa Tephra as a critical datum for earliest human impact in northern New Zealand. *Journal of Archaeological Science, 25*, 533-544.

Newnham, R. M., Vandergoes, M. J., Garnett, M. H., Lowe, D. J., Prioir, C., & Almond, P. C. (2007). Test of AMS 14C of pollen concentrations using tephrochronology. *Journal of Quaternary Science, 22*(1), 37-51.

Newnham, R. M., Vandergoes, M. J., Sikes, E., Carter, L., Wilmshurst, J. M., Lowe, D. J., et al. (2012). Does the bipolar seesaw extend to the terrestrial southern mid-latitudes? *Quaternary Science Reviews, 36*, 214-222.

Nowaczyk, N. R. (2001). Logging of magnetic susceptibility. In W. M. Last, & J. P. Smol (Eds.), *Tracking Environmental Change Using Lake Sediments: basin analysis, coring, and chronological techniques* (Vol. 1, pp. 155-170). Dordrecht: Kluwer Academic Publishers.

Page, M. J., Trustrum, N. A., & Dymond, J. R. (1994). Sediment budget to assess the geomorphic effect of a cyclonic storm, New Zealand. *Geomorphology, 9*(3), 169-188.

Page, M. J., Trustrum, N. A., Orpin, A. R., Carter, L., Gomez, B., Cochran, U. A., et al. (2010). Storm frequency and magnitude in response to Holocene climate variability, Lake Tutira, north-eastern New Zealand. *Marine Geology, 270*, 30-44.

Parris, A. S., Bierman, P. R., Noren, A. J., Prins, M. A., & Lini, A. (2009). Holocene paleostorms identified by particle size signatures in lake sediments from the northeastern United States. *Journal of Paleolimnology, 43*(1), 29-49.

Pepper, A. C., Shulmeister, J., & Nobes, D. C. (2004). Possible ENSO signals prior to the Last Glacial Maximum, during the last deglaciation and the early Holocene, from New Zealand. *Geophysical Research Letters, 31*.

Pocknall, D. T. (1980). Modern pollen rain and Aranuian vegetation from Lady Lake, north Westland, New Zealand. *New Zealand Journal of Botany, 18*(2), 275-284.

Putnam, A. E., Schaefer, J. M., Denton, G. H., Barrell, D. J., Finkel, R. C., Anderson, B. G., et al. ((August) 2012). Regional climate control of glaciers in New Zealand and Europe during the pre-industrial Holocene. *Nature Geoscience - Advance online publication*.

Rattenbury, M. S., Cooper, R. A., & Johnston, M. R. (1998). *Geology of the Nelson Area.* 1:250 000 Geological Map 9, Institute of Geological & Nuclear Sciences, Lower Hutt, New Zealand.

Renwick, J., & Tompson, D. (2006). The southern annular mode and New Zealand climate. *Water and Atmosphere (NIWA), 14*, 24-25.

Reynolds, R. L., Rosenbaum, J. G., & Thompson, R. S. (2008). *Mineralogic Causes of Variations in Magnetic Susceptibility of Late Pleistocene and Holocene Sediment from Great Salt Lake, Utah.* Reston, Virginia: U. S. Geological Survey.

Reynolds, R. L., Rosenbaum, J. G., Rapp, J., Kerwin, M. W., Bradbury, J. P., Adam, D., et al. (2004). *Record of Late Pleistocene Glaciation and Deglaciation in the Southern Cascade Range. I. Petrological Evidence from Lacustrine Sediment in Upper Klamath Lake, Southern Oregon.* USGS staff - published research.

Roser, B. P., Cooper, R. A., Nathan, S., & Tulloch, A. J. (1996). Reconnaissance sandstone geochemistry, provenance, and tectonic setting of the lower Paleozoic terranes of the West Coast and Nelson, New Zealand. *New Zealand Journal of Geology and Geophysics, 39*(1), 1-16.

Ryan, M. T., Dunbar, G. B., Vandergoes, M. J., Neil, H. L., Hannah, M. J., Newnham, R. M., et al. (2012). Vegetation and climate in Southern Hemisphere mid-latitudes since 210 ka: new insights from marine and terrestrial pollen records from New Zealand. *Quaternary Science Reviews, 48*, 80-98.

Saarinen, T., & Petterson, G. (2001). Image analysis techniques. In W. M. Last, & J. P. Smol (Eds.), *Tracking Environmental Change Using Lake Sediments: physical and geochemical methods* (pp. 23-39). Dordrecht: Kluwer Academic Publishers.

Sandgren, P., & Snowball, I. (2001). Application of mineral magnetic techniques to paleolimnology. In W. M. Last, & P. J. Smol (Eds.), *Tracking Environmental Change Using Lake Sediments: physical and geochemical methods* (pp. 217-237). Dordrecht: Kluwer Academic Publishers.

Sandiford, A., Newnham, R., Alloway, B., & Ogden, J. (2003). A 28 000-7600 cal yr BP pollen record of vegetation and climate change from Pukaki Crater,

northern New Zealand. *Palaeogeography, Palaeoclimatology, Palaeoecology, 201*, 235-247.

Schallenberg, M., Goff, J., & Harper, M. A. (2012). Gradual, catastrophic and human induced environmental changes from a coastal lake, southern New Zealand. *Sedimentary Geology, 273-274*, 48-57.

Shulmeister, J., Fink, D., & Augustinus, P. C. (2005). A cosmogenic nuclide chronology of the last glacial transition in North-West Nelson, New Zealand—new insights in Southern Hemisphere climate forcing during the last deglaciation. *Earth and Planetary Science Letters, 233*, 455-466.

Sporka, F., Stefkova, E., Bitusik, P., Thompson, A. R., Agusti-Panareda, A., Appleby, P. G., et al. (2002). The paleolimnological analysis of sediments from high mountain lake NiÓné Terianske pleso in the High Tatras (Slovakia). *Journal of Paleolimnology, 28*, 95-109.

Steart, D. C., Greenwood, D. R., & Boon, P. I. (2009). The chemical constraints upon leaf decay rates: Taphonomic implications among leaf species in Australian terrestrial and aquatic environments. *Review of Palaeobotany and Palynology, 157*, 358-374.

Stephens, T., Atkin, D., Augustinus, P., Shane, P., Lorrey, A., Street-Perrott, A., et al. (2012). A late glacial Antarctic climate teleconnection and variable Holocene seasonality at Lake Pupuke, Auckland, New Zealand. *Journal of Paleolimnology, 48*, 785-800.

Striewski, B., Mayr, C., Flenley, J., Naumann, R., & Turner, G. (2009). Multi-proxy evidence of late Holocene human-induced environmental changes at Lake Pupuke, Auckland (New Zealand). *Quaternary International, 202*, 69-93.

Sweetapple, P. J., & Fraser, K. W. (1992). Litterfall from a mixed red beech (*Nothofagus fusca*)-silver beech (*Nothofagus menziesii*) forest, central North Island, New Zealand. *New Zealand Journal of Botany, 30*(3), 263-269.

Talbot, M. R. (2001). Nitrogen isotopes in palaeolimnology. In W. M. Last, & J. P. Smol (Eds.), *Tracking Environmental Change Using Lake Sediments: Physical and Geochemical Methods* (Vol. 2, pp. 401-439). Dordrecht: Kluwer Academic Publishers.

Talbot, M. R., & Laerdal, T. (2000). The Late Pleistocene-Holocene palaeolimnology of Lake Victoria, East Africa, based upon elemental and isotopic analyses of sedimentary organic matter. *Journal of Paleolimnology, 23*, 141-164.

Tiljander, M., Ojala, A., Saarinen, T., & Snowball, I. (2002). Documentation of the physical properties of annually laminated (varved) sediments at a sub-annual to decadal resolution for environmental interpretation. *Quaternary International, 88,* 5-12.

Turner, G. M. (1997). Environmental magnetism and magnetic correlation of high resolution lake sediment records from Northern Hawke's Bay, New Zealand. *New Zealand Journal of Geology and Geophysics, 40,* 287-298.

Turner, G. M., & Lillis, D. A. (1994). A palaeomagnetic secular variation record for New Zealand during the past 2500 years. *Physics of the Earth and Planetary Interiors, 83,* 265-282.

Turney, C. S., McGlone, M. S., & Wilmshurst, J. M. (2003). Asynchronous climate change between New Zealand and the North Atlantic during the last deglaciation. *Geology, 31,* 223-226.

Vaasma, T. (2008). Grain-size analysis of lacustrine sediments: a comparison of pre-treatment methods. *Estonian Journal of Ecology, 57*(4), 231-243.

Vandergoes, M. J., Dieffenbacher-Krall, A. C., Newnham, R. M., Denton, G. H., & Blaauw, M. (2008). Cooling and changing seasonality in the Southern Alps, New Zealand during the Antarctic Cold Reversal. *Quaternary Science Reviews, 27,* 589-601.

Vanhoutte, K., Verleyen, E., Kilroy, C., Sabbe, K., Dasseville, R., & Vyverman, W. (2006). Journal of Paleolimnology Journal of Paleolimnology. *Journal of Paleolimnology, 57,* 83-93.

Velle, G., Bjune, A. E., Larsen, J., & Birks, H. B. (2010). Holocene climate and environmental history of Brurskardstjørni, a lake in the catchment of Øvre Heimdalsvatn, south-central Norway. *Hydrobiologia, 642,* 13-34.

Walker, M. J., Berkelhammer, M., Bjorck, S., Cwynar, L. C., Fisher, D. A., Long, A. J., et al. (2012). Formal subdivision of the Holocene Series/Epoch: a Discussion Paper by a Working Group of INTIMATE (Integration of ice-core, marine and terrestrial records) and the Subcommission on Quaternary Stratigraphy (International Commission on Stratigraphy). *Journal of Quaternary Science, 27*(7), 649-659.

Walker, M., Johnsen, S., Rasmussen, S. O., Popp, T., Steffensen, J.-P., Gibbard, P., et al. (2009). Formal definition and dating of the GSSP (Global Stratotype Section and Point) for the base of the Holocene using the Greenland NGRIP ice core, and selected auxiliary records. *Journal of Quaternary Science, 24*(1), 3-17.

Wardle, P. (1991). *Vegetation of New Zealand.* Cambridge: Cambridge University Press.

Weber, M. E., Reichelt, L., Pfeiffer, M., Korff, B., Thurow, J., & Ricken, W. (2010). BMPix and PEAK tools: New methods for automated laminae recognition and counting—Application to glacial varves from Antarctic marine sediment. *Geochemistry, Geophysics, Geosystems, 11*(3).

Williams, P. W., King, D. N., Zhao, J.-X., & Collerson, K. D. (2004). Speleothem master chronologies: combined Holocene ^{18}O and ^{13}C records from the North Island of New Zealand and their palaeoenvironmental interpretation. *The Holocene, 14*, 194-208.

Williams, P. W., King, D. N., Zhao, J.-X., & Collerson, K. D. (2005). Late Pleistocene to Holocene composite speleothem ^{18}O and ^{13}C chronologies from South Island, New Zealand—did a global Younger Dryas really exist? *Earth and Planetary Science Letters, 230*, 301-317.

Williams, P. W., Neil, H. L., & Zhao, J.-X. (2010). Age frequency distribution and revised stable isotope curves for New Zealand speleothems: palaeoclimatic implications. *International Journal of Speleology, 39*, 99-112.

Wilmshurst, J. M., McGlone, M. S., Leathwick, J. R., & Newnham, R. M. (2007). A pre-deforestation pollen-climate calibration model for New Zealand and quantitative temperature reconstructions for the past 18 000 years BP. *Journal of Quaternary Science, 22*(5), 535-547.

Wratt, D. S., Tait, A., Griffiths, G., Espie, P., Jessen, M., Keys, J., et al. (2006). Climate for crops: integrating climate data with information about soils and crop requirements to reduce risks in agricultural decision-making. *Meteorological Applications, 13*, 305-315.

Yan, P., Shi, P., Gao, S., Chen, L., Zhang, X., & Bai, L. (2002). ^{137}Cs dating of lacustrine sediments and human impacts on Dalian Lake, Qinghai Province, China. *Catena, 47*, 91-99.

Appendices

Appendix A: mixdist routine

Appendix B: UoW Herbarium catalogued reference species that were used to identify plant macrofossils

Appendix C: Absolute abundance of plant macrofossils and additional notes

Included on CD

Appendix D: Grain size

Appendix E: Magnetic susceptibility

Appendix F: Isotope data

Appendix A: mixdist routine

Operating Rmix

By David Haberlah, Ben Love and Craig Strong – over a 12mnth period.

Three major activities;

1. converting MSA data into Rmix compatible input file
2. running syntax in Rmix
3. refining fits

Converting MSA data into Rmix compatible input file

- Rmix input data needs to have two columns of data; log10 um and vol %.
- Using the "mixdata_calc_sheet.xls" paste in exported listing data from the Multisizer. Note there are three tabs in this xls sheet from three different projects, all sheets do same job.
- Copy columns E and F
- Paste into notepad and save as a txt file.
- If you save the files with a simple filename it simplifies the Rmix syntax. In fact if you save successive samples with the same filename (e.g. x.txt) you don't need to change you syntax, HOWEVER you MUST ensure that you are saving to the correct folder to ensure that you are processing the correct sample !!!
- Should save the txt file in: C:\Program Files\R\R-2.9.0\library\mixdist\data

Running syntax in Rmix

- the syntax required is found in the attached txt file "Mix Syntax Cheat Sheet.txt" – have this file open also to allow easy cut and paste
- Open up R
- At prompt copy and paste in first line of syntax : "library(mixdist)" [enter]
  This tells R that it will be working with the package mixdist

- Paste in second line: "data(x)" [enter]
  This tells R the file name it will be looking for

- Paste in third line: "x<-as.mixdata(x)" [enter]
  Reads the txt file and identifies that input data is in correct format (nb x is the data filename).

- Paste in fourth line: "plot(x)" [enter]
  Produces a simple line plot of the distribution – i.e. the psd .

- Paste in fifth line: "fitx1<-
  mix(x,mixparam(mu=c(0.1,1.2),sigma=c(0.2),pi=c(0.2)),"norm",mixconstr(conpi="NONE",conmu="NONE",consigma="NONE",fixpi=c(NULL),fixmu=c(NULL),fixsigma=c(NULL)))" [enter]

This is the cruncher !!!! there is scope here to alter the analysis – number of parameters, type of distribution, constricting or free floating analysis etc etc. Essentally the above is for a distribution with 2 populations at (0.1 and 1.2 modal positions, setting the std dev (sigma) at a nominal size of 0.2 and a nominal proportion of 0.2. Unlike the old version you don't have to make the pi = 1, Rmix will just spit out the best fit.

- Paste in sixth line: "plot(fitx1)" [enter]
  Plots the populations against the overall population, i.e. visual representation of best fit. Note the condition of the fit for refinement if required

- Paste in seventh line: "summary(fitx1)" [enter]
  Presents all the numerical data associated with the fit. Best to write this down if unhappy with fit and start making adustments to the numbers specified in line five.

<u>Constructing refits in Rmix</u>

The program is sequential in processing (I think) that is, it will sort of build on what it has already done for the one sample and rework with this data. It is important to have a knowledge of the last set of parameters just produced and then start modifying the syntax against this

- To re run syntax (e.g. step 5), when in the RGui at the > prompt just use the 'up' arrows on your keyboard to scroll through the last used line of syntax.
- Just scroll up to e.g line 5, change the parameters (mu, pi, sigma) and hit enter to action the request.
- Of course then need to scroll up to re run line 6 (plot function) and then line 7 (numerical summary).

To run a new sample, just create a new txt file, save as the 'x.txt' in the original folder (i.e. overwrite the prexisting file) and then scroll up to line one of code. Then scroll back down the list of codes again.

Appendix B: UoW Herbarium catalogued reference species that were used to identify plant macrofossils

Reference species	Waikato Herbarium number	Location	Altitude (m)
Nothofagus menziesii	Waik-15271-P0606 Waik-303-P0607	Waikato Ecological Region Uruwera's	1219 m
Nothofagus fusca	Waik-19085	Mossoman Bush Block, King Country	240 m
Nothofagus solandri var. cliffortioides	Waik-15171	Craigieburn Ecological District	860 m
Libocedrus bidwillii	Waik-3399	Ohakuni TNP	1000 m
Phyllocladus alpinus		Ketetahi Track, Mt Tongariro	1200 m
Dracophyllum lingifolium	Waik-5484	Mt Manuoha	1402 m

Appendix C: Absolute abundance of plant macrofossils and additional notes

Plant identification									
Depth	**Species**	**Abundance**	**Leaf**	**Seed**	**Root**	**Stem**	**Fragments**	**Photos**	**Measurements**
0	*Dracophyllum longifolium*	Rs					1	5	
	Carex grass	Ss					4	3, 9	
	Libocedrus bidwillii	Rs					2	8	
	Aquatic seed pod	Rs					1	4	
	Unidentified 1.							6, 7	
	Unidentified 2.	Ss					3	10	
	Unidentified 3. Small leaf		1					8	
	Unidentified 4. Moss							11, 12	
	Unidentified 5. Grass							13, 14	
5	*Nothofagus cliffortioides*	RL	1					15, 16, 17, 18	
	Carex sp.	Rs					1	19	
	Unidentified 1. Grass	Ss					3	20	~5 mm
	Unidentified 2. Small leaf		1					21	~ 5 mm
	Unidentified 3. Grass-2						1	22	~10 mm
	Unidentified 4. Possible seed?			4				23, 24	
	Unidentified 5. Possible seed?			1				25, 26	~3 mm
	Unidentified 6. Grass?	Rs					2	27, 28	

	Unidentified 7. Moss						1	29	
	Unidentified 8. Grass?						1		
10	*Nothofagus cliffortioides*	RL	1					31, 32	
15	Unidentified 1. Moss?						1	33	
	Unidentified 2. possible seed?			1					
20	Unidentified 1. Seed?			1				34 (m 4.0)	
	Unidentified 2. Moss?	AM					Multiple	35 (m 2.0)	
	Unidentified 3. Small leaf		1					36 (m 2.5)	~3 mm

25	Unidentified 1. Moss-1							37 (m 2.0)	
	Unidentified 2. Moss-2						2	38, 39 (m 1.6)	~4-6 mm
30	*Libocedrus bidwillii*		1					L.bid 30 cm, 40, 41 (m 0.8)	
	Unidentified 1. Seed coat?	Ss					3	42 (m 3.2), 43 (m 5.0)	
	Unidentified 2. Moss	Mm					6		
	Unidentified 3. Grass, flax	Cs					10	44, 45 (m 1.6)	2-3 mm
	Unidentified 4. Grass						1	46 (m 1.6)	
	Unidentified 5. Moss?	Ss					3	47	
35	Unidentified 1. Leaf	RL	2					048 (m 1.25), 49 (m 2.5), 50 (m 3.2), 51 (m	~6 mm

								10.0)	
	Unidentified 2. Moss	Rs					2	52	
	Unidentified 3. Seed capsule?						1	53 (m 2.0), 54 (m 3.2), 55 (m 3.2)	
	Unidentified 4. Grass	Ms					5		
	Unidentified 5. seed coat?						1	56	
40	No Big macros, all micro and broken frags								
45	Same as above								

50	Unidentified 1. Moss								
	Unidentified 2. Grass?								
55	No macros								
	Some of U1-15 cm								
60	*Libocedrus bidwillii*	Mm	2				5	57 (m 1.0), 58 (m 1.25), 59 (m 1.25), 60 (m 3.2) 61	

65	Unidentified 1. Moss								
	Unidentified 2. Mix of frags								
70	Unidentified 1. Moss								
75	Unidentified 1. small leaf		1				2	2, 62 (1.6), 63 (m 3.2)	
	Unidentified 2. Moss?								

	Unidentified 3. Grass						1	64 (m 1.6)	
	unidentified 4.						1	65 (m 2.0)	
	Unidentified 5. stem?						1	66 (2.0), 67 (m 4.0)	
	Unidentified 6.						1	68 (m 3.2), 69 (m 5.0)	
80	Unidentified 1. Moss								
	Unidentified 2.						1	70 (m 2.5)	
	Unidentified 3.						1	71 (m 2.0)	
	Unidentified 4.		1					72 (m 3.2), 73 (m 6.3)	~2 mm
	Unidentified 5.		1					74 (m 2.5)	~2-3 mm
	Unidentified 6. leaf fragment						1	75 (2.5), 76 (m 6.3)	~2-3 mm
	Unidentified 7. Grass								
	Unidentified 8.							77 (m 2.0), 78 (m 6.3)	
	Unidentified 9. Monocote?						1	79 (m 3.2), 80 (m 6.3)	
85	Unidentified 1. Moss								

90	Unidentified 1.						1	81 (m 1.6), 82 (m 4.0), 83 (m 5.0), 84 (m 3.2)	
	Unidentified 2.								
95	Unidentified 1. Moss								
	Nothofagus menziessii	RL	1					85 (m 1.6), 92 (m 1.6), 93, 94	
	Nothofagus fusca	RL	1					86 (m 0.8), 87 (m 1.0)	
	Nothofagus undifferentiated	SL					8	88 (1.6)	
	Libocedrus sp.						1		
100	Very small fargments								
	Nothofagus sp.	RL					2		

105	Unidentified 1. Grass								
	Unidentified 2. Leaf stem?							1	
	Unidentified 3. Bark?							1	
	Unidentified 4.							2	
110	Unidentified 1. Moss	AL						large amount	
	Nothofagus menziessii	SL						5	
	Nothofagus undifferentiated	Cs						13	2-3 mm
	Nothofagus sp.	Rs		1				97 (m 1.25)	
	Unidentified 2. Stem	Rs				2		98 (m 1.25)	
	Unidentified 3. Leaf, poss hebe odora	Rs	1					99 (m 2.5), 105 (m 4.0)	2-3 mm
	Unidentified 4. Moss						1	106 (m 2.5)	
	Phyllocladus	RL	1					96 (m 0.8)	

115	*Nothofagus menziessii*	RL	1					114 (m 0.8)	
	Nothofgus undifferentiated	Rs					3		
120	*Nothofagus menziessii*	RL	1					116 (m 0.8)	
	Nothofagus sp.	Rs					1	120 (m 1.25)	
	Unidentified 1.						1		
	Unidentified 2. Grass								
	Unidentified items							121 (m 1.0), 122 (m 1.6)	
	Nothofagus fusca	RL	1					117 (m 0.8)	
	Phyllocladus or *Nothofagus*	RL					1	118 (m 0.8)	
125	*Nothofagus menziessii*	RL	4					123, 124, 125, 126 (m 0.8),	
	Nothofagus undifferentiated	As					24	128 (m 1.0)	Ranging from 2-4 mm
	Unidentified 1. Grass	Ss					5		
	Unidentified 3.					3			
	Unidentified 4.	Rs					4		
	Nothofagus fusca	RL	2					127 (m	

								1.25),129 (m 1.0)	
130	*Nothofagus menziessii*	RL					3	133 (m 0.8)	
	Nothofagus sp.	CM					14		
	Unidentified 1. Stems	Rs				3		132 (m 1.0)	
135	*Nothofagus menziessii*	SL					6	134, 135, 136 (m 0.8), 137 (m 1.0)	
	Nothofagus sp.	Ss					7	138 (m 1.0)	2-4 mm
	Unidentified 1.	Cs					11	139 (m 1.0)	
	Unidentified 2. Monocote	Rs					2	140 (m 2.0)	
140	*Nothofagus menziessii*	CL					11	141 (m 0.8), 142 (m 1.0)	Large frag 5-6 mm
	Nothofagus fragments	Ss					8	143 (m 0.8)	

145	Nothofagus sp. ?	Cs					12		2-4 mm
	Undifferenciated leaves with stems	Rs					4		
	Unidentified 1. Leaf, poss *Plantago*	Rs	1					144 (m 3.2), 145 (m 4.0), 146 (m 2.0)	1x3 mm
	Unidentified 2. Moss/liverwort						1	147 (m 1.6)	
	L. bidwillii	Rs					1	148 (m 2.0)	
	Unidentified 3. Grass	Rs					3		
	Unidentified 4. Grass	Rs					4		5-10 mm
	Undifferenciated fragments	SM					9		
150	Nothofagus sp.	Ss					9	149 (m 1.25)	2-4 mm
	Unidentified 1. Small leaf, poss *Celmisia*	Rs	1					150 (m 2.5), 151 (m 4.0), 152 (m 4.0)	2-3 mm
	Undifferentiated frags	Rs					4		2-4 mm

155	*Nothofagus menziessii*	Rm	1				2	153 (m 0.8)	
	Seed	Rs	1						
	Undifferentiated fragments	Am					16+		
	Unidentified 1. Leaf		1				1	155 (m 1.6)	
	Unidentified 2. Moss						1		
	Unidentified 3. Moss-2						1	156 (m 2.5)	
161	*Nothofagus menziessii*	RL	2					157 (m 0.8), 158 (m 1.25)	
	Nothofagus sp.	Rs					4		
	Unidentified fragments	AM					15		
	Unidentified 1. Grass						2		
165	*Nothofagus menziessii*	RL	2					159 (m 0.8), 160 (m 0.8)	
	leaf fargments-poss nothofagus	Ss					8		1-2 mm
	Undifferenciated fragments	Ss					9		0.5-1 mm
	Unidentified 1. Grasses						2		
	Unidentified 2.- *Hymenophyllum*?						1	161 (m 3.2), 162 (m 2.0)	10 mm
	Unidentified 3. Liverwort							163 (m 2.0)	

	Unidentified 4.							164 (m 1.6)	
	Unidentified 5.							165 (m 2.5), 166 (m 0.2)	15 mm
170	Unidentified 1. grass						4		
	Unidentified 2. Notho frags?						6		
	Unidentified 3. moss								
175	Nothofagus sp.	Cs					leaf frags 10		1-2 mm
	Unidentified 1. grass	Rs					4		
	Unidentified 2. moss	Rs					1		
180	*Nothofagus menziessii*	RL	1 1/2					167 (m 1.0)	4-5 mm
	Nothofagus sp. Leaf frags	Cs					11	168 (m 1.0)	1-3 mm
	Stem-possible nothofagus	Rs				1		169 (m 1.25)	
	Unidentified 1. Grass	Ss					6		2-3 mm

	Unidentified 2. Moss	RL					1		4-5 mm
	Unidentified 3. leaf stems	Rs					2		
186	*Nothofagus menziessii*	ML	3					170 (m 0.8), 171 (m 0.8), 172 (m 0.8)	
	Nothofagus fusca	RL					1	173 (m 0.8)	
	Nothofagus sp. Leaf fragments	Mm					9		
	Unidentified 1. Grass	Ms					8		1-2 mm
	Undifferentiated fragments U2								
190	*Nothofagus menziessii*	RL	1					174 (m 0.8)	
	Nothofagus sp. Leaf frags	Cs					13		1-3 mm
	Large stem-possibly nothofagus							175 (m 0.8)	6-7 mm
	Unidentified 1. moss							176 (m 1.25)	6-7 mm
	Unidentified 2. small leaf		1					177 (m 2.0)	
195	Nothofagus sp. Fragments	Ss					3	178 (m 1.0)	
	Undifferentiated fragments	Ms					7		1-2 mm

200	*Nothofagus menziessii*	RL	1					179 (m 0.8)	
	Unidentified 1. Grass	As					16		2-3 mm
	Unidentified 2. Moss						1		
	Nothofagus fragments						1		
	Stem of leaf						1		
	Liver wort?						2	180 (m 1.6)	
	Unidentified fragments						15		1-2 mm
205	*Nothofagus menziessii*	RL	2					181, 182 (m 0.8)	
	Unidentified 1. Moss						1		
	Unidentified 2. Undiff frags						7		1-2 mm
210	*Nothofagus sp. Pos fusca*	RL	0.5					183 (m 0.8)	

	Nothofagus menziessii	SL	4					184 (m 0.8)	
	Nothofagus sp.	Mm					5		1-5 mm
	Unidentified 1. Grass	Ss					4		
	Undifferentiated fragments	Ms					7		1-2 mm
215	*Nothofagus menziessii*	RL	1						
	Nothofagus sp.	Ss					3		1-2 mm
	Undifferentiated fragments	Cs					12		1-2 mm
220	*Nothofagus menziessii*	RL	1					186 (m 0.8)	
	Nothofagus sp.	Ms					8		2-4 mm
	Unidentified 1. Grass	Ss					3		1-2 mm
	Unidentified 2. undiff frags	Ms					7		
	Unidentified 3. Moss??						1	187 (m 2.0)	
225	*Nothofagus cliffortioides*	RL	1					190 (m 1.0),	

								191 (m 1.6)	
	Root-possibly N.menziessii or podocarp	RL			1			188 (m 0.8), 189 (m 2.0)	
	Nothofagus menziessii	RL	1 1/2 leaf					192 (m 0.80), 193 (m 1.25)	
	Unidentified 1. Grass	Ms					9		1-2mm
	Nothofagus sp. leaf frags	Ss					4		1-2 mm
230	*Nothofagus menziessii*	SL	2				1	194, 195, 196 (m 0.8)	
	Nothofagus sp. Undiff	Mm					6		large: 3-5 mm, small: 1-2 mm
	Unidentified 1. Grass	Cs					10		1-2 mm
	Unidentified 1. Moss	Rs					2		3-4 mm
	Undifferentiated fragments	Ms					6		1-2 mm
235	*Nothofagus menziessii*	RL	2					197, 198 (m 0.8)	
	Nothofagus sp. Frags	Ms					6		2-4 mm
	Unidentified 1. moss/liverwort	Ss					4	199 (m 1.0)	2-4 mm
	Unidentified 2. Grass	Cs					11	200 (m 1.6)	1-2 mm

	Unidentified 3. Stems					1			
	Unidentified 4.undiff frags	As					15		1-2 mm
	Unidentified 5. Moss? Unerground rhio						6	201 (m 2.5)	2-3 mm
	Unidentified 6. small leaf		1					202 (m 2.5)	1-2 mm
240	*Nothofagus menziessii*	RL					2		
	Nothofagus sp. Frags	Cs					11		1-3 mm
	Unidentified 1. Grass	Ms					6		1-2 mm
	Unidentified 2. Stem?					1		204 (m 1.25), 205 (m 2.0)	
245	*Nothofagus menziessii*	ML	2				4	206 (m 0.8), 207 (m 0.8)	4-5 mm
	Nothofagus sp. Frags	Ms					8		1-2 mm
	Unidentified 1. Grass	Ms					5		1-2 mm
	Unidentified 2. Stems?	SL					4		4-5 mm
	Unidentified 3. Undiff fragments	Ss					4		1-2 mm
	Unidentified 4. ?							208 (m 2.0)	
250	Unidentified 1. leaf? Or							209 (m 0.8)	5-7 mm

	flattened seed								
	Unidentified 2. stem	Rm				2		210 (m 0.8)	10-12 mm & 2-3 mm
	U3. Nothofagus sp. Frags	Rs					2		2-3 mm
	Unidentified 4. Grass	Rs					2		1-2 mm
	Unidentified 5. Root?				1			211 (m 2.0)	
255	*Nothofagus menziessii*	RL	1					212 (m 0.8)	
	Unidentified 1. wood fragments	ML					5		3-7 mm
	Nothofagus leaf fragments	Ms					6		1-4 mm
	Unidentified 2. Grass, moncote	As					17	213 (1.6)	1-2 mm
	Undifferentiated fragments	As					19		2-3 mm
	Unidentified 3. Seed-possible Nothofagus	Rs		1				214 (m 1.0)	
260	Nothofagus sp leaf frags	Rs	1						
	Unidentified 1. Stems	SL					3	216 (m 1.0)	4-5 mm
	Unidentified 2. Grass	Rs					2		1-2 mm
	Nothofagus menziessii	RL	1					215 (m 0.8)	

265	Unidentified 1. moss/aquatic plants	Cs					10	217, 218 (m 1.25)	
	Unidentified 2. Wood							219 (m 0.8)	~15 mm
	Nothofagus sp leaf	ML					5	220 (m 0.8)	4-5 mm
	Unidentified 3. Stem	Rs				1			
	Unidentified 4. Grass	Ms					9	221 (m 0.8)	1-2 mm
	Libocederus bidwillii	Rs					1	222 (m 2.5)	
	Unidentified 6. Undiff frags								
270	Unientified 1. Monocote	Ms					7	223, 224 (m 1.0)	3-4 mm
275	Unientified 1. Monocote	Mm					8		2-5 mm

280	Unidentified 1. moss						1		4x1 mm
285	Unidentified 1. Fibrous monocots	Am					19	225 (m 0.8)	2-6mm
	Nothofagus sp. Fragments	Sm					3	226, 227 (m 1.6)	2-6 mm
	Libocedrus bidwillii?	Rs					1		2-3 mm
	Unidentified 2. Leaf-alpine herb	Rs	1					228 (m 1.25)	6-7 mm
290	No macrofossils-unidentified fragments								

295	Unidentified 1. Bark	CL					10	229 (m 0.8)	large: 10-20 mm, Small: 4-6 mm
	Unidentified 2. Moss/aquatic plants	Sm					4		2-7 mm
	Nothofagus menziessii	RL					1	230 (m 1.0)	
	Unidentified 3. Grass	Ss					4		2-4 mm
	Unidentified fragments								
	Unidentified 4. Small leaf							231 (m 1.6)	~3 mm
300	Nothofagus sp. -possible menziessii	RL	1					232 (m 0.8)	
	Unidentified 1. leaf or flattened seed	Rs					1	233 (m 1.0), 243 (m 1.6)	
	Unidentifiifed frag						1		

305	Unidentified 1. Grass	Ss					4	235 (m 2.0)	
	Unidentified 2. Root structures herb?	ML					6	236 (m 1.25)	10-15 mm
310	Unidentified 1. Bark-1	RL					2		10-12 mm
	Unidentified 1. Bark-2	Cs					13	237 (m 0.8)	2-4 mm
	Unidentified 3. Monocots	Cs					12		1-2 mm
315	Unidentified 1. Grass	As					15		2-4 mm

320	Unidentified 1. Moss	RL					2		4-5 mm
	Unidentified 2. Grass	Rs					2		1-2 mm
325	Unidentified 1. Stems	Mm				3	3		8-10 mm & 3-4 mm
	Unidentified 2. Grass	ML					5		4-5 mm
	Unidentified 3. Moss						1		18-20 mm
330	No macrofossils-Unidentified fragments						2		

335	Unidentified 1. Grass	Ms					5		2-4 mm
	Unidentified fragments	Ss					4	238 (m 2.0)	4-6 mm
	Unidentified 2. Veination of leaf	Rs					1	239 (m 1.25)	
340	Unidentified 1. Grass	Rs					2		2-4 mm
	Dracophyllum						1	240 (m 1.0), 241 (m 2.0)	5-6 mm
345	Unidentified 1. Bark?	Cm					14		2-14 mm

350	Unidentified 1. Moss/aquatic plants	Sm					4	242 (m 1.0)	3-7 mm
	Unidentified 2. Posible seed coat						1	243 (m 2.0)	
	Unidentified fragments								
	Unidentified 3. fibrous grass	Ms					6	244 (m 1.6)	2-3 mm
355	Unidentified 1. Moss	Rs					2		2-3 mm
	Unidentified 2. Grass	Ss					4		2-3 mm
	Unidentified 3. Wood	Ms					6		3-4 mm
360	No macros								

365	Unidentified 1. possible grass	Rs					2	245 (m 1.6)	3-4 mm
370	Unidentified 1. Grass	Cm					11	246 (m 0.8)	6-7 & 4-5 mm
	Unidentified 2. Moss/liverwort	ML					5	247 (m 0.8), 248 (m 1.6), 249, 250 (m2.0)	10-20 mm
	Undifferentiated fragments	Ms					9	251 (m 1.0)	2-5 mm
	Unidentified 3. Moss-2	Rs					2	252 (m 1.25)	2-4 mm
375	No macros								

380	No macros								
385	No macros								
390	No macros								

395	No macros								
400	Unidentified 1. Moss	Rs					1		2-3 mm
	Unidentified 2. Grass?	Ss					3		
405	No macros								

410	Unidentified 1. Moss/aquatic/liverwort	Sm					3	253 (m 0.8), 254 (m 1.6)	10 mm stem 3mm leaves
	Unidentified 2. Moss-2	Rs					1	255 (m 0.8), 256 (m 1.25)	
	Unidentified 3. Moss-3	Ms					6	257 (m 1.6)	
	Unidentified 4. Moss-4	Sm					4	258 (m 1.6), 259 (0.8), 260 (m 1.25)	x1 large fragment 30-40 mm
	Unidentified 5. Grass	Ms					5		
	Unidentified 6. Bark	Ss					3		
415	No macros								

420	Unidentified 1. Moss	Cm					13	262 (m 2.5), 263 (m 1.0)	3-7 mm
425	No macros								
430	Unidentified 1. Moss/aquatic plant	SL					4	264 (1.0), 265 (m 2.0)	10-20 mm 1mm wide

435	Unidentified 1. Moss/aquatic	Am					Clumps	266 (m 1.6)	
	Unidentified 2. Moss	Ms					5	267 (m 1.0)	
	Unidentified 3. Grass	Ss					4	278 (m 1.0)	
440	Unidentified 1. Moss/aquatic	Rs					2	269 (m 1.0)	3-4 mm
445	No macros								

450	Unidentified 1. Moss/aquatic	Cm					Clumps	270 (m 1.6)	
	Unidentified 2. Grass	Ss					4		
455	Unidentified 1. Aquatic plant						1	273 (m 1.25)	
	Unidentified 2. Moss	Ms					5	271 (m 1.25), 272 (m 1.0)	
	Unidentified 3. Aquatic? Same as 430 cm?						2	274 (m 1.25)	
460	Unidentified 1. Moss/roots	Ms					6	275 (m 1.0)	2-4 mm
	Unidentified 2. Grass	Ms					5		2-3 mm

465	No macros								
470	No macros								
475	Unidentified 1. Moss/aquatic	Ms					7	276 (m 1.6)	2-4 mm
	Unidentified 2. Moss-2						2	277 (m 1.25)	
	Unidentified 3. Grass	Rs					1	278 (m 2.0)	1-2 mm
	Unidentified 4. Stems?						2		2-3 mm

480	No macros								
485	No macros								
490	No macros								

495	No macros								
500	No macros								
505	Unidentified 1. Moss/grass	Ms					8		1-2 mm

510	Unidentified 1. undiff frags	Cs					12		1-2 mm
515	Unidentified 1. Grass	Cs					12	279 (m 2.0)	1-2 mm
	Unidentified 2. Moss	Rs					1	280 (m 1.6), 281 (m 2.5)	
520	Unidentified 1. Grass	Rs					1		2-3 mm

525	No macros								
530	Unidentified 1. Grass	Rs					1		1-2 mm
535	Unidentified 1. Grass	Rs					4		1-2 mm
	Unidentified 2. Leaf	Rs	1					282 (m 3.2)	2 mm

540	No macros								
545	Unidentified 1. Grass?								10 mm
550	Unidentified 1. Moss	Ms					5	283 (m 2.5), 284 (m 2.5)	2-3 mm

555	Unidentified 1. Moss	Ss					3		1-2 mm
560	Unidentified 1. Moss-1	Cs					10	285 (m 1.6)	1-2 mm
	Unidentified 2. Moss-2						1	286 (m 2.5)	2-3 mm
	Unidentified 3. Possible grass?								